

Dear Editor,

We wish to thank you and the referees for your precious time in reviewing our paper and providing valuable comments. It was your valuable and insightful comments that led to possible improvements in the current version. We have carefully considered the comments and tried our best to address every one of them. Below we provide the point-by-point responses to referees' comments. Texts in italic are the referees' comments (C), those in black bold style are our responses (AR), and texts marked in red are relevant changes in the manuscript. The page and line numbers in this letter refer to the marked-up version. We hope that you will find the changes satisfactory.

Sincerely,

Bahar Bahrami on behalf of the co-authors  
bahreh.bahrami@ufz.de  
Department of Computational Hydrosystems  
UFZ, Leipzig, Germany

## Referee # 1

Dear Referee,

Thank you for your time and attentions on this work. The comments and suggestions are very useful to improve our manuscript. We paid detailed attention to all comments and have addressed all of them below accordingly.

### General comments

*Bahrami et al. developed a forest development model requiring few parameters linked with a phenology submodel predicting gross primary productivity (GPP) and leaf area index (LAI). They evaluated model performance at a selection of FLUXNET sites and performed a parameter sensitivity analysis determining the most sensitive parameters and optimal site-specific values as well as a set of compromise parameter values for larger regions. The model can be coupled with a hydrologic model, which could improve both water and carbon flux simulations. The model is well developed and performs reasonably well at broad-leaved forest sites. The language and description of certain parts of the manuscript, however, should be improved before publication. Especially the Introduction and parts of the Results and Discussion are unclear and should be better explained. I would suggest*

*rewriting most of the Introduction section to explain the cited literature and its relevance to the manuscript better. Generally, the model is explained well, but certain parts of the description can be made clearer (see specific comments below). The manuscript contains a lot of technical corrections (typos and grammatical mistakes), which should be corrected.*

**We appreciate the reviewer's suggestions! We have revised the manuscript based on all the general and specific comments raised by the reviewer and rewrote most of the introduction. We have also carefully proofread the manuscript and have made several technical corrections, and hope that the revised manuscript will meet with your requirements.**

### **Specific comments and technical corrections**

*C 1) l. 5: Add "the" water cycle*

**AR 1) We added it to the sentence [Pg. 1, l. 5].**

*"... which is of critical significance in and closely linked to the water cycle."*

*C 2) l. 38: Use "sequestering" instead of "sequestrating" (also in l. 69, 79).*

**AR 2) We have modified the sentence as follows [Pg. 3, l. 76], [Pg. 4, l. 95], [Pg. 4, l. 108].**

*"... the extent to which ecosystems are capable of sequestering it, ..."*

*"... the rubisco enzyme uses the ATP energy from the light response to sequester the atmospheric carbon dioxide ..."*

*"The amount of sequester carbon as biomass ..."*

*C 3) l. 43: In "60% of the global net forest sink" do you mean the "global net carbon sink"?*

**AR 3) Thank you for this remark. We meant the temperate broad-leaved forest contribute around 60% of the global net carbon sink among all type of forests. We have made the sentence clearer now as below [Pg. 2, l. 50].**

*"Generally, forests are recognized as biomes with high carbon sequestration capacity (Lal and Lorenz, 2012) where temperate broad-leaved forest contribute to approximately 60% of the global net carbon sink of forests (Pan et al., 2011; Reinmann and Hutyra, 2017)."*

*C 4) l. 44: Specify what kind of ecosystems you mean; I haven't heard it defined as "vegetation GPP", just GPP. You could say "vegetated ecosystems". "Plant photosynthesis" already implies that it comes from vegetation.*

**AR 4:) Thank you for the suggestion. We have accordingly revised the sentence [Pg. 3, l. 78].**

“The total carbon uptake from the atmosphere into the vegetated ecosystems by plant photosynthesis is known as gross primary production (GPP).”

*C 5) l. 45: GPP and ecosystem respiration are of similar magnitude and which one is larger depends on whether the ecosystem is a sink or source of CO<sub>2</sub>. I would rephrase this.*

**AR 5) Thanks for this suggestion. We modified the sentence to make it clearer [Pg. 3, l. 79].**

“GPP is the primary driver of the land carbon sink (Spielmann et al., 2019; Zhou et al., 2021) and the largest flux within the carbon cycle (Schaefer et al., 2012; Foley and Ramanakuty, 2003).”

*C 6) l. 46: Be more specific what you mean with “has a direct effect on moderating climate and environment”, especially the effect on the environment.*

**AR 6) Thanks for the suggestion. We have added sentences to better explain the effect on climate and environment [Pg. 3, l. 81].**

“Accurate estimation of GPP directly influences carbon budget assessments as well as estimates of the amount of stored carbon in the plant leaf pool. Accurate carbon budget assessment, in turn, promotes understanding of the feedbacks between the terrestrial biosphere and the climate system (Zhou et al., 2021; Huang et al., 2022).”

*C 7) ll. 46-50: Be more specific about what “adverse effects of a changing climate” you mean! The second part of the sentence applies to any climatic conditions not only under a changing climate. To relate this part of the sentence to the first part about climate change, discuss its effects on temperature, water availability, radiation, etc. Otherwise, the reason for mentioning a changing climate here is unclear.*

**AR 7) Thank you for the comment. We have revised the paragraph following your valuable suggestion [Pg. 2, l. 42].**

“Vulnerability due to climate change can be attributed to different ecosystem stresses (Nathalie et al., 2006; Cholet et al., 2022) including high temperatures that decrease enzymes activity and the rate of carbon uptake as well as soil water limitation causing hydraulic failure or carbon starvation, reducing plant photosynthetic capacity, and early senescence (Imadi et al., 2016) in temperate forest ecosystems. In addition to these stresses, some environmental changes such as radiation change associated with increased cloudiness or atmospheric aerosols can also increase plant productivity, e.g. due to an increased fraction of diffused radiation (Knohl and Baldocchi, 2008).”

*C 8) l. 50: Favourable climate in what respect? I’m not sure what you want to express here and how, for example, the winter season is favourable for the vegetation.*

**AR 8) Thank you for this comment. We had put “favorable” mistakenly instead of “temperate”. It has been revised as follows [Pg. 3, l. 59].**

“Temperate DBF biomes are characterized by having a temperate climate with four distinct seasons and a temperature-driven canopy structure.”

*C 9) l. 51: “The plant canopy capacity and seasonality are expressed by leaf area index (LAI)” -¿ Rephrase this! What exactly do you mean with “plant canopy capacity” and LAI itself does not express seasonality. Changes in LAI do.*

**AR 9) Thank you for this comment. Here by plant canopy capacity we meant the capacity to exchange the fluxes. We have rephrased the sentence accordingly [Pg. 3, l. 61].**

“The plant canopy capacity for water and carbon exchange is strongly related to seasonal variation in leaf development (Seo and Kim, 2021).”

*C 10) l. 52: Reference? Maybe make it clearer that with “total green leaf area” you mean two-sided, as opposed to one-sided leaf area in broadleaf canopies, or total needle surface area in conifers.*

**AR 10) We revised the sentence and added the reference as follows [Pg. 3, l. 62].**

“Leaf area index (LAI) is a dimensionless quantity, defined as one-sided area of green leaf per unit horizontal ground surface area (Nathalie, 2003; Fang et al., 2019).”

*C 11) l. 53: Be more specific or add a reference here.*

**AR 11) We made the sentence more specific and added a reference [Pg. 3, l. 64].**

“LAI can be estimated either by direct field measurements, inferred using remote sensing or be simulated by vegetation carbon cycle models (Fang et al., 2019).”

*C 12) ll. 54-55: Rephrase this to make it clearer! Yes, LAI affects transpiration, but GPP does as well.*

**AR 12) Thanks for the comments. We have rephrased the sentence to make it clearer [Pg. 3, l. 67].**

“LAI is a key biophysical plant variable, representing vegetation state, affecting not only the sequestration of carbon from the atmosphere via photosynthesis but also the release of water to the atmosphere through transpiration (Fang et al., 2019).”

*C 13) ll. 56-57: If you mention water balance components affected by LAI, I would include canopy evaporation as well.*

**AR 13) Thanks for this comment. Canopy evaporation and interception are added to the sentence [Pg. 5, l. 129].**

“(e.g., plant transpiration and canopy evaporation)”

*C 14) l. 68: Unnecessary to have both “later” and “in the next step”. Could just say “in the dark reactions of the Calvin cycle, ...”.*

**AR 14) Thanks. It has been revised accordingly [Pg. 4, l. 95].**

“In the dark reactions of the Calvin cycle, the rubisco enzyme uses the ATP energy from ...”

*C 15) l. 71: “specifically at scales larger than the leaf level” -¿ Above, you only mention that GPP is determined at the leaf level in the EK approach. You don’t say how it is up-scaled to the canopy level or larger scales.*

**AR 15) Thanks for the comment. We agree with the reviewer. The sentence with the last part was confusing and it has been removed during revision [Pg. 4, l. 96].**

“This approach requires the specification of a relatively large number of parameters for governing processes.”

*C 16) ll. 76-77: Rephrase to make it clearer! It isn’t clear that you mean that APAR is a product of PAR and fPAR, which is the biome-specific LUE parameter.*

**AR 16) We have revised the sentence to make it clearer. The APAR is a product of PAR and fPAR. We revised the sentence as follows [Pg. 4, l. 103].**

“In this approach, ecosystem GPP is a function of absorbed photosynthetically active radiation (APAR) and a biome specific LUE parameter (Gamon, 2015; Springer et al., 2017). APAR is a product of incident photosynthetically active radiation (PAR) and the fraction of PAR (fPAR) absorbed by plant leaves.”

*C 17) l. 78: “The LUE” -¿ Say either “the LUE parameter” or “fPAR”. You aren’t talking about LUE itself here.*

**AR 17) Thanks for pointing this out. Indeed, this should be mentioned [Pg. 4, l. 106].**

“The LUE parameter corresponds to the vegetation conversion efficiency of solar radiation into biomass and is defined as the amount of carbon produced per unit of absorbed PAR (Monteith, 1977; Yuan et al., 2014).”

*C 18) ll. 81-82: “CFLUX (Turner et al., 2006), EC-LUE (Yuan et al., 2007), MODIS-GPP (Running et al., 2004), VPM (Xiao et al., 2004), and CASA” -¿ Define what these abbreviations stand for!*

**AR 18) We have now added the complete name of the models [Pg. 4, l. 113].**

“carbon cycle model (CFLUX)..., eddy covariance- light use efficiency (EC-LUE) ..., moderate resolution imaging spectroradiometer-gross primary production (MODIS-GPP) ..., vegetation photosynthesis model (VPM) ..., and Carnegie-Ames-Stanford Approach (CASA)...”

*C 19) l. 86: Why specifically central Europe? If you mention it, explain why as well!*

**AR 19) Thanks for the question. Central Europe was mistakenly put here. We have rephrased the sentence as follows [Pg. 4, l. 117].**

“These two key biophysical variables are generally sensitive to cloud contamination leading to gaps in their temporal and spatial coverage throughout the year”

*C 20) ll. 86-89: Unclear what you mean. Be more specific!*

**AR 20) Thanks for the comment. We have revised the sentence as follows [Pg. 4, l. 120].**

“These gaps are sources of uncertainty in satellite-based fPAR and LAI products which, in turn, may induce errors in quantifying GPP (Rahman et al., 2022).”

*C 21) ll. 89-101: The purpose of this paragraph isn't really clear, as several different models are mentioned, but their limitations aren't clearly explained!*

**AR 21) Thanks for the comment. We have revised the paragraph to make it clearer. Here, in general, we wanted to mention previous efforts of models simulating LAI using GPP. The limitations for TETIS-VEG are that it is only applicable for evergreen forests, and also that the source code is not freely available. Regarding, the SGPD-TS model, although it simulates LAI but its limitation is that it uses a linear relationship between steady-state GPP and LAI. In this way, GPP is used as a proxy of LAI which utilizes a conversion ratio when maximum GPP has been reached. However, it has been earlier shown that maximum GPP saturates at LAI values above  $4 \text{ m}^2 \text{m}^{-2}$  (Lee et al., 2019); and this may potentially introduce uncertainty during simulation of LAI when the LAI of stands exceed values of  $4 \text{ m}^2 \text{m}^{-2}$ . Many of these models have been developed and validated at specific sites and their broader applicability across a diverse range of climatic conditions has yet been not demonstrated [Pg. 5, l. 131].**

“The LUE principle and leaf growth have been successfully implemented in the TETIS-VEG ecohydrology model (Francés et al., 2007; Pasquato et al., 2015). The TETIS-VEG model is, however, adapted for evergreen forest biome. In other words, the TETIS-VEG model lacks representation of a dynamic leaf phenology relevant in the deciduous broad-leaved forests. Another approach to simulate GPP and LAI is adopted in the simplified growing production day time-stepping scheme (SGPD-TS) model (Xin et al., 2019). The SGPD-TS model, however, does not represent leaf growth and allocation to leaf pool, but establishes a linear relationship between steady-state GPP and LAI. In this way, GPP is used as a proxy of LAI, utilizing a conversion ratio when maximum GPP has been reached. However, it has been shown that simulated GPP saturates at high LAI values (e.g., above  $4.5 \text{ m}^2 \text{m}^{-2}$  (Lee et al., 2019) and (Pan et al., 2021)). High LAI values are often common in deciduous broad-leaved forests, thus, relying on maximum GPP to derive LAI might introduce a bias at elevated LAI. Another more general challenging aspect for these models is the identification of model parameters that are site or location specific. Previous applications often have been limited to one calibration site (Francés et al., 2007); but they need to be thoroughly cross-validated for their applicability across a diverse range of climatic

conditions”

*C 22) l. 105: Explain what specifically you mean with “readily available observational datasets across eddy flux tower stations”*

**AR 22) Thanks for this comment. We meant the most common available data set among eddy flux tower stations that are easy to obtain, i.e., can be downloaded. We made the sentence clearer by specifying the name of variables [Pg. 5, l. 150].**

“The parsimonious approach and level of model complexity are designed to make use of readily available observational dataset for abiotic forcing across eddy flux tower stations such as air temperature, vapour pressure deficit, soil moisture, photosynthetic photon flux density.”

*C 23) ll. 180: “changes of vapour pressure deficit” should be “changes in vapour pressure deficit”.*

**AR 23) Thanks for the comment. We changed the sentence accordingly [Pg. 8, l. 229].**

“The canopy photosynthesis rate is strongly related to changes in vapour pressure deficit ...”

*C 24) l. 200: It is unclear what you mean with “using the cumulative root fraction up to each layer”. What is the cumulative root fraction used for, if the root fraction for each layer is multiplied by the soil moisture content of that layer?*

**AR 24) Thanks for raising this question. For the calculation of a root-zone weighted soil moisture, we used information on depth (layer) specific soil moisture and fraction of roots in each soil layer. The latter is estimated using formulations provided by Jackson et al., 1996 – in which the cumulative root fraction at a specified depth can be expressed by an asymptotic (power law) equation along with a biome specified parameter (in our case for DBF is 0.966; see Eq. 11). We then deduce the root fraction for a specific soil layer from this cumulative root fraction estimates (see Eq. 12). Another point is that the root fractions are normalized to 100%. We have created a schematic representation here to better explain this averaging part [Pg. 9, l. 249].**

Depth[cm]	$R_{C_i}$	$R_{I_i}$	$\theta_i$	$\theta_i$ ( $\theta_i * R_{I_i}$ )
0	0	0	0	0
0-10	0.29	0.31	13	4.1
10-20	0.50	0.22	14	3.1
20-30	0.64	0.15	12	1.9
30-40	0.74	0.11	12	1.3
40-50	0.82	0.07	15	1.2
50-80	0.93	0.012	20	2.5

$\sum \theta_i = \theta$  (daily effective)  
 Normalized: dividing by 0.93  
 Ex. For the last day of data

“Then, to estimate the root fraction in each individual layer (Eq. 12), we use the calculated cumulative root fraction up to each layer subtracted from the corresponding fraction of the previous layer (see Eq. 11).”

C 25) l. 228: “photosynthetical”, not “photosynthetically”.

AR 25) Thanks, modified to photosynthetical [Pg. 10, l. 279].

“is the sum of photosynthetical carbon uptake by plants (GPP)”

C 26) l. 251: Do you mean “growing season length”?

AR 26) Here we refer to  $L_g$  parameter which is a threshold in degree day for the duration of leaf growing length from budburst day up to the day of maximum canopy leaf cover. This parameter, with the same description, is adapted from Yue and Unger, 2015. We revised the sentence to make it clearer [Pg. 10, l. 302].

“The  $L_g$  parameter is a calibrated constraint in degree day, representing the period of leaf growth from budburst to maximum leaf cover (Yue and Unger, 2015)”

C 27) l. 286: Why have “used” twice in the sentence?

AR 27) Thanks for pointing this typing mistake. We have deleted the second one [Pg. 12, l. 338].

“There are two widely used allocation schemes in vegetation models based on: ... ”

C 28) l. 288: It should be “BIOME-BGC” (also in l. 369).

AR 28) Thanks. We modified the text [Pg. 12, l. 340], [Pg. 15, l. 434].

“... or BIOME-BGC (Hidy et al., 2016).” “... (BIOME-BGC; Hidy et al., 2016)”

C 29) Equation 28: It should be 0 for  $T_c \leq T(t)$ .

AR 29) Thank you for noticing. It was indeed a typo in the text. We modified the third part of Eq. 28 as following [Pg. 13, l. 371].



$T_0, T_c \leq T(t)$

*C 30) l. 339: Either use “we” or remove the “and” and add a “.”.*

**AR 30)** Thanks for the comment. We removed “and” [Pg. 13, l. 391].

“This study focuses on deciduous broad-leaved forests biome type. We selected tower sites distributed over Europe and North America to ensure a representative spatial coverage”

*C 31) l. 342: Be more specific what you mean with “long missing data at some sites”.*

**AR 31)** Indeed this sentence was not very clear. We meant that in some of the FLUXNET sites there were continually long periods of missing data such as years of missing data for PPFD where we excluded those years. For example, in the US-Ha1 site, even though the dataset in FLUXNET web page are available from 1991 to 2012, there is a long period of missing data for PPFD from 1991 to 2003. Therefore, our simulation starts in 2003. We added the following sentences to make it clearer [Pg. 14, l. 394].

“We further screened out the data at each site to the years with minimal gap in input data. For example, there were some long period of gaps (i.e., years) within the continuously recorded FLUXNET dataset for photosynthetic photon flux density (PPFD), which we excluded those years in the simulations (e.g., a continuous period of missing PPFD in the US-Ha1 dataset from 1991-2003)”

*C 32) l. 350-351: Make it clearer whether the soil moisture and soil texture variables are optional or required for the model.*

**AR 32)** Thanks for this suggestion. The text is now revised. In fact, the soil moisture (SM) and soil texture variables are optional for running the model. We had SM related information only for the DE-HoH site and therefore the application of soil moisture module was possible for only this site. In contrast, the model was run without the SM module for the other studied sites. While revising the text, we removed the word “required”. Based on the change in this sentence we also removed “However” at the beginning of the next sentence [Pg. 14, l. 408].

“Soil moisture (SM) and soil textural properties need to be provided to the model, if the model should also consider soil moisture stress. We investigated ...”

*C 33) l. 359: “obtained” not “collected” via personal communication.*

**AR 33)** Thanks for the suggestion. We changed “collected” to “obtained” [Pg. 14, l. 418].

“The LAI field measurements were obtained via personal communication to site contact persons: ...”

*C 34) l. 360: Maybe say “a subset of 4 sites was selected based on data availability” instead of “based on the responses a subset of 4 sites are used”.*

**AR 34) Thanks for suggestion. We modified the text [Pg. 14, l. 419].**

“; and a subset of 4 sites (DE-HoH, DE-Hai, US-MMS, and US-Ha1) was selected based on data availability”

*C 35) l. 364: What do you mean with "closest methods"? Are these methods both used at the same site or is one of the methods used at each site?*

**AR 35) We meant at one of the sites the fisheye method is used and at the others the LAI-2000 method. According to Ariza-Carricondo et al. (2019), these two methods agree very well with each other providing nearly similar of LAI across different sites. We have revised the texts accordingly [Pg. 14, l. 421].**

“The observation-based LAI data were obtained using common procedures with either the LAI-2000 instrument (Gower and Norman, 1991) at the DE-Hai, US-MMS, and US-Ha1 or the fisheye (DHP) technique ((Bonhomme, R. and Chartier, P., 1972; Ariza-Carricondo et al., 2019)) at the DE-HoH site, respectively. These two methods agree very well according to Ariza-Carricondo et al. (2019) and are thus considered to yield comparable values also across different sites.”

*C 36) ll. 368-371: Explain the different water stress functions better instead of just mentioning their names.*

**AR 36) Thanks for the suggestion. We also noticed that we had put the CASA model in a wrong category. We also added FORMIND in the text where soil moisture stress is considered in the model. We revised the text and add to the sentence accordingly to explain this part better [Pg. 15, l. 429].**

“The impact of water availability on the canopy photosynthesis (i.e., soil water deficit and atmospheric water deficit), in vegetation models is structured in two ways: individually or in combination with each other. Recently, plant hydraulic theory has also been introduced to reflect the vegetation water stress in Community Land Model (CLM5), which is beyond the scope of this study (Kennedy et al., 2019). In some models, water stress is quantified as an overall stress from both atmosphere and soil ((GLO-PEM; Prince and Goward, 1995), (BIOME-BGC; Hidy et al., 2022)). For instance, in the GLO-PEM model the water stress condition is reflected by an estimated and potential evapotranspiration, a relative drying rate scalar for potential water extraction, and a volumetric soil moisture content (more details together with equations can be found in (Zhang et al., 2015)). Some other models account for the water stress only due to the atmospheric drought ((CASA; Potter et al., 1993), (MOD17 algorithm; Running et al., 2000)). For example, in the MOD17 algorithm, only the atmospheric variable VPD and its two parameters,  $v_{min}$  and  $v_{max}$ , are used to calculate water stress factor to predict GPP (Running et al., 2000). In some other models such as FORMIND (Fischer et al., 2016) and EC-LUE (Yuan et al., 2007) only the soil moisture deficit is reflected. For instance, in the FORMIND model, the impact of atmospheric water deficit (VPD impact) is not presented; but the soil moisture deficit is represented by volu-

metric soil water content and soil parameters (soil field capacity, permanent wilting point, and minimum soil water content)..”

C 37) l. 375: *It should be “in 2018”.*

**AR 37) Modified [Pg. 15, l. 447].**

“... on simulated GPP over the DE-HoH site during the drought in 2018.”

C 38) l. 390: *In “the literature”.*

**AR 38) Modified [Pg. 16, l. 462].**

“In this study during the GSA, the parameters vary over boundaries reported in the literature’s.”

C 39) l. 420: *Do you not spin up the model for a longer time period? How can soil C and other C pools be spun up after one year or do you fully spin up the model with the default parameter values only?*

**AR 39) Thanks for the question. Here we focus on temperate forests and only on the above ground carbon pool confined to the canopy and leaf pool. The leaf pool at the end of each annual active growing season reaches to zero and the next year start almost from a bare canopy and zero carbon in the leaf pool. Therefore, we do not spin up the model for long period where it is indeed more relevant for compartment such as soil carbon, which we are not simulating the carbon in soil or other pools.**

C 40) l. 466: *“in (Eq. 3)” -¿ either remove the brackets or put the “in” into the brackets as well.*

**AR 40) Modified [Pg. 18, l. 542].**

“LUE in (Eq. 3).”

C 41) l. 468: *Add “the” in front of “Farquhar photosynthesis scheme”.*

**AR 41) Added [Pg. 18, l. 545].**

C 42) l. 469: *Add “the” in front of “photosynthesis process”.*

**AR 42) Added [Pg. 18, l. 546].**

C 43) l. 474: *Switch order to “also showed”.*

**AR 43) Added [Pg. 18, l. 550].**

The multiplicative coefficient of canopy reflectance, C, and the light extinction coefficient, k, parameters in the fPAR formulation (Eq. 4) based on Lambert-Beer’s law also showed substantial sensitivities.

C 44) ll. 474-475: *Rephrase! I don’t think you need both “typically” and “by default”.*

*Make it clearer what you're doing differently, if you mention that the parameters are "typically" fixed.*

**AR 44) "Typically" is removed. We added to text to make it clearer. This investigation helps to explore the model sensitivities to the often hidden parameters with the possibility to properly constrain the model [Pg. 18, l. 551].**

*"Notably, these parameters are fixed to constant values by default in the fPAR formulation in similar studies (e.g., Xiao et al. (2004) and Xin et al. (2019)); whereas, here, we let these parameters ( $C$  and  $k$ ) vary at  $\pm 20\%$  level of their fixed values."*

*C 45) l. 479: Instead of saying "the impact", specify what kind of impact (e.g., strong, weak) and say "VPD" or "the VPD variable".*

**AR 45) Revised [Pg. 18, l. 556].**

*"the strong impact of VPD ..."*

*C 46) l. 480: It should be "the" next environmental factor constraining "GPP".*

**AR 46) Modified [Pg. 18, l. 557].**

*"The next environmental factor constraining GPP ..."*

*C 47) l. 481: It should be "at the DE-HoH site".*

**AR 47) Modified [Pg. 18, l. 558].**

*C 48) l. 484: Remove "the" in front of  $\theta_r$  (also in l. 486).*

**AR 48) Modified [Pg. 19, l. 562].**

*C 49) l. 485: Add "a" in front of "soil matric potential".*

**AR 49) Added [Pg. 19, l. 562].**

*C 50) ll. 487-489: Be more specific what you would use as parameters?*

**AR 50) Thank you for this remark. With the text mentioned there, we wish to emphasise that empirical coefficients in pedo-transfer functions, linking soil textural properties (like sand or clay contents) with hydraulic characteristics (like permanent wilting points, field capacity), can be considered as parameters. To this end, we have provided references of previous studies also emphasising this aspect. We have revised the text as follows [Pg. 19, l. 565].**

*"Pedo-transfer functions (PTFs) link soil textural properties (e.g., sand, clay contents) to soil parameters (e.g.,  $\theta_r$ ) and various functional forms have been developed in past decades (Van Looy et al., 2017). Empirical coefficients of PTFs can also be regarded as model parameters (Samaniego et al., 2010; Kumar et al., 2013; Schweppe et al., 2021)."*

*C 51) ll. 490: Remove "the" in front of "simulated GPP".*

**AR 51) Modified [Pg. 19, l. 571].**

“.. is also a major contributor to simulated GPP ...”

*C 52) l. 491: Add “the” in front of “LAI calculation”.*

**AR 52) Modified [Pg. 19, l. 572].**

“.. the LAI calculation ...”

*C 53) l. 497: Say “at some sites”, not “in”.*

**AR 53) Modified [Pg. 19, l. 578].**

“... at some sites ...”

*C 54) ll. 497-498: Either use just “b” or “The b parameter”.*

**AR 54) Modified [Pg. 19, l. 579].**

“... The b parameter ...”

*C 55) l. 499: Add “the” in front of “temperature factor”.*

**AR 55) Added [Pg. 19, l. 580].**

“... the temperature factor ...”

*C 56) l. 501: With “informative” do you mean “sensitive”?*

**AR 56) Indeed. We meant that parameter is sensitive and thus is informative [Pg. 19, l. 583].**

*C 57) l. 502: It should be “favourable conditions”.*

**AR 57) Modified [Pg. 19, l. 585].**

*C 58) ll. 504-505: “little impact of environmental stresses due to temperature on GPP during the growing season” -¿ What about outside the growing season? Are the temperature stress parameters just less significant than your phenology submodel parameters? Also, could this not be site-dependent? At some sites, heat might impact GPP during the growing season.*

**AR 58) Indeed what limits the  $\text{CO}_2$  assimilation and gross primary productivity outside of the growing season is the temperature stress. we have revised the text as follows [Pg. 19, l. 583]:**

“In other words, temperature stress limits the  $\text{CO}_2$  assimilation and gross primary productivity outside of the growing season. Phenology parameters play their roles during the growing season. This period indicates favourable condition for plant growth when the temperature stress is mostly not active. Therefore, temperature stress parameters do not significantly influence the modelled GPP. In agreement with our results, Yuan et al. (2007) also reported little impact of environmental stresses due to temperature on GPP during the growing sea-

son. It is worth mentioning that the temperature stress is still applied during the growing season, but as the upper-most limits of temperature ( $T_{low}=-2$  °C and  $T_{high}=38$  °C) do not occur frequently, unless during cold, heat stresses (such as heat years in 2018 and 2019 at the DE-HoH site), the sensitivity of GPP to temperature parameters are less pronounced during the growing season.”

*C 59) ll. 506-507: Rephrase to make your point clearer! Unclear what you mean with "a group of daily LAI". Close the bracket after Figure 5.*

**AR 59)** As it can be seen from the PCM simulations and in agreement with previous studies, GPP output saturates and becomes insensitive to LAI values above  $4\text{ m}^2\text{m}^{-2}$ . For instance, the simulated LAI at DE-HoH site during the summer period, with maximum LAI usually above 4, an ensemble of LAI's from 4 to  $5\text{ m}^2\text{m}^{-2}$  correspond to a much narrower resulting GPP at each time step. We modified the sentence to make it clearer [Pg. 19, l. 592].

“This effect can also be seen in the LAI simulation (e.g., at DE-HoH site) where an ensemble of simulated LAI at each time step during the maturity phase, (i.e., in Figure 7), did not cause much difference in the corresponding GPP output (i.e., in Figure 5).”

*C 60) l. 522: Why "might"? Do they?*

**AR 60)** Thanks for the question. In the PCM, the LAI and GPP are simultaneously simulated in the model. Since the SLA is one of the parameters directly related to LAI, while LAI is, in turn, related to resulting GPP, we interpret that when SLA impacts GPP, it can only be through the LAI. However, we use “might” for a further caution. We changed the “might” word to “likely” [Pg. 20, l. 610].

“Since the LAI output in the model depends on GPP, the studies mentioned above reporting the SLA impact on GPP likely apply for LAI output as well (Li et al., 2016; Arsenault et al., 2018).”

*C 61) l. 527: Add "the" in front of "Fluxnet2015".*

**AR 61)** Added [Pg. 20, l. 615].

*C 62) l. 532: Explain what you mean with "allowing the canopy to reach to its maximum". Instead of "Next important contribution of parameters to the LAI output are those", maybe say something like "Other parameters the LAI output is sensitive to are ..." or "The LAI output is also sensitive to the parameters ..."*

**AR 62)** The  $L_b$  parameter is the maximum LAI that the ecosystem can sustain. Within PCM the carbon allocation to the leaf pool is maintained until the canopy LAI reaches that maximum value. More detail can be find in (Pasquato et al., 2015). We also modified the sentence [Pg. 20, l. 619]

“The  $L_b$  parameter (Eq. 24), also exhibits a marked sensitivity for the LAI output (Figure

3b) because it directly affects how long carbon allocation to the leaf pool continues until the canopy LAI reach to its maximum value at canopy closure (see (Eq. 26). Other parameters the LAI output is sensitive to are those governing the leaf phenology in the phenology submodel,  $L_g$  (Eq. 18),  $F_s$  (Eq. 22),  $b$  (Eq. 20),  $r$  (Eq. 20) (i.e., in Figure 3b)."

C 63) l. 536: "Lg parameter" -¿ Add "the" or remove "parameter".  
AR 63) Added [Pg. 20, l. 625].

C 64) l. 538: "cold accumulation in degree day" -¿ Below you call it "cold degree days". Choose one name and define what it is! Just say "leaf fall" instead of "the leaf fall event".  
AR 64) Thank you for the comment. We acknowledge that the sentence was not easy to understand. In fact, the cold accumulation in degree day and cold degree days here do not refer to the name of the parameter but are statements to help describing. To avoid confusion we have removed them from the revised manuscript.  $F_s$  (or leaf fall threshold) is a coldness threshold in degree day, below which leaf shed starts (more detail can be found in Yue and Unger (2015)). The phenology submodel in the PCM is adapted from Yue and Unger (2015) who describe it very well. So instead of explaining in more detail, we point the readers to Yue and Unger (2015)). We revised the sentences to avoid confusion [Pg. 20, l. 627].

"This parameter represents a coldness threshold for leaf fall in degree day. If the cumulative cold degree days from summer solstice (FDD) becomes equal or less than this threshold, then leaves start falling (more detail can be found in (Yue and Unger, 2015)). For instance, a higher threshold would lead to an early leaf shedding, especially in the cold climates where cumulative cold degree days can be reached faster. Therefore, the between site variation of this parameter is not surprising, given the differences in temperature and accumulated cold degree days among study sites. "

C 65) l. 539: "lower cold degree days accumulation" -¿ "Accumulated cold degree days"? Why does a lower value trigger earlier leaf fall?

AR 65) We thank reviewer for this comment. Given the cold degree days accumulation and the negative sign for these values, the word "lower" is changed to "higher". Therefore, A higher value indicates that the accumulated cold degree days (FDD) can reach to or become less than this threshold earlier and leaves start falling. We modified the text [Pg. 21, l. 629].

"For instance, a higher threshold would lead to an early leaf shedding, especially in the cold climates where cumulative cold degree days can be reached earlier."

C 66) ll. 546-547: Make clearer what you mean! Why would LAI always decrease, when you change these parameters? Don't you vary the value by +/- 20%?? Also, you say that GPP is less sensitive to these parameters than LAI, but then you explain the sensitivity of



*LAI by a reduced GPP?*

**AR 66)** We agree that the justification looks confusing! We indeed vary the values by  $\pm 20\%$ ; the LAI can either decrease or increase to reflect these variations. we have added another sentence to the previous one to better clarify this aspect [Pg. 21, l. 638].

“It might partly be due to the reduced/raised assimilated carbon (GPP) by canopy respiration which, in turn, might decrease/increases the available carbon to be allocated to leaf biomass and affect the resultant LAI. In addition to that, to best of our knowledge, it is the first time that these parameters are thoroughly analysed within a sensitivity analysis framework, and we yet might not be able to find a reason or explanation for this pattern in this study. This calls for future studies to further investigate this aspect.”

*C 67) ll. 547-548: How is the sentence “Furthermore, the evaluation of Sobol’ indices convergence (see Figure 4) showed relative stability of sensitivity indices at around 8 000 model evaluations.” connected to the previous sentences?*

**AR 67)** Indeed, it was not the best place for this sentence. It is an independent piece of information about SA. We have therefore replaced this sentence to the end of section 3.1 [Pg. 18, l. 532].

*C 68) l. 551: Instead of “informative parameters” maybe say “The X most sensitive parameters?”*

**AR 68)** We would like to mention that the SA has been conducted for each site individually and the X number of most sensitive parameters at each site vary between 8 to 14. We therefore opted to say informative parameters without attaching specific number to to that retains the generality of the mentioned text. Nevertheless, we have added more clarification in the revised text [Pg. 21, l. 646].

“... only the most sensitive parameters (depending on the SA result at each site, number of the most sensitive parameters vary between 8 to 14 parameters)...”

*C 69) l. 571: Instead of “validity” maybe use “performance”.*

**AR 69)** Modified [Pg. 22, l. 667].

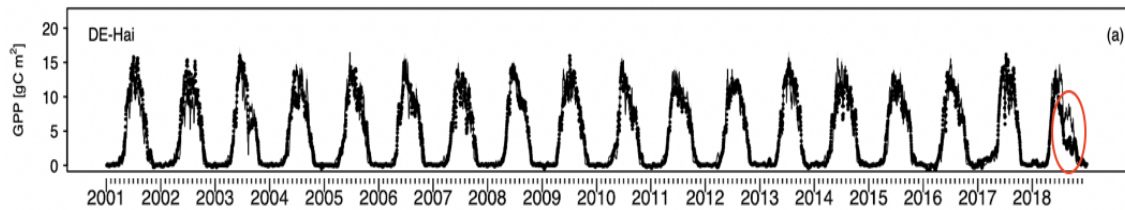
“Taken together, our model exhibits a reasonable performance...”

*C 70) l. 580: “where the model overestimated GPP” -; You mention poor performance due to a lack of soil moisture data and a lack of moisture. Why would GPP be overestimated then?*

**AR 70)** Thanks for the question. We believe this is due to omitting information on soil water stress. Where soil moisture data is not available (everywhere except the DE-HoH site), soil moisture stress is not accounted for, leading to a overestimation of GPP during times of water limitation. At the DE-Hai site in the late summer 2018, where the model does not account for soil moisture stress, due to unavailability of



relevant soil moisture information, the GPP is overestimated. The figure below shows the overestimation of GPP at DE-Hai during summer 2018 in a red ellipse.



However, since the soil moisture information was available at the DE-HoH site and the stress factor was applied in the GPP estimation, we were able to compare simulations with and without water stress. When accounting for water stress, the median of GPP output ensembles showed a good agreement with the observed GPP. We also showed that GPP at the DE-HoH site is overestimated without accounting for soil moisture stress factor in the supplemental figure S1.

*C 71) l. 599: Why was the decision made not to include non-structural carbohydrates in the model, if it is specifically made for deciduous broadleaf trees?*

**AR 71) In fact, at the beginning of model set-up, we were not aware of it. Only after analysing the result and looking for reasons for the disagreement, we learnt about non-structural carbohydrates and believe they are the cause of the slightly lagging phase in simulating LAI at the beginning of growing season as compared to the field measurements. Also, note that PCM currently comes without a complete carbon allocation scheme to all pools, which would be a pre-requisite to account for carbon storage. Therefore, in this first version of the PCM the non-structural carbohydrates are not represented in the model. We have acknowledge this part in the manuscript and this leaves the room for further model development.**

*C 72) l. 602: “Eventually” is unnecessary.*

**AR 72:) Modified [Pg. 23, l. 705].**

*C 73) l. 615: “also even” -; Use “also” or “even”, not both.*

**AR 73) Modified [Pg. 23, l. 718].**

*C 74) Figure 1 caption: It should be “PAR: photosynthetically active radiation”. Why do you define certain abbreviations that are in the rectangles but not all of them?*

**AR 74) Thanks. We have modified the “PAR: photosynthetically active radiation” as suggested. All the rectangles are the processes defined in the model except the LUE parameter and Photoperiod variable. Since LUE is one of the most important parameters in the model, we show this parameter in the figure. Also photoperiod is an**

inherent variable and part of autumn phenology which its representation in the figure helps to distinguish between spring and autumn phenology. However, we understand that showing them in rectangles was confusing. We now show these two important variables in ellipse.

“Variables in ellipse show LUE and photoperiod.”

*C 75) Table 1: You talked about excluding certain years with missing data. Are these the time periods you actually used?*

**AR 75) Thanks for this reminder! Actually, the time periods in the table show the original time series downloaded from the Fluxnet2015 site. The actual simulation time periods, with exclusion of the first year – first year is needed for the calculation of budburst day of subsequent year –, are the time series shown in the figure S4, S5, and S6 for different sites. We added another column with a name as “Simulation period”.**

“US-MMS: 1999-2014, US-Oho: 2004-2013, IT-Ro1: 2001-2006, US-Ha1: 2003-2012, FR-Fon: 2005-2014, DE-Hai: 2000-2018, DE-HoH: 2014-2018, CA-Oas: 1996-2010, DK-Sor: 2006-2013. Please see the response to the AR 9 response to the Referee#2 for more detail.”

*C 76) Figure 5 caption: I think you mean “shaded areas”. Why do you only have the shading for short periods at certain sites?*

**AR 76) Modified to “shaded area”. And thanks for the question. As explained in Section 2.2.4, to account for the predictive uncertainty, we selected an ensemble of model runs (outputs) at each site that lie within the top 5% of all the performance metrics. Based on that, at some sites there may be more and at others less ensemble members. Regarding certain and short period, as it can be obviously seen at the DE-HoH site, it shows more uncertainty during drought periods on 2018 and 2019 and emphasis the role of soil moisture stress factor and associated parameters (namely root distribution coefficient and permanent wilting point parameters). Even small variation in the above mentioned parameters makes a larger difference in resultant GPP.**

*C 77) What ensemble are you talking about? Is it an ensemble of the model output using different parameter values?*

**AR 77) Yes, indeed! Out of a total of 10000 parameter sets sampled from their a priori defined ranges (Table 3) at each site we choose the informative parameter sets. Here, the grey shaded area corresponds to the resultant ensemble output members.**

## Referee # 2

Dear Referee,

Thank you very much for your time and attentions on this work. The comments and suggestions are very useful to improve our manuscript. We paid detailed attention to all comments and have addressed all of them below accordingly. We also would like to thank you for the introducing new papers, they are indeed very interesting and helpful.

### General comments

*Bahrami and colleagues presented a manuscript describing the Parsimonious Canopy Model (PCM v1.0), that estimates gross primary productivity and leaf area index. The manuscript is well written (with some technical notes below) and, in my opinion, useful since the authors provides the code for the PCM in R. I have two main concerns: Please consider including in the title: “Developing a Parsimonious Canopy Model (PCM v1.0) to Predict Forest Gross Primary Productivity and Leaf Area Index on deciduous broad-leaved forest” or something that limits to the actual coverage of the study. Right now, the model only has been tested in this type of ecosystems (with good performance), and the actual title kind of oversells the coverage.*

**We appreciate the reviewer’s overall positive assessment to our work. We understand the reviewer remark regarding title and therefore have revised the title that now more clearly state the “deciduous broad-leaved forest” for which we have developed and tested our model. The revised title is:**

**”Developing a Parsimonious Canopy Model (PCM v1.0) to predict forest gross primary productivity and leaf area index on deciduous broad-leaved forest”**

*The phenology module. It is not clear if the phenology module estimates the start and end of the growing seasons using the warm-up period and then these values are used in the subsequent years. If so, this is a limitation of the model, since the SOS and EOS can be different over the years, influencing the carbon uptake period. At the end the annual sum might be correct/similar, however for incorrect reasons. This should be clearly stated in the limitation of the model, if it is the case.*

**Thanks for these remarks! In fact, the phenology module is run for each year. It uses the number of chill days (it counts days with daily mean temperature less than 5 degree centigrade) from winter solstice of the previous year as a variable which influences the budburst occurrence of each next year. We used the warm up period term referring to the last 10 to 11 days of each previous year that are eventually required for estimating variables in the phenology module for its uninterrupted run in the subsequent year. Indeed, what we observed using phenology module was differ-**

ent SOS's and EOS's during the study period at each site. And the start and end of carbon uptake is exactly in accordance with the SOS and EOS in each individual year.

## Specific comments and technical corrections

C 1) Please check the use of the expression “e.g.”, in the text it is used as “e.g.,” with the comma, while in the abstract is not.

AR 1) Thanks. We changed “e.g.” to “e.g.,” over the text.

C 2) Please check over the text the use of “R<sup>2</sup>” in uppercase, it should be in lowercase since it is a 1:1 comparison.

AR 2) We modified “R<sup>2</sup>” to “r<sup>2</sup>” in the text.

C 3) Over the text, please use italics when referring to a parameter (i.e., coefficients/parameters from Table 3).

AR 3) Thanks for the comment. We used italics when referring to parameters in the text accordingly.

C 4) Epsilon is in Eq. 3, not Eq. 4, please correct.

AR 4) Thanks for noticing. We modified the equation number to Eq. 3 [Pg. 7, l. 195].

C 5) L217-218. Please check the references in this sentence.

AR 5) Thanks. We Modified the sentence [Pg. 9, l. 268].

“According to Granier et al. (1999) and Fischer et al. (2016) the *scw* ...”

C 6) L260. If  $f_{SP} = f_{ST}$  (Eq 21), why not make it simple since Eq 18?

AR 6) Thanks for your kind suggestion. By keeping this equation, we wanted to be consistent with the autumn phenology (Eq. 25), which is the next part where photo-period factor  $f_{dl}$  also plays a role.

C 7) L288. It should be BIOME-BGC (check this all over the text), please check if this version also includes the MUSSO

AR 7) Thanks for the comment. We added the latest version as Biome-BGCMuSo v6.2. [Pg. 12, l. 340].

C 8) L346-347. How is the PAR-PPFD conversion done?

AR 8) Thanks for the question. We use the Fluxnet2015 PPFD variable in  $\mu\text{mol m}^{-2} \text{s}^{-1}$  and convert it to PAR in  $\text{MJ m}^{-2} \text{day}^{-1}$  as following:

$4.5 \mu\text{mol m}^{-2} \text{s}^{-1} = 0.000001 \text{ MJ m}^{-2} \text{day}^{-1}$ , then multiplied to 86400 to get the

corresponding daily values.

$$\text{PAR} = \text{PPFD-IN} * 0.000001 / 4.5 * 86400$$

*C 9) L348-349. Does this mean that the phenology submodel parameters are fixed according to the warm-up year to the subsequent years? Are there implications for using this? Could the authors report the values of the start and end of the growing season for each year of simulation?*

**AR 9)** We actually meant that since the phenology module for each individual year needs the number of chilling days from the previous year, the very first year of the observation period cannot be included in the simulations. Instead it is used to determine the budburst day of the first modelling year. For instance if the study period is from 2006 to 2013 then the simulation starts from 2007 to 2013. We acknowledge this sentence was not clear enough. We added to the sentence to make this clearer. In the following we also report the range of simulated Phenological transition dates including the start and end of the growing season (Julian date) for each year of simulation at the DE-HoH site.

Year	Start of growing Season	Maturity state	Start of leaf fall	End of growing Season
2015	109-123	162-186	257-270	296-298
2016	111-122	163-183	270	297-298
2017	101-129	168-183	251-270	290-298
2018	103-112	146-168	270-272	296-298
2019	105-114	154-179	271-273	297-298

“In other words, since the phenology module for each individual year needs the number of chilling days from the previous year, the very first year of observations is not included in the simulations. It is only used for to calculate budburst day of the first simulation year.”

*C 10) L476. Please check the references in this sentence.*

**AR 10) Modified [Pg. 18, l. 553].**

“... in similar studies (e.g., Xiao et al. (2004) and Xin et al. (2019)); ...”

*C 11) L486. Please check this reference (Hirmas et al., 2018, Nature) for increasing the discussion on how soil parameters should not be fixed. I liked this! Hirmas, D.R., Giménez, D., Nemes, A. et al. Climate-induced changes in continental-scale soil macroporosity may intensify water cycle. Nature 561, 100–103 (2018). <https://doi.org/10.1038/s41586-018-0463-x>*

**AR 11)** Thanks for providing this reference. We added it to the discussion part of the revised manuscript [Pg. 19, l. 568].

“Hirmas et al. (2018) also showed that soil retention properties can change in time. For example, climate change may induce rapid changes in the soil macroporosity and the associated soil hydraulic properties. Those may alter the feedback between climate and land surface.”

*C 12) L503-504. “Therefore, corresponding parameters do not significantly influence the modelled GPP”. This sentence is ambiguous, since I cannot interpret to which parameters the authors are referring to (i.e., temperature stress or phenology).*

**AR 12) Thanks for the comment. What we tried to explain is that in general upon arrival of favourable condition for plant growth, the period between SOS and EOS, temperature stress and the corresponding parameter roles on the GPP is less pronounced. To make this clearer, we have revised the texts [Pg. 19, l. 586].**

“Therefore, temperature stress parameters do not significantly influence the modelled GPP.”

*C 13) L508. Please check how the references are used.*

**AR 13) Thanks. We modified the sentence [Pg. 20, l. 595].**

“This is in agreement with the previous studies of Jung et al. (2007) and Lee et al. (2019), which showed that GPP output saturates and becomes insensitive at LAI values above  $4 \text{ m}^2 \text{ m}^{-2}$ .”

*C 14) L571-583. This might be a good reference (Vargas et al) for the discussion of drought and Mediterranean ecosystems. Vargas, R., Sonnentag, O., Abramowitz, G. et al. Drought Influences the Accuracy of Simulated Ecosystem Fluxes: A Model-Data Meta-analysis for Mediterranean Oak Woodlands. Ecosystems 16, 749–764 (2013). <https://doi.org/10.1007/s10021-013-9648-1>*

**AR 14) Thanks for this reference. We have added it to the discussion part [Pg. 22, l. 574].**

“Vargas et al. (2013), also discussed inter-annual dynamics of soil moisture effect on GPP flux in Mediterranean ecosystems using five process-oriented ecosystem models including water balance. They observed a systematically underestimation of GPP in the models that were accounting for soil water balance. Those underestimations may have been related to the complex nature of Mediterranean ecosystems, e.g., due to deep roots and an important role of the lower canopy. In contrast, here we overestimate the GPP and believe that this is due to lack of local information on soil moisture stress. More information of soil moisture stress is therefore expected to improve the model. Overall, they emphasize the importance of drought conditions and the complex nature of Mediterranean ecosystems in representing forest dynamics, including GPP flux.”

*C 15) In Tables 4-5, I recommend to the authors to report the linear regression coefficients (slope and intercept), not only RMSE and  $r^2$ , so the reader can know the biases.*

**AR 15) The linear regression coefficients are now added to the tables.**

## References

- Ariza-Carricondo, C., Mauro, F., Op de Beeck, M., Roland, M., Gielen, B., Vitale, D., Ceulemans, R., and Papale, D.: A comparison of different methods for assessing leaf area index in four canopy types, *Central European Forestry Journal*, 65, <https://doi.org/10.2478/forj-2019-0011>, 2019.
- Arsenault, K., Nearing, G., Wang, S., Yatheendradas, S., and Peters-Lidard, C.: Parameter Sensitivity of the Noah-MP Land Surface Model with Dynamic Vegetation, *Journal of Hydrometeorology*, 19, <https://doi.org/10.1175/JHM-D-17-0205.1>, 2018.
- Bonhomme, R. and Chartier, P.: The interpretation and automatic measurement of hemispherical photographs to obtain sunlit foliage area and gap frequency, *Israel J. Agric. Res.*, 22, 53–61, 1972.
- Cholet, C., Houle, D., Sylvain, J.-D., Doyon, F., and Maheu, A.: Climate Change Increases the Severity and Duration of Soil Water Stress in the Temperate Forest of Eastern North America, *Frontiers in Forests and Global Change*, 5, 879 382, <https://doi.org/10.3389/ffgc.2022.879382>, 2022.
- Fang, H., Baret, F., Plummer, S., and Schaepman-Strub, G.: An Overview of Global Leaf Area Index (LAI): Methods, Products, Validation, and Applications, *Reviews of Geophysics*, 57, 739–799, <https://doi.org/https://doi.org/10.1029/2018RG000608>, 2019.
- Fischer, R., Bohn, F., Dantas de Paula, M., Dislich, C., Groeneveld, J., Gutiérrez, A. G., Kazmierczak, M., Knapp, N., Lehmann, S., Paulick, S., Pütz, S., Rödig, E., Taubert, F., Köhler, P., and Huth, A.: Lessons learned from applying a forest gap model to understand ecosystem and carbon dynamics of complex tropical forests, *Ecological Modelling*, 326, 124–133, <https://doi.org/https://doi.org/10.1016/j.ecolmodel.2015.11.018>, next generation ecological modelling, concepts, and theory: structural realism, emergence, and predictions, 2016.
- Foley, J. and Ramankutty, N.: A primer on the terrestrial carbon cycle: What we don't know but should, 2003.
- Francés, F., Velez, J., and Velez, J.: Split-parameter structure for the automatic calibration of distributed hydrological models, *Journal of Hydrology*, 332, 226–240, <https://doi.org/10.1016/j.jhydrol.2006.06.032>, 2007.

- Gamon, J. A.: Reviews and Syntheses: optical sampling of the flux tower footprint, *Biogeosciences*, 12, 4509–4523, <https://doi.org/10.5194/bg-12-4509-2015>, 2015.
- Gower, S. and Norman, J.: Rapid Estimation of Leaf Area Index in Conifer and Broad-Leaf Plantations, *Ecology*, 72, 1896–1900, <https://doi.org/10.2307/1940988>, 1991.
- Granier, A., Bréda, N., Biron, P., and Villette, S.: A lumped water balance model to evaluate duration and intensity of drought constraints in forest stands, *Ecological Modelling*, 116, 269–283, [https://doi.org/https://doi.org/10.1016/S0304-3800\(98\)00205-1](https://doi.org/https://doi.org/10.1016/S0304-3800(98)00205-1), 1999.
- Hidy, D., Barcza, Z., Marjanović, H., Ostrogović Sever, M. Z., Dobor, L., Gelybó, G., Fodor, N., Pintér, K., Churkina, G., Running, S., Thornton, P., Bellocchi, G., Haszpra, L., Horváth, F., Suyker, A., and Nagy, Z.: Terrestrial ecosystem process model Biome-BGCMuSo v4.0: summary of improvements and new modeling possibilities, *Geoscientific Model Development*, 9, 4405–4437, <https://doi.org/10.5194/gmd-9-4405-2016>, 2016.
- Hidy, D., Barcza, Z., Hollós, R., Dobor, L., Ács, T., Zacháry, D., Filep, T., Pásztor, L., Incze, D., Dencső, M., Tóth, E., Merganičová, K., Thornton, P., Running, S., and Fodor, N.: Soil-related developments of the Biome-BGCMuSo v6.2 terrestrial ecosystem model, *Geoscientific Model Development*, 15, 2157–2181, <https://doi.org/10.5194/gmd-15-2157-2022>, 2022.
- Hirmas, D., Giménez, D., Nemes, A., Kerry, R., Brunsell, N., and Wilson, C.: Climate-induced changes in continental-scale soil macroporosity may intensify water cycle, *Nature*, 561, <https://doi.org/10.1038/s41586-018-0463-x>, 2018.
- Huang, X., Zheng, Y., Zhang, H., Lin, S., Liang, S., Li, X., Ma, M., and Yuan, W.: High spatial resolution vegetation gross primary production product: Algorithm and validation, *Science of Remote Sensing*, 5, 100 049, <https://doi.org/https://doi.org/10.1016/j.srs.2022.100049>, 2022.
- Imadi, S., Gul, A., Dikilitas, M., Karakas, S., Sharma, I., and Ahmad, P.: Water stress: Types, causes, and impact on plant growth and development, pp. 343–355, <https://doi.org/10.1002/9781119054450.ch21>, 2016.
- Jung, M., Vetter, M., Herold, M., Churkina, G., Reichstein, M., Zaehle, S., Ciais, P., Viovy, N., Bondeau, A., Chen, Y., Trusilova, K., Feser, F., and Heimann, M.: Uncertainties of modeling gross primary productivity over Europe: A systematic study on the effects of using different drivers and terrestrial biosphere models, *Global Biogeochemical Cycles*, 21, <https://doi.org/10.1029/2006GB002915>, 2007.



- Kennedy, D., Swenson, S., Oleson, K. W., Lawrence, D. M., Fisher, R., Lola da Costa, A. C., and Gentine, P.: Implementing Plant Hydraulics in the Community Land Model, Version 5, *Journal of Advances in Modeling Earth Systems*, 11, 485–513, <https://doi.org/10.1029/2018MS001500>, 2019.
- Knohl, A. and Baldocchi, D.: Effects of diffuse radiation on canopy gas exchange processes in a forest ecosystem, *Journal of Geophysical Research, Biogeosciences*, 113, G02 023, doi:10.1029/2007JG000 663, <https://doi.org/10.1029/2007JG000663>, 2008.
- Kumar, R., Samaniego, L., and Attinger, S.: Implications of distributed hydrologic model parameterization on water fluxes at multiple scales and locations, *Water Resources Research*, 49, <https://doi.org/10.1029/2012WR012195>, 2013.
- Lal, R. and Lorenz, K.: Carbon Sequestration in Temperate Forests, pp. 187–202, <https://doi.org/10.1007/978-94-007-4159-1-9>, 2012.
- Lee, H., Park, J., Cho, S., Lee, M., and Kim, H.: Impact of leaf area index from various sources on estimating gross primary production in temperate forests using the JULES land surface model, *Agricultural and Forest Meteorology*, p. 107614, 2019.
- Li, J., Wang, Y., Duan, Q., Lu, X., Pak, B., Wiltshire, A., Robertson, E., and Ziehn, T.: Quantification and attribution of errors in the simulated annual gross primary production and latent heat fluxes by two global land surface models, *Journal of Advances in Modeling Earth Systems*, 8, <https://doi.org/10.1002/2015MS000583>, 2016.
- Monteith, J. L.: Climate and the Efficiency of Crop Production in Britain, *Philosophical Transactions of the Royal Society of London Series B*, 281, 277–294, <https://doi.org/10.1098/rstb.1977.0140>, 1977.
- Nathalie, B.: Ground-based measurements of leaf area index: A review of methods, instruments and current controversies, *Journal of experimental botany*, 54, 2403–17, <https://doi.org/10.1093/jxb/erg263>, 2003.
- Nathalie, B., Huc, R., Granier, A., and Dreyer, E.: Temperate forest trees and stands under severe drought: A review of ecophysiological responses, adaptation processes and long-term consequences, <http://dx.doi.org/10.1051/forest:2006042>, 63, <https://doi.org/10.1051/forest:2006042>, 2006.
- Pan, N., Wang, S., Wei, F., Shen, M., and Fu, B.: Inconsistent changes in NPP and LAI determined from the parabolic LAI versus NPP relationship, *Ecological Indicators*, 131, 108 134, <https://doi.org/https://doi.org/10.1016/j.ecolind.2021.108134>, 2021.

- Pan, Y., Birdsey, R., Fang, J., Houghton, R., Kauppi, P., Kurz, W., Phillips, O., Shvidenko, A., Lewis, S., Canadell, J., Ciais, P., Jackson, R., Pacala, S., McGuire, A., Piao, S., Rautiainen, A., Sitch, S., and Hayes, D.: A Large and Persistent Carbon Sink in the World's Forests, *Science* (New York, N.Y.), 333, 988–93, <https://doi.org/10.1126/science.1201609>, 2011.
- Pasquato, M., Medici, C., Friend, A., and Frances, F.: Comparing two approaches for parsimonious vegetation modelling in semiarid regions using satellite data, *ECOHYDROLOGY*, 8, 1024–1036, 2015.
- Potter, C. S., Randerson, J. T., Field, C. B., Matson, P. A., Vitousek, P. M., Mooney, H. A., and Klooster, S. A.: Terrestrial ecosystem production: A process model based on global satellite and surface data, *Global Biogeochemical Cycles*, 7, 811–841, <https://doi.org/https://doi.org/10.1029/93GB02725>, 1993.
- Prince, S. and Goward, S.: Global Primary Production: A Remote Sensing Approach, *Journal of Biogeography*, 22, 815, 1995.
- Rahman, A., Zhang, X., Houser, P., Sauer, T., and Maggioni, V.: Global Assimilation of Remotely Sensed Leaf Area Index: The Impact of Updating More State Variables Within a Land Surface Model, *Frontiers in Water*, 3, 789 352, <https://doi.org/10.3389/frwa.2021.789352>, 2022.
- Reinmann, A. B. and Hutrya, L. R.: Edge effects enhance carbon uptake and its vulnerability to climate change in temperate broadleaf forests, *Proceedings of the National Academy of Sciences*, 114, 107–112, <https://doi.org/10.1073/pnas.1612369114>, 2017.
- Running, S., Nemani, R., Heinsch, F., Zhao, M., Reeves, M., and Hashimoto, H.: A Continuous Satellite-Derived Measure of Global Terrestrial Primary Production, *BioScience*, 54, 547–560, [https://doi.org/10.1641/0006-3568\(2004\)054\[0547:ACSMOG\]2.0.CO;2](https://doi.org/10.1641/0006-3568(2004)054[0547:ACSMOG]2.0.CO;2), 2004.
- Running, S. W., Thornton, P. E., Nemani, R., and Glassy, J. M.: Global Terrestrial Gross and Net Primary Productivity from the Earth Observing System, pp. 44–57, Springer New York, New York, NY, <https://doi.org/10.1007/978-1-4612-1224-9-4>, 2000.
- Samaniego, L., Kumar, R., and Attinger, S.: Multiscale parameter regionalization of a grid-based hydrologic model at the mesoscale, *Water Resources Research*, 46, <https://doi.org/https://doi.org/10.1029/2008WR007327>, 2010.
- Schaefer, K., Schwalm, C. R., Williams, C., Arain, M. A., Barr, A., Chen, J. M., Davis, K. J., Dimitrov, D., Hilton, T. W., Hollinger, D. Y., Humphreys, E., Poulter, B., Raczka,

- B. M., Richardson, A. D., Sahoo, A., Thornton, P., Vargas, R., Verbeeck, H., Anderson, R., Baker, I., Black, T. A., Bolstad, P., Chen, J., Curtis, P. S., Desai, A. R., Dietze, M., Dragoni, D., Gough, C., Grant, R. F., Gu, L., Jain, A., Kucharik, C., Law, B., Liu, S., Lokipitiya, E., Margolis, H. A., Matamala, R., McCaughey, J. H., Monson, R., Munger, J. W., Oechel, W., Peng, C., Price, D. T., Ricciuto, D., Riley, W. J., Roulet, N., Tian, H., Tonitto, C., Torn, M., Weng, E., and Zhou, X.: A model-data comparison of gross primary productivity: Results from the North American Carbon Program site synthesis, *Journal of Geophysical Research: Biogeosciences*, 117, <https://doi.org/https://doi.org/10.1029/2012JG001960>, 2012.
- Schweppe, R., Thober, S., Kelbling, M., Kumar, R., Attinger, S., and Samaniego, L.: MPR 1.0: A stand-alone Multiscale Parameter Regionalization Tool for Improved Parameter Estimation of Land Surface Models, *Geoscientific Model Development Discussions*, 2021, 1–40, <https://doi.org/10.5194/gmd-2021-103>, 2021.
- Seo, H. and Kim, Y.: Role of remotely sensed leaf area index assimilation in eco-hydrologic processes in different ecosystems over East Asia with Community Land Model version 4.5 – Biogeochemistry, *Journal of Hydrology*, 594, 125 957, <https://doi.org/https://doi.org/10.1016/j.jhydrol.2021.125957>, 2021.
- Spielmann, F. M., Wohlfahrt, G., Hammerle, A., Kitz, F., Migliavacca, M., Alberti, G., Ibrom, A., El-Madany, T. S., Gerdel, K., Moreno, G., Kolle, O., Karl, T., Peressotti, A., and Delle Vedove, G.: Gross Primary Productivity of Four European Ecosystems Constrained by Joint CO<sub>2</sub> and COS Flux Measurements, *Geophysical Research Letters*, 46, 5284–5293, <https://doi.org/https://doi.org/10.1029/2019GL082006>, 2019.
- Springer, K., Wang, R., and Gamon, J.: Parallel Seasonal Patterns of Photosynthesis, Fluorescence, and Reflectance Indices in Boreal Trees, *Remote Sensing*, 9, 691, <https://doi.org/10.3390/rs9070691>, 2017.
- Turner, D., RITTS, W., STYLES, J., YANG, Z., COHEN, W., Law, B., and THORNTON, P.: A diagnostic carbon flux model to monitor the effects of disturbance and interannual variation in climate on regional NEP, *Tellus B*, 58, 476 – 490, <https://doi.org/10.1111/j.1600-0889.2006.00221.x>, 2006.
- Van Looy, K., Bouma, J., Herbst, M., Koestel, J., Minasny, B., Mishra, U., Montzka, C., Nemes, A., Pachepsky, Y. A., Padarian, J., Schaap, M. G., Tóth, B., Verhoef, A., Vanderborght, J., van der Ploeg, M. J., Weihermüller, L., Zacharias, S., Zhang, Y., and Vereecken, H.: Pedotransfer Functions in Earth System Science: Challenges and Perspectives, *Reviews of Geophysics*, 55, 1199–1256, <https://doi.org/https://doi.org/10.1002/2017RG000581>, 2017.

- Vargas, R., Sonnentag, O., Abramowitz, G., Carrara, A., Chen, J., Ciais, P., Correia, A., Keenan, T., Kobayashi, H., Ourcival, J., Papale, D., Pearson, D., Pereira, J., Piao, S., Rambal, S., and Baldocchi, D.: Drought Influences the Accuracy of Simulated Ecosystem Fluxes: A Model-Data Meta-analysis for Mediterranean Oak Woodlands, *Ecosystems*, 16, 749–764, <https://doi.org/10.1007/s10021-013-9648-1>, 2013.
- Xiao, X., Zhang, Q., Braswell, B., Urbanski, S., Boles, S., Wofsy, S., Moore, B., and Ojima, D.: Modeling gross primary production of temperate deciduous broadleaf forest using satellite images and climate data, *Remote Sensing of Environment*, 91, 256–270, <https://doi.org/10.1016/j.rse.2004.03.010>, 2004.
- Xin, Q., Dai, Y., and Liu, X.: A simple time-stepping scheme to simulate leaf area index, phenology, and gross primary production across deciduous broadleaf forests in the eastern United States, *Biogeosciences*, 16, 467–484, <https://doi.org/10.5194/bg-16-467-2019>, 2019.
- Yuan, W., Liu, S., Zhou, G., Zhou, G., Tieszen, L., Baldocchi, D., Bernhofer, C., Gholz, H., Goldstein, A., Goulden, M., Hollinger, D., Hu, Y., Law, B., Stoy, P., Vesala, T., and Wofsy, S.: Deriving a light use efficiency model from eddy covariance flux data for predicting daily gross primary production across biomes, *Agricultural and Forest Meteorology*, 143, 189–207, <https://doi.org/10.1016/j.agrformet.2006.12.001>, 2007.
- Yuan, W., Cai, W., Xia, J., Chen, J., Liu, S., Dong, W., Merbold, L., Law, B., Arain, A., Beringer, J., Bernhofer, C., Black, A., Blanken, P. D., Cescatti, A., Chen, Y., Francois, L., Gianelle, D., Janssens, I. A., Jung, M., Kato, T., Kiely, G., Liu, D., Marcolla, B., Montagnani, L., Raschi, A., Rouspard, O., Varlagin, A., and Wohlfahrt, G.: Global comparison of light use efficiency models for simulating terrestrial vegetation gross primary production based on the LaThuile database, *Agricultural and Forest Meteorology*, 192–193, 108–120, <https://doi.org/10.1016/j.agrformet.2014.03.007>, 2014.
- Yue, X. and Unger, N.: The Yale Interactive terrestrial Biosphere model version 1.0: description, evaluation and implementation into NASA GISS ModelE2, *Geoscientific Model Development*, 8, 2399–2417, <https://doi.org/10.5194/gmd-8-2399-2015>, 2015.
- Zhang, L., Zhou, D., Fan, J.-W., and Hu, Z.: Comparison of four light use efficiency models for estimating terrestrial gross primary production, *Ecological Modelling*, 300, 30–39, <https://doi.org/10.1016/j.ecolmodel.2015.01.001>, 2015.
- Zhou, H., Yue, X., Lei, Y., Tian, C., Ma, Y., and Cao, Y.: Large Contributions of Diffuse Radiation to Global Gross Primary Productivity During 1981–2015, *Global Biogeochemical Cycles*, 35, <https://doi.org/10.1029/2021GB006957>, 2021.

# Developing a Parsimonious Canopy Model (PCM v1.0) to Predict Forest Gross Primary Productivity and Leaf Area Index on deciduous broad-leaved forest

Bahar Bahrami <sup>\*1</sup>, Anke Hildebrandt<sup>1,2</sup>, Stephan Thober<sup>1</sup>, Corinna Rebmann<sup>1</sup>, Rico Fischer<sup>3</sup>, Luis Samaniego<sup>1</sup>, Oldrich Rakovec<sup>1,4</sup>, and Rohini Kumar<sup>1</sup>

<sup>1</sup> Department of Computational Hydro-system, Helmholtz Centre for Environmental Research-UFZ, Leipzig, Germany

<sup>2</sup> Friedrich Schiller University Jena, Institute of Geoscience, Terrestrial Ecohydrology, Burgweg 11, 07745 Jena, Germany

<sup>3</sup> Department of Ecological Modelling, Helmholtz Centre for Environmental Research-UFZ, Leipzig, Germany

<sup>4</sup> Faculty of Environmental Sciences, Czech University of Life Sciences Prague, Praha-Suchbát 16500, Czech Republic

**Correspondence:** Bahar Bahrami (bahareh.bahrami@ufz.de)

**Abstract.** Temperate forest ecosystems play a crucial role in governing global carbon and water cycles. However, unprecedented global warming poses fundamental alterations to forest ecological functions (e.g., carbon uptake) and forest biophysical variables (e.g., leaf area index). Quantification of forest carbon uptake, gross primary productivity (GPP), as the largest carbon flux has a direct consequence on carbon budget estimations. Part of this assimilated carbon stored in leaf biomass is related to the leaf area index (LAI), which is of critical significance in and closely linked to the water cycle. There already exist a number of models to simulate dynamics of LAI and GPP, however, the level of complexity, demanding data, and poorly known parameters often prohibit the model applicability over data-sparse and large domains. In addition, the complex mechanism associated with coupling the terrestrial carbon and water cycles poses a major challenge for integrated assessments of interlinked processes (e.g., accounting for temporal ~~dynamic~~ dynamics of LAI for improving water balance estimations and soil moisture availability for enhancing carbon balance estimations). In this study, we propose a parsimonious forest canopy model (PCM) to predict daily dynamics of LAI and GPP with few required input which is also suitable for integration into state-of-the-art hydrologic models. The light use efficiency (LUE) concept is central to PCM (v1.0), coupled with a phenology submodel. PCM estimates total assimilated carbon based on conversion efficiency of absorbed photosynthetically active radiation into biomass. Equipped with the coupled phenology submodel, the total assimilated carbon partly converts to leaf biomass from which prognostic and temperature-driven LAI is simulated. The model combines modules for estimation of soil hydraulic parameters based on ~~the so-called~~ pedotransfer functions and vertically weighted soil moisture considering the underground root distribution, when soil moisture data is available. We test the model on deciduous broad-leaved forest sites in Europe and North America selected from the FLUXNET network. We analyze the model parameter sensitivity on the resulting GPP and LAI and identified on average 10 common sensitive parameters at each study site (e.g., LUE, SLA, etc). Model performance is evaluated in a ~~verification~~ validation period using in situ measurements of GPP and LAI (when available) at eddy covariance flux towers. The model adequately captures the daily dynamics of observed GPP and LAI at each study site (Kling-Gupta-Efficiency; KGE

\*Corresponding author (bahareh.bahrami@ufz.de)

varies between 0.79 and 0.92). Finally, we investigate the cross-location transferability of model parameters and derive a compromise parameter set to be used across different sites. The model also showed robustness with the compromise single set of parameters, applicable to different sites, with an acceptable loss in model skill (on average  $\pm 8\%$ ). Overall, in addition to the satisfactory performance of the PCM as a stand-alone canopy model, the parsimonious and modular structure of the developed PCM allows for a smooth incorporation of carbon modules to existing hydrologic models. Thereby, it facilitates the seamless representation of coupled water and carbon cycle components, i.e. prognostic simulated vegetation leaf area index (LAI) would improve the representation of the water cycle components (e.g.i.e., evapotranspiration), while GPP predictions would benefit from simulated soil water storage from a hydrologic model.

## 1 Introduction

As the climate ~~is changing~~changes, the future functionality and resilience of terrestrial ecosystems are expected to change in numerous ways. Fundamentally, terrestrial ecosystems (such as temperate forests) drive the life-sustaining exchanges of matter and energy between land and atmosphere (e.g., carbon dioxide / water vapor exchange). However, increased concentrations of greenhouse gases and projected global warming (IPCC, 2021), contribute to unprecedented extreme climate events and changes in ecosystem functioning and productivity (Malhi et al., 2020). ~~Depending on the frequency and intensity of extreme events together with other aspects of anthropogenic change, ecosystem patterns and processes such as~~ This affects forest ecosystems by altering growth, timing of life cycle events (Nigatu, 2019), carbon dioxide uptake, and water vapour release can be altered, potentially irreversibly (Grimm et al., 2013). Given the importance of carbon dioxide as a principal greenhouse gas that drives global climate change and the extent to which ecosystems are capable of sequestering it, there has been growing attention toward the quantification of carbon fluxes/stocks and understanding the role of the terrestrial ecosystems in regulating the exchange of carbon between land and atmosphere (Beer et al., 2010) rates (Luyssaert et al., 2007; Senf et al., 2018; Forzieri et al., 2021) among other climate-related disturbances. Vulnerability due to climate change can be attributed to different ecosystem stresses (Nathalie et al., 2006; Cholet et al., 2022) including high temperatures that decrease enzymes activity and the rate of carbon uptake as well as soil water limitation causing hydraulic failure or carbon starvation, reducing plant photosynthetic capacity, and early senescence (Imadi et al., 2016) in temperate forest ecosystems. In addition to these stresses, some environmental changes such as radiation change associated with increased cloudiness or atmospheric aerosols can also increase plant productivity, e.g. due to the increased fraction of diffused radiation (Knohl and Baldocchi, 2008). Temperate forest ecosystems, including deciduous broad-leaved forest (DBF), ~~are known as an integral part of global carbon cycle and contribute to climate change mitigation~~ play an indispensable role in mitigating climate change (Estoque et al., 2022) by removing carbon from the atmosphere (Reinmann and Hutya, 2017). Forests (Pan et al., 2011; Reinmann and Hutya, 2017). Generally, forests are recognized as biomes with high carbon sequestration capacity (Lal and Lorenz, 2012) equivalent to around where temperate broad-leaved forest contribute to approximately 60% of the global net forest sink (Reinmann and Hutya, 2017). The total carbon uptake from the atmosphere into the ecosystems by plant photosynthesis is known as vegetation gross primary production (GPP). GPP is the largest flux within the carbon cycle (Schaefer et al., 2012; Foley and Ramankutty, 2003) and has a direct

55 ~~effect on moderating climate and environment by sequestering anthropogenically emitted CO<sub>2</sub>. In turn, these ecosystems are~~  
~~also vulnerable to the adverse effects of changing climate (Luyssaert et al., 2007; Senf et al., 2018; Forzieri et al., 2021) where~~  
~~the spatial pattern of vulnerability is controlled by environmental conditions (Forzieri et al., 2021). Specifically, environmental~~  
~~constraints, such as temperature, water availability, and radiation control vegetation productivity and regulate the rate of GPP~~  
~~(Yuan et al., 2014). The carbon sink of forests (Pan et al., 2011; Reinmann and Hutya, 2017). Temperate DBF biomes are~~  
 60 ~~characterized by favourable climate in having a temperate climate with~~ four distinct seasons ~~with and~~ a temperature-driven  
~~canopy structure. The plant canopy capacity and seasonality are expressed by leaf for water and carbon exchange is strongly~~  
~~related to seasonal variation in leaf development (Seo and Kim, 2021). Leaf area index (LAI) (Wang et al., 2019). The LAI~~  
~~is defined as one half the total green leaf area is a dimensionless quantity, defined as one-sided area of green leaf per unit~~  
~~horizontal ground surface area (Nathalie, 2003; Fang et al., 2019). LAI can be estimated by field measurements and either by~~  
 65 ~~direct field measurements, inferred using remote sensing or be simulated by the fractional accumulated carbon stored in the leaf~~  
~~pool within vegetation carbon cycle models (Fang et al., 2019). Water availability plays a key role in carbon uptake and leaf~~  
~~development, affecting the carbon cycle. This In addition, LAI is a key biophysical plant variable affects not only sequestering,~~  
~~representing vegetation state, affecting not only the sequestration of carbon from the atmosphere via photosynthesis but also the~~  
~~release of water to the atmosphere through transpiration (Yang et al., 2017). However, accounting for a dynamic representation~~  
 70 ~~of vegetation characteristics (e.g., leaf area index) relevant (Fang et al., 2019). Therefore, in hydrologic models considering~~  
~~carbon cycle components (such as dynamic LAI related to the leaf carbon pool) are crucial for accurate estimation of water~~  
~~balance components (e.g., plant transpiration) in most of conceptual hydrologic models is not properly considered, especially~~  
~~for the assessment of climate change impacts on water balance components (Wegehenkel, 2009; Asaadi et al., 2018). the water~~  
~~budget.~~

75 Given the importance of carbon dioxide as a principal greenhouse gas that drives global climate change and the extent to  
which ecosystems are capable of sequestering it, there has been growing attention toward the quantification of carbon fluxes and  
pools and understanding the role of terrestrial ecosystems, including DBF ecosystems, in regulating the exchange of carbon  
between land and atmosphere (Beer et al., 2010). The total carbon uptake from the atmosphere into vegetated ecosystems  
by plant photosynthesis is known as gross primary production (GPP). GPP is the primary driver of the land carbon sink  
 80 (Spielmann et al., 2019; Zhou et al., 2021) and the largest flux within the carbon cycle (Schaefer et al., 2012; Foley and Ramankutty, 2003)  
. Accurate estimation of GPP directly influences carbon budget assessments as well as estimates of the amount of stored  
carbon in the plant leaf pool. Accurate carbon budget assessment, in turn, promotes understanding of the feedbacks between  
the terrestrial biosphere and the climate system (Zhou et al., 2021; Huang et al., 2022).

Many models have been successfully developed to estimate GPP, spanning a range of complexity and representation of  
 85 physical and biological processes (Che et al., 2014; Arora, 2002; Ostle et al., 2009). ~~The~~ GPP models are generally divided  
 into three categories ~~of including~~ empirical, enzyme kinetic (EK), and light use efficiency (LUE) models (Schaefer et al., 2012).  
~~The In~~ first category, ~~the~~ empirical models, are data-oriented approaches where statistical relationships between inferred GPP  
 from flux observations (eddy ~~covariance–EC~~ covariance–EC) and observed environmental conditions are established; ~~and those~~  
~~Those~~ inferred relationships are then expanded ~~to into~~ large scales ranging from regional to global levels (Beer et al., 2010;

Schaefer et al., 2012). The second category, the enzyme kinetic (EK) approach, represents leaf scale GPP as a result of a complex set of biophysical and biochemical reactions. This includes first, the light reaction (in which light energy splits water molecules, travelling from the soil to leaf chloroplasts, into O<sub>2</sub>, electrons, and H<sup>+</sup> to produce electron carrier molecule (the reduced form of nicotinic adenine dinucleotide phosphoric acid; NADPH) and energy storage (adenosine triphosphate; ATP). ~~Later, in the next step for dark reaction (Calvin cycle)~~ In the dark reactions of the Calvin cycle, the rubisco enzyme uses ~~the~~ ATP energy from the light response to ~~sequester the atmospheric CO<sub>2</sub>~~ sequester the atmospheric carbon dioxide into organic carbon (Farquhar et al., 1980; Collatz et al., 1992). This approach requires the specification of a relatively large number of parameters for governing processes, ~~whose acquisition (through direct measurements) is not straightforward – specifically at scales larger than the leaf level~~. Finally, the last category for the GPP estimation is a widely used approach based on the light use efficiency (LUE) concept, relevant for its applications over larger scales ~~at (regional and global)~~ (Potter et al., 1993; Yuan et al., 2007). By implementing simplified relationships that hold at the ecosystem level and avoiding a detailed parameterization of leaf-level processes, the LUE concept is particularly relevant for quantifying the carbon budget at landscape and larger scales (Street et al., 2007; Wei et al., 2017) and coupling with the hydrologic models (Street et al., 2007; Wei et al., 2017). In this approach, ecosystem GPP is ~~related to a function of~~ absorbed photosynthetically active radiation (APAR) ~~as a and a biome specific LUE parameter (Gamon, 2015; Springer et al., 2017)~~ APAR is a product of incident photosynthetically active radiation (PAR) ~~by a and the~~ fraction of PAR (fPAR) absorbed by plant leaves ~~through a biome specific LUE parameter~~. The LUE ~~is a parameter corresponds to the~~ vegetation conversion efficiency ~~factor of absorbed of solar~~ radiation into biomass and is defined as the amount of carbon produced per unit of absorbed PAR (~~Yuan et al., 2014~~) (Monteith, 1977; Yuan et al., 2014). The amount of ~~sequestered sequestered~~ carbon as biomass will then be allocated to different plant carbon pools (i.e. leaf, stems, and roots) controlled by the relative demand exerted by these pools at different periods (Arora, 2002).

Several LUE models have been successfully applied for estimating the ecosystem GPP ~~such as, CFLUX (Turner et al., 2006), EC-LUE (Yuan et al., 2007), MODIS-GPP (Running et al., 2004), VPM (Xiao et al., 2004), and CASA (Potter et al., 1993) at different spatial and temporal scales (Wei et al., 2017; Law et al., 2000; Coops et al., 2005)~~ at different spatial and temporal scales (Law et al., 2000; Coops et al., 2005; Wei et al., 2017) such as the carbon cycle model (CFLUX; Turner et al., 2006), eddy covariance-light use efficiency (EC-LUE; Yuan et al., 2007), moderate resolution imaging spectroradiometer-gross primary production (MODIS-GPP; Running et al., 2004), vegetation photosynthesis model (VPM; Xiao et al., 2004), and the Carnegie-Ames-Stanford Approach (CASA; Potter et al., 1993). However, despite the large potential of these LUE models, they are highly dependent on satellite-based ~~data observations~~ such as remotely sensed LAI and fPAR (Wang et al., 2017). These two key biophysical variables are generally sensitive to cloud contamination (~~Chen et al., 2019; Zhu et al., 2013~~) leading to leading to gaps in their temporal and spatial ~~gaps, particularly over areas like central Europe. It has also been documented that the coverage throughout the year (Rahman et al., 2022). These gaps are sources of uncertainty in~~ satellite-based fPAR and LAI products ~~are subjected to uncertainty, and that which, in turn,~~ may induce errors in quantifying GPP (~~Wang et al., 2017~~). Overall, several (Rahman et al., 2022).

Several factors, including either high demand of required data and computation in ~~detailed models~~ the detailed biogeochemical model (e.g., EK models) or dependency of existing simplified LUE models on satellite data ~~might hinder the application in~~



125 ~~simulating GPP and /or LAI hinders the coupling~~ of existing models ~~Concerning estimation of LAI and its impact on water~~  
~~balance, the utilization of carbon uptake and leaf biomass growth has been used~~ with hydrologic models. Currently, within most  
of the conceptual hydrologic models dynamic vegetation characteristics and LAI are not properly considered. As mentioned  
earlier, such a representation is relevant for accurate estimation of water balance components (i.e., plant transpiration and  
canopy evaporation), and especially for the assessment of climate change impacts on the water cycle (Wegehenkel, 2009; Asaadi et al., 2018)

130 ~

The LUE principle and leaf growth have been successfully implemented in the TETIS-VEG ecohydrology model (Francés  
et al., 2007; Pasquato et al., 2015). The TETIS-VEG model is ~~however adapted for the evergreen forest, thus it is not applicable~~  
~~over deciduous~~, however, adapted for evergreen forest biome. In other words, the TETIS-VEG model lacks representation  
of a dynamic leaf phenology relevant in the deciduous broad-leaved ~~forest with a distinct seasonal leaf development dynamic~~  
135 ~~forests~~. Another approach to simulate GPP and LAI is adopted in ~~the~~ simplified growing production day time-stepping scheme  
(SGPD-TS) model (Xin et al., 2019). The SGPD-TS model, however, does not ~~use the leaf biomass growth concept, rather~~  
~~it represent leaf growth and allocation to leaf pool, but~~ establishes a linear relationship between steady-state GPP and LAI.  
In this way, GPP is used as a proxy of LAI, ~~utilising~~ ~~utilizing~~ a conversion ratio when maximum GPP has been reached.  
However, it has been shown that ~~modelled simulated~~ GPP saturates at high LAI values (~~Lee et al., 2019~~) (e.g., above  $4.5\text{ m}^2\text{m}^{-2}$ )  
140 (~~Lee et al., 2019~~) and (~~Pan et al., 2021~~). High LAI values are often common in deciduous broad-leaved forests, thus, relying  
on maximum GPP to derive LAI might introduce a bias at elevated LAI. ~~This may potentially introduce uncertainty when~~  
~~calculating the conversion ratio to simulate LAI~~. Another more general challenging aspect for these models is the ~~specification~~  
~~of effective model parameters such that they can seamlessly operate at different scales and locations~~ ~~identification of model~~  
~~parameters that are site or location specific~~. Previous applications ~~often have~~ ~~have often~~ been limited to ~~a one~~ calibration site  
145 (Francés et al., 2007); but they need to be thoroughly cross-validated for their applicability across a diverse range of climatic  
conditions. ~~The overarching aim~~

~~The overarching aims~~ of this study are to propose a parsimonious model (i) to simulate daily dynamics of GPP and LAI  
~~over of~~ deciduous broad-leaved forest at a medium level of complexity (ii) also suitable for integration in existing hydrologic  
and ecologic models. We simulate processes related to the carbon cycle in the canopy at a forest stand of undetermined size,  
150 ~~utilizing using~~ the LUE approach with implementation of a phenology submodel. The parsimonious approach and level of  
model complexity are ~~adapted based on~~ ~~designed to make use of a~~ readily available observational ~~datasets~~ ~~dataset~~ for abiotic  
~~forcing~~ across eddy flux tower stations ~~such as air temperature, vapour pressure deficit, soil moisture, and photosynthetic~~  
~~photon flux density~~. We apply a global sensitivity analysis to investigate model parameters' sensitivity to the model's output  
variables (i.e., GPP and LAI). Finally, we assess the generality and robustness of the underlying model parameterizations and  
155 demonstrate the model applicability over different sites conducting a cross-location transferability experiment.

## 2 Methodology

### 2.1 Model overview

The PCM model developed and presented in this study aims at providing a parsimonious representation of daily development of biomass of leaf (Bl) coupled to simulated gross primary productivity (GPP) over deciduous broad-leaved forest (DBF) ecosystems. Analogous to most of the LUE models treating the entire vegetation canopy as a big extended leaf (Guan et al., 2021), the PCM operates over forest stand scale and adapts parameters mainly from a biome properties look-up table (BPLUT) (Running et al., 2000). Parameters such as specific leaf area index (~~SLA~~SLA) in PCM represent an effective community-weighted parameters. Figure 1 shows a schematic representation of the PCM structure including carbon fluxes/stocks and interconnected processes related to plant canopy for DBF biomes. We focus on simulating Bl, which is related to LAI via the specific leaf area index parameter. The simulated LAI is, in turn, used in the calculation of the GPP.

PCM uses a daily time step during which it simulates the processes of carbon uptake, leaf respiration, carbon allocation, and carbon decay from the leaf pool (canopy) using a mass balance equation (Istanbulluoglu et al., 2012; Yue and Unger, 2015; Pasquato et al., 2015; Melton and Arora, 2016; Ruiz-Perez et al., 2017). The main governing equation to simulate the daily development of GPP(t) and Bl(t) is:

$$\frac{dBl(t)}{dt} = (GPP(t) - R_e(t))\lambda(t) - D(t) \quad (1)$$

where Bl(t) is leaf biomass, GPP(t) is gross primary productivity,  $R_e(t)$  is leaf respiration,  $\lambda(t)$  is carbon allocation coefficient and D(t) is leaf decay components at day t. All terms on the right hand side are calculated in the modules of the PCM. The LAI (related to Bl(t) in Eq. 1) is defined as:

$$LAI(t) = Bl(t) \cdot SLA \cdot f_{cov} \quad (2)$$

where SLA is specific leaf area index, and  $f_{cov}$  is the vegetation fractional coverage. In the following sections, the modeling approaches implemented for each submodel component are described in detail. A summary of the model inputs and underlying parameters is provided in Tables 2 and 3, respectively.

#### 2.1.1 Gross Primary Productivity

The theoretical soundness and practical convenience of the ~~LUE~~LUE concept in estimating terrestrial GPP has been the main core of several model developments (Monteith, 1972; Wei et al., 2017; Running et al., 2000; Arora, 2002; Schaefer et al., 2012; Zhang et al., 2015) at the regional and global scales (Potter et al., 1993; Yuan et al., 2007; Xiao et al., 2004; Running et al., 2000). In this study, we likewise utilize the LUE approach, which theoretically relies on the concept of interception of photosynthetically active radiation by plant leaves and converting ~~it~~the intercepted radiation into biomass through energy to biomass efficiency factor (i.e. ~~LUE~~LUE factor). As expressed in Eq. 1, the PCM simulation starts with assimilation of the carbon flux (GPP) by leaf component. The GPP flux (Eq. 3) is estimated as a product of incident photosynthetically active radiation (PAR), by fPAR, which is a fraction of PAR being absorbed by plant leaf, and an ~~LUE~~LUE factor, multiplied by a

modifier factor when environmental constraints present ( $\epsilon$ ).

$$GPP(t) = LUE \cdot \epsilon(t) \cdot PAR(t) \cdot fPAR(t) \quad (3)$$

Where  $LUE$  is biome-specific unstressed (or maximum) vegetation light use efficiency parameter.  $fPAR$  is calculated as following (Ruimy et al., 1999; Xiao et al., 2004; Wu, 2012; Yuan et al., 2007) (Ruimy et al., 1999; Xiao et al., 2004; Yuan et al., 2007) :

$$fPAR(t) = c \cdot (1 - e^{-(k \cdot LAI(t))}) \quad (4)$$

where  $c$  refers to maximum absorption at full light interception in deciduous broad-leaved forest biomes (Monsi and Saeki, 1953; Ruimy et al., 1994) and  $k$  is the light extinction coefficient parameter.

$\epsilon$  (Eq. 4.3) is an overall and integrated modifier that corresponds to environmental stress factors. The overall modifier factor diminishes light use efficiency of vegetation from its potential value during unfavorable environmental conditions (Potter et al., 1993). These unfavorable conditions include for example high and/or low temperature  $fT$ , water availability  $fSM$ , and elevated vapor pressure deficit  $fVPD$  stress factors (Zhang et al., 2015; Pasquato et al., 2015).

In general, calculation of  $\epsilon$  across different ~~LUE~~LUE models can be expressed either in minimum (Eq. 5) or multiplicative (Eq. 6) approaches to integrate different environmental stress factors. On the one hand, models such as Eddy Covariance-Light Use Efficiency (EC-LUE; (Yuan et al., 2007)) uses Liebig law of minimum stress that emphasise the most limiting resource to constrain GPP (Eq.5). On the other hand models such as Carnegie-Ames-Stanford Approach (CASA; (Potter et al., 1993)) and Vegetation Photosynthesis Model (VPM; (Xiao et al., 2004)) follow a multiplicative approach of stresses (Eq.6). In the present study, we opt for the first approach to integrate different stress factors and to calculate the  $\epsilon$ .

The first approach (minimum) is expressed as follows (Running et al., 2000; Sitch et al., 2003; Prince and Goward, 1995).

$$\epsilon(t) = \min(fT(t), fVPD(t), fSM(t)) \quad (5)$$

The second approach can be written in a multiplicative way as:

$$\epsilon(t) = fT(t) \cdot fVPD(t) \cdot fSM(t) \quad (6)$$

The individual stress factors are dimensionless scalars ranging between zero (full stress) and one (no stress), and are introduced in more detail in the following section.

### 2.1.2 Environmental constrains and GPP

**I) Temperature stress factor ( $fT$ ):** The first reduction factor,  $fT$ , on GPP due to air temperature is calculated by including two factors corresponding to low temperature  $\rho_l$  (cold) and high temperature  $\rho_h$  (heat) stress effects (Eqs. 7,8,9) (Sitch et al., 2003; Fischer et al., 2016; Rödiger et al., 2017).

$$fT(t) = \rho_l(t) \cdot \rho_h(t) \quad (7)$$

The stress induced by the cold stress factor ( $\rho_l(t)$ ) can be calculated as:

$$\rho_l = (1 + e^{k_0 \cdot (k_1 - T(t))})^{-1}, \quad (8)$$

where,

$$k_0 = \frac{2 \ln(0.01/0.99)}{(T_{low} - T_{cold})}, k_1 = 0.5(T_{low} + T_{cold})$$

220

The heat stress factor is calculated as:

$$\rho_h(t) = 1 - 0.01 \cdot e^{k_2 \cdot (T(t) - T_{hot})}, \quad (9)$$

$$k_2 = \frac{\ln(0.99/0.01)}{(T_{high} - T_{hot})}$$

225

where  $T(t)$  is daily mean air temperature,  $T_{low}$  and  $T_{high}$  are DBF biome-specific parameters representing high and low temperature limits for  $CO_2$  assimilation, respectively.  $T_{hot}$  and  $T_{cold}$  are the monthly mean air temperature of the warmest and coldest months, respectively, that a DBF biome can cope with, respectively (Boons-Prins, 2010; Bohn et al., 2014; Fischer et al., 2016; Rödig et al., 2017).

**II) Vapour Pressure Deficit stress factor (fVPD):** The canopy photosynthesis rate is strongly related to changes of in vapour pressure deficit (VPD) (Konings et al., 2017; Xin et al., 2019), as photosynthesis declines due to stomata closure (Yuan et al., 2019) when atmospheric VPD increases. It can be modelled as follows in Eq. 10 (Jolly et al., 2005):

$$fVPD(t) = \max \left( \min \left( 1 - \frac{VPD(t) - v_{min}}{v_{max} - v_{min}}, 1 \right), 0 \right) \quad (10)$$

where  $VPD(t)$  is daily vapour pressure deficit,  $v_{min}$  and  $v_{max}$  denote lower and upper thresholds for photosynthetic activities, respectively. The fVPD value of one indicates no stress on GPP, whereas there is full stress when the fVPD becomes zero; values between zero and one result in partial and linear reduction on the GPP.

**III) Soil Moisture stress factor (fSM):** In general, the impact of soil water deficit on photosynthesis in vegetation models is represented as a generic soil moisture stress function using either modeled or field observation soil moisture content (Cox et al., 1999; Granier et al., 2000; Fischer et al., 2016). Here, we use field observations from different vertical soil profiles including volumetric soil moisture content and soil textural properties (wherever available) to calculate the soil moisture stress factor, fSM.

Essentially, the soil moisture influence on plant productivity depends not only on soil moisture over the entire profile but also on the available soil water to the plant roots. Therefore, to estimate the availability of water to plants, the characteristics of the root system, including rooting depths and its distribution at different soil depths, are essential factors to be considered (Ostle et al., 2009). Thus, we include plant rooting distribution in our analysis, following Jackson et al. (1996), to take into account the root fraction at different soil depths, and weight the soil moisture content layer-wise according to the present fraction of roots in that layer. In doing so, we calculated cumulative root fraction ( $R_{c_i}$ ) from the surface to a certain depth ( $d$ ) in the soil profile for each layer ( $i$ ) using the biome specific parameter,  $\beta$  as follows (Eq. 11) (Jackson et al., 1996):

$$R_{c_i} = 1 - \beta^{d_i} \quad (11)$$

Then, ~~using the cumulative root fraction up to each layer, the~~ to estimate the root fractions in each layer fraction in each individual layer ( $R_i$  are estimated and then (Eq. 12), we use the calculated cumulative root fraction up to each layer subtracted from the corresponding fraction of the previous layer (see Eq. 11). Next,  $R_i$  is multiplied with the corresponding observed soil moisture content of that layer to calculate the soil moisture contribution from each layer individually ~~-(Eq. 13).~~ Later, by summing up the soil moisture contributions from all individual layers ( $\theta_i$ ), a daily effective soil moisture content,  $\theta(t)$ , over the soil column is obtained (Eq. 12-14).

$$R_i = R_c - R_{c_{i-1}} \quad (12)$$

$$\theta_i = \theta_i \cdot R_i \quad (13)$$

$$\theta(t) = \Sigma(\theta_i) \quad (14)$$

Similarly to other stress terms, the soil moisture stress factor varies between 0 and 1; and is quantified as follows (Eq. 15).

$$fSM(t) = \max \left( \min \left( \frac{\theta(t) - \theta_r}{\theta_{MSW} - \theta_r}, 1 \right), 0 \right) \quad (15)$$

where  $\theta(t)$  is daily effective soil moisture,  $\theta_r$  and  $\theta_{MSW}$  are water storage corresponding to the permanent wilting point and the critical point below which transpiration is limited, respectively.  $\theta_{MSW}$ , representing minimum soil water content for unstressed photosynthesis (Hartge, 1980; Granier et al., 1999; Fischer et al., 2014), is calculated as follows:

$$\theta_{MSW} = \theta_r + scw \cdot (\theta_s - \theta_r) \quad (16)$$

where  $\theta_s$  is soil water content at field capacity, ~~sew- $scw$~~  is a constant threshold commonly set at 0.4, and a calibration parameter in PCM. ~~sew- $scw$~~  is a physiological threshold defined as critical relative soil water content at which tree transpiration begins to decrease Granier et al. (1999). According to ~~Granier et al. (1999); Fischer et al. (2016) the sew~~ Granier et al. (1999) and Fischer et al. (2016) the  $scw$  value does not vary significantly between soil and plant species and can be considered as a constant value. The  $\theta_r$  and  $\theta_s$  correspond to soil matric potentials of -1.5 and -0.033 MPa, respectively.

When the daily effective soil moisture content is above a minimum soil water content ( $\theta_{MSW}$ ; Eq. 16), there is no stress to limit photosynthesis, while below the  $\theta_{MSW}$  point, there is a linear increase in stress as water content decreases until  $\theta_r$  is reached. At this point, the soil water stress factor becomes zero with full limitation on photosynthesis and GPP (Harper et al., 2021).

### 2.1.3 Canopy respiration

To allow estimation of daily changes in carbon in the leaf pool (Eq. 1), the release of carbon to the atmosphere from leaf respiration ( $R_e$ ) has to be calculated. This flux is part of gained carbon (i.e., GPP) consumed for self-maintenance requirements

in the leaf pool. In fact, canopy net primary productivity ( $NPP_{\text{canopy}}$ ), which is net available carbon ready to be allocated among different plant pools, is the sum of ~~photosynthetically~~ photosynthetical carbon uptake by plants (GPP) reduced by  
 280 carbon loss via leaf respiration ( $R_e$ ) (Pasquato et al., 2015; Running et al., 2000; Melton and Arora, 2016).

We use the well-established modified Arrhenius equation (Eq. 17) (Lloyd and Taylor, 1994; Sitch et al., 2003; Perez, 2016) to calculate the leaf respiration. The  $R_e$  flux is a function of air temperature, carbon mass of leaf pool, and a tissue-specific carbon to nitrogen ratio, given as:

$$R_e(t) = \frac{rr \cdot Bl(t)}{CNr} \cdot e^{p_1 \cdot \left( \frac{1}{p_2} - \frac{1}{T(t)+p_3} \right)} \quad (17)$$

285 where  $rr$  represents the leaf respiration rate,  $Bl$  the carbon mass of leaf pool (leaf biomass),  $p_1, p_2, p_3$  are parameters in the Arrhenius equation,  $CNr$  is carbon to nitrogen ratio in leaves, and  $T$  is daily mean air temperature.

#### 2.1.4 Vegetation phenology module

We incorporated a phenology submodel into our model using the approach defined in Yue and Unger (2015). This submodel calculates temperature-dependent phenological factors for spring and autumn,  $f_{ST}$  and  $f_{AT}$  respectively. These factors range  
 290 from 0 to 1 throughout the year, to determine the timing of spring budburst (once the spring temperature dependent factor sets up to increase above zero), maturity (when the spring temperature-dependent factor approaches to 1), autumn senescence (once the product of autumn temperature-dependent and photo-period factors start off to decrease below 1), and dormancy phenophases (once the product of autumn temperature-dependent and photo-period factors approach zero). The second phenological factor in the autumn and dormancy phenology is photo-period ( $f_{dl}$ ) factor and depends on day length. The photo-period factor together  
 295 with the temperature-dependent factor regulate the leaf senescence. The phenology submodel determines the above-mentioned four phenological transition dates on which a simple allocation of assimilated carbon to the leaf pool is based. Below, we provide details of each phenological factor and events.

**I) Spring phenology ( $f_{SP}$ ):** The growing season starts with the budburst day, which is the beginning of canopy development and the time when green tips of leaf show up. It is estimated using a temperature-dependent phenological factor  $f_{ST}$  as follows  
 300 (Eq. 18):

$$f_{ST} = \begin{cases} \min \left( 1, \frac{GDD - G_b}{L_g} \right) & GDD \geq G_b \\ 0 & \text{otherwise} \end{cases} \quad (18)$$

where GDD is growing degree day ~~and~~  $G_b$  is budburst threshold value. ~~The  $L_g$  is a parameter for growing length parameter is~~ a calibrated constraint in degree day, representing the period of leaf growth from budburst to maximum leaf cover (Yue and Unger, 2015). The accumulation of growing degree day (GDD) (Eq. 19) from winter solstice day is calculated as below:

$$305 \quad GDD = \sum_{i=1}^n \max(T_{10} - T_b, 0) \quad (19)$$

Where  $T_{10}$  is 10-day average air temperature,  $T_b$  is base temperature for the budburst ( $5^{\circ}\text{C}$ ).

$G_b$  in the estimation of  $f_{ST}$  (Eq. 18) is a threshold value for budburst to occur and is calculated as follows:

$$G_b = a + b \cdot e^{(r \cdot \text{NCD})} \quad (20)$$

where  $a$ ,  $b$ , and  $r$  are parameters for the budburst threshold. NCD is counted as number of chill days between the previous winter  
310 solstice day and the beginning of the successive year. Given the GDD and  $G_b$  estimates, temperature-dependent phenological  
factor ( $f_{ST}$ ) is then applied to calculate the spring phenology ( $f_{SP}$ ) (Eq. 21).

$$f_{SP} = f_{ST} \quad (21)$$

**II) Autumn phenology ( $f_{AP}$ ):** For the autumn phenology the product of two phenological factors, temperature  $f_{AT}$  and  
photo-period  $f_{dl}$  factors, is considered to estimate timing of senescence and dormancy. The autumn temperature-dependent  
315 factor,  $f_{AT}$ , (Eq. 22), is obtained as follows:

$$f_{AT} = \begin{cases} \max(0, 1 + \frac{(\text{FDD} - F_s)}{L_f}) & \text{FDD} \leq F_s \\ 1 & \text{otherwise} \end{cases} \quad (22)$$

where  $F_s$  is a threshold in degree day for leaf fall, and  $L_f$  is a threshold in degree day for the duration and length of the leaf  
falling period (more detail can be found in Yue and Unger (2015)). FDD (Eq. 23) is an accumulative falling degree day from  
summer solstice day which is known as a cumulative cold summation method (Yue and Unger, 2015) and it can be calculated  
320 as:

$$\text{FDD} = \sum_{i=1}^m \min(T_{10day} - T_s, 0) \quad (23)$$

where  $T_{10day}$  is 10-day average air temperature,  $T_s$  is base temperature for leaf fall at  $20^{\circ}\text{C}$ .

In addition to temperature factor  $f_{AT}$ , autumn senescence timing is regulated via photo-period factor  $f_{dl}$ , which is calculated  
based on day length (dl) period, together with lower ( $dl_{min}$ ) and upper ( $dl_{max}$ ) limits of day length affecting leaf fall as in  
325 Eq. 24.

$$f_{dl} = \begin{cases} \max(0, \frac{dl - dl_{min}}{dl_{max} - dl_{min}}) & dl \leq dl_{max} \\ 1 & \text{otherwise} \end{cases} \quad (24)$$

Where  $dl$  is the day length in minutes.  $dl_{min}$  and  $dl_{max}$  are the lower and upper limits of day length for the period of leaf fall,  
respectively. The autumn phenology ( $f_{AP}$ ) is finally calculated as a product of  $f_{AT}$  and  $f_{dl}$  (Eq. 25):

$$f_{AP} = f_{AT} \cdot f_{dl} \quad (25)$$

330 The predicted phenological transition dates from spring  $f_{SP}$  and autumn  $f_{AP}$  phenology factors determine the budburst-  
maturity and senescence-dormancy events, respectively. Based on this information, a fractional allocation to and decay from  
the leaf pool is considered (as detailed below).

### 2.1.5 Carbon allocation to and decay from the leaf pool

The next step of the carbon pathway in Eq. 1 is allocation to and decay of assimilated carbon from the leaf pool. The leaf biomass state variable (BI) in Eq. 1 is updated at a daily time-step, based on changes in gain and loss of carbon in the leaf pool. The allocation and decay processes are both key physiological processes in the vegetation models to govern the partitioning of growth among different plant carbon pools and are critical determinants of plant productivity (Haverd et al., 2016; Xia et al., 2017). There are two widely used allocation schemes ~~used~~ in vegetation models based on: (1) fixed allocation coefficients, and (2) allocation driven by allometric constraints. The first scheme uses a fixed allocation ratio to individual plant's carbon pools (e.g., used in CASA (Friedlingstein et al., 1999) or ~~BIOM-BGC(Hidy et al., 2016)~~ BIOME-BGC(Hidy et al., 2022)). In this scheme, the allocation ratio is constant within different plant development stages. In the second scheme, a fraction of carbon is allocated in such a way that it satisfies allometric relationships that exist between various plant compartments (Malhi et al., 2011; Gim et al., 2017). In the case of allocation to leaf, the allometric relationship is based on the relative mass of canopy – so-called maximum  $L_b$  – that a plant can support with a certain stem mass and height. We adopted an allocation scheme that mainly depends on an updated daily carbon status of the leaf pool. We use the maximum values of balanced LAI supported by the system (Eq. 26) based on a previous study conducted by Fleischer et al. (2013). Instead of considering it as a fixed value, we vary  $L_b$  within a range of  $\pm 1m^2/m^2$ , and consider it as one of the model parameters.

$$\lambda(t) = 1 - \frac{LAI(t)}{L_b} \quad (26)$$

Where  $\lambda(t)$  is the carbon allocation ratio to the leaf pool and  $L_b$  is the maximum LAI that can be supported by plants.

Provided with the identified major phenological transition dates from the phenology submodel – i.e., budburst, maturity or steady growth, senescence, and dormancy – the calendar year is accordingly divided into four main stages. During the early growing season, once the climate condition becomes favourable to plant growth and ~~the~~ budburst occurs, carbon allocation to leaf,  $\lambda$  (Eq. 26), is relatively a large fraction. This means that the largest part of carbon will be partitioned towards leaf and is being used for growth during the early growing season (Gim et al., 2017). Given the value for balanced LAI supported by the system (Fleischer et al., 2013), the carbon allocation slowly decreases with an increase in LAI until the leaf mass reaches that balanced LAI. As soon as the canopy approaches a full leaf state (i.e. maturity phenophase), the carbon allocation ratio to the leaf is held at its minimum – a small portion is used for maintenance respiration during this steady growth stage. We set the leaf allocation ratio during the maturity phase to a value of 5% from the assimilated carbon, following the recent version of the Noah-MP model's leaf allocation scheme (Gim et al., 2017).

After the steady growth and maturity phase, the leaf senescence phase approaches and the leaf-loss processes start to play the main role in moderating the mass-balance of canopy and the corresponding LAI seasonality. The loss of carbon via the leaf fall in PCM is simulated based on the calculated senescence and dormancy transition dates via the phenology submodel, such that when the simulation time-step approaches to the senescence date, the model linearly decreases the leaf biomass until the leaf biomass reaches to nearly zero at the beginning of the dormancy phase.

Concerning the leaf loss processes, PCM also accounts for the leaf losses due to cold stress ( $O_C$ ) (Eq. 27), drought stress ( $O_D$ ) (Eq. 29), and normal loss of the leaf ( $O_N$ ) (Eq. 30) following schemes of the CLASSIC model (Melton and Arora, 2016).



The leaf loss due to the cold stress is given by:

$$O_C(t) = O_{Cmax} \cdot (Cs(t))^3 \quad (27)$$

where,  $O_{Cmax}$  is the maximum leaf loss rate parameter and  $Cs$  is a cold stress factor value. The cold stress factor (Eq. 28),  
 370 ranging between 1 (full stress) and 0 (no stress), is calculated as:

$$Cs(t) = \begin{cases} 1 & T(t) \leq (T_c - 5) \\ 1 - \frac{T(t) - (T_c - 5)}{5} & (T_c - 5) < T(t) < T_c \\ 0 & T_c \leq T(t) \end{cases} \quad (28)$$

where  $T(t)$  is air temperature and  $T_c$  is a biome specific temperature threshold below which leaf damage is expected.

Similar to the  $O_C$ , the leaf loss rates due to drought stress  $O_D$  (Eq. 29) is calculated using the fSM stress factor (through the soil moisture stress submodel) and a  $O_{Cmax}$  maximum leaf loss rate parameter associated with the drought stress.

$$375 \quad O_D(t) = O_{Dmax} \cdot (1 - fSM(t))^3 \quad (29)$$

The third leaf loss term represents the loss rates due to a Normal decay  $O_N$  driven by biome specific leaf lifespan ( $\tau = 1$  for DBF in Eq. 30) given by:

$$O_N(t) = 1/(365 \cdot \tau) \quad (30)$$

Finally, the total decay of leaves  $D(t)$  consists of contributions from all individual losses (Melton and Arora, 2016); and can  
 380 be given as follows (Eq. 31):

$$D(t) = Bl(t) \cdot (1 - e^{-(O_C(t) + O_D(t) + O_N(t))}) \quad (31)$$

where  $O_C$ ,  $O_D$ , and  $O_N$  are the leaf loss rates due to cold stress, drought stress, and normal decay, respectively.

In summary, the proposed PCM model comprises the submodels mentioned above in a hierarchical chain, starting with the carbon uptake via the initial leaf biomass state variable and continues with daily partitioning of that assimilated carbon together  
 385 with daily decay from leaf compartment to calculate the leaf biomass production increment. This biomass increment is later added up to the state variable from the previous time step to update the leaf biomass for the current time step. Finally, to update the LAI that is required for the GPP estimation over the next time step, the current leaf biomass is converted to LAI according to Eq. 2.

## 2.2 Model set-up and experimental design

### 390 2.2.1 Study sites and datasets

This study focuses on deciduous broad-leaved ~~forests biome type and forest biome types~~. We selected tower sites distributed over Europe and North America to ensure a representative spatial coverage. Sites were excluded if data of fewer than five years

consecutive years of observations were available. We further screened out the data at each site to the years with minimal gap in input data, ~~in particular,~~. For example, there were some long period of gaps (i.e., years) within the continuously recorded FLUXNET dataset for photosynthetic photon flux density variable and its associated frequent and long missing data at some sites (PPFD), which we excluded those years in the simulations (e.g., a continuous period of missing PPFD in the US-Ha1 dataset from 1991-2003). Applying the above criteria, nine sites with varying temporal coverage were retained for the analyses (Fig. 2). The general site information is presented in Table 1. Daily flux and meteorological forcing data are from ecosystem stations available from the free fair-use FLUXNET2015 Tier 1 global collection database ([https://fluxnet.org/data/download-](https://fluxnet.org/data/download-data/) data/, last access: June 2021) (Pastorello et al., 2020). The input data required to drive the PCM comprises: air temperature (T), photosynthetic active radiation (PAR) (i.e. converted from PPFD in  $\mu\text{mol m}^{-2} \text{s}^{-1}$ ) and vapor pressure deficit (VPD) (Table 2). The tower-based GPP estimations, GPP\_NT\_VUT\_REF from the FLUXNET2015 dataset are used for model calibration. We used the first year of the time series as a warm-up period, during which the chilling days and thermal requirement in the phenology submodel are counted. ~~Optional variables to establish the model include~~ In other words, since the phenology module for each individual year needs the number of chilling days from the previous year, the very first year of observations is not included in the simulations. The very first year of observations is only used for to calculate budburst day of the first simulation year. The warm up period, here, refers to the last 10 to 11 days of each previous year that are eventually required for estimating variables in the phenology module for its uninterrupted run in the subsequent year. When simulating the soil moisture stress in establishing the model is desired, soil moisture (SM) and soil textural properties, ~~are required to simulate the soil moisture stress development. However, we are also included.~~ We investigate the soil moisture stress impact only at the Hohes Holz (DE-HoH) site in Germany with soil moisture data available up to 80 cm depth. In regard to calculating the soil moisture stress in PCM, a pedotransfer function following Zacharias and Wessolek (2007) is implemented to estimate site-specific  $\theta_s$  and  $\theta_r$  values. This (pedotransfer) submodel receives soil textural properties (sand, clay contents, and bulk density) obtained from field observations of spatially distributed soil profiles as input. It provides the required field capacity ( $\theta_s$ ) and permanent wilting point ( $\theta_r$ ) to calculate  $\theta_{MSW}$  and the corresponding soil moisture stress term fSM in the calculation of  $\epsilon$  (Eq. 5). To maintain the consistency with the vertically weighted soil moisture,  $\theta_s$  and  $\theta_r$  are estimated as weighted average values of individual layer-specific  $\theta_s$  and  $\theta_r$  taking the respective root fractions as a weighting factor. Other required parameters in the model related to different processes, are listed in Table 3. The LAI field measurements were ~~collected~~ obtained via personal communication to site contact persons; and ~~based on the responses~~ a subset of 4 sites (DE-HoH, DE-Hai, US-MMS, and US-Ha1 (<https://harvardforest1.fas.harvard.edu/exist/apps/datasets/showData.html?id=hf069>, last access: 05 January 2022)) ~~are used~~ was selected based on data availability to evaluate the modeled LAI. The observation-based LAI measurements ~~are data were~~ obtained using common procedures ~~of with either the~~ LAI-2000 instrument (~~Gower and Norman, 1991~~) and fisheye technique (~~Bonhomme, R. and Chartier, P., 1972~~) (~~Gower and Norman, 1991~~) at the DE-Hai, US-MMS, and US-Ha1 or the fisheye (DHP) technique (~~Bonhomme, R. and Chartier, P., 1972; Ariza-Carricondo et al., 2019~~) at the DE-HoH site, respectively. These two methods ~~are considered as the closest methods yielding similar values among other techniques and, therefore, provide consistent measurements~~ agree very well according to Ariza-Carricondo et al. (2019) and are thus considered to yield comparable values also across different sites (Ariza-Carricondo et al., 2019).

### 2.2.2 Model structure and set up

The impact of water availability on the canopy photosynthesis (i.e., soil water deficit and atmospheric water deficit), in vegetation models is structured in two ways; individually or in combination with each other. Recently, plant hydraulic theory has also been introduced to reflect the vegetation water stress in Community Land Model (CLM5), which is beyond the scope of this study (Kennedy et al., 2019). In some models, water stress is quantified as an overall stress from both atmosphere and soil-moisture (GLO-PEM; Prince and Goward, 1995), (Biom-BGC; Hidy et al., 2016), while some soil ((GLO-PEM; Prince and Goward, 1995), (BIOME-BGC; Hidy et al., 2022)). For instance, in the GLO-PEM model the water stress condition is reflected by an estimated and potential evapotranspiration, a relative drying rate scalar for potential water extraction, and a volumetric soil moisture content (more details together with equations can be found in (Zhang et al., 2015)). Some other models account for the water stress due to either only due to the atmospheric drought (CASA; Potter et al., 1993), ((CASA; Potter et al., 1993), (MOD17 algorithm; Running et al., 2000)), or soil moisture drought (EC-LUE; Yuan et al., 2007), only the atmospheric variable VPD and its two parameters,  $v_{min}$  and  $v_{max}$ , are used to calculate water stress factor to predict GPP (Running et al., 2000). In some other models such as FORMIND (Fischer et al., 2016) and EC-LUE (Yuan et al., 2007) only the soil moisture deficit is reflected. For instance, in the FORMIND model, the impact of atmospheric water deficit (VPD impact) is not presented; but the soil moisture deficit is represented by volumetric soil water content and soil parameters (soil field capacity, permanent wilting point, and minimum soil water content). In order to determine, how stress should be represented in the final version of PCM, we conducted two sets of preliminary model experiments to examine: (1) whether inclusion of fSM, additionally to the other stress factors affects the results, and (2) the effect of alternative integration approaches (i.e. Liebig law and multiplicative approaches, see Section 2.1.1) on simulated GPP over the DE-HoH site during the drought in 2018. Since the best model skill of the PCM was achieved, when incorporating all stress factors (fT, fVPD, and fSM) in the calculation of the overall environmental stress; and using the minimum integration approach (Eq. 6), this structure was selected for the final setup (see Figures in Supplement, Figure S1 and Figure S2). With regard to specific considerations in LAI simulations, the model starts with the simulation using a fixed initial LAI state variable to begin the carbon assimilation once weather conditions become more favourable for plant growth. Following the CABLE model parameterizations (Li et al., 2018), we set the initial LAI value to 0.35. We also consider a local maximum LAI (so-called  $L_b$  in this study), obtained from reported values in literature (Fleischer et al., 2013), that individual mature forest can sustain at canopy closure. However, the local maximum LAI is, later in the calibration step, allowed to vary within  $\pm 1\text{m}^2\text{m}^{-2}$  of the reported value. The  $L_b$  constrains the simulated LAI up to the reported value at each site across years.

### 2.2.3 Global sensitivity analysis

Despite the simplicity of parsimonious models, assessing model robustness remains a fundamental step when building and developing a model. One of the powerful and invaluable tools for robustness assessment is global sensitivity analysis (GSA) to test the underlying model parameterizations and inform about sensitive model parameters for the subsequent parameter inference. In general, the GSA can be performed to understand the influence of parameters perturbations on modeled simulations

and to determine the informative parameters that contribute the most to an output behavior (Iooss and Lemaître, 2014; Cuntz et al., 2016; Rakovec et al., 2014). In this study during the GSA, the parameters vary over boundaries reported in ~~literature~~the literature's. In case there were no ~~bounds-reports of upper and lower bounds were~~ available for some parameters (e.g., phenological parameters from Yue and Unger (2015)), we varied them at  $\pm 20\%$  level of their default values. We utilize the Sobol' variance-based sensitivity method (Saltelli et al., 1999) with Sobol2002 formula (Saltelli, 2002), in which decomposition of the output variance is performed in terms of Sobol' indices. The Sobol' First order index (Si) and total-order Sobol' index (ST) express the share of output variance associated with a given parameter  $i$  and the share of output variance where all parameters are varied except the parameter  $i$ , respectively. These indices range between 0 to 1; with zero value indicating that the model output is entirely insensitive to the respective parameter changes. The closer the value is to 1, the more important and sensitive the respective parameteris. Generally, the model parameters deem sensitive, if the sensitivity index is above a certain threshold value. Here in this study, we report the total-order Sobol' index and set the selection threshold at 1% (Tang et al., 2007), meaning that if the variation of a given parameter contributes to a change greater than 1%, then that parameter is recognized as an informative parameter. In contrast, non-informative parameters are reported as parameters with Sobol' indices below 1%. Given the focus of the present study on two main output variables (i.e. GPP and LAI), we use the time mean for both outputs over the entire period for the sensitivity analysis at each study site. However, the results are expected to differ not only according to the site and selected target output but also between the individual years if a specific year is of interest to be investigated (Göhler et al., 2013; Hou et al., 2012). To conduct the sensitivity analysis, we opt to choose all coefficients in the empirical equations as adjustable parameters (Table 3). It helps to explore the model sensitivities of often hidden parameters to properly constrain the model (Cuntz et al., 2016). Overall, we apply the global sensitivity analysis in all study sites for the common 29 parameters and analyse the sensitivity of the soil moisture stress parameters together with other parameters only for the DE-HoH site at which representative soil moisture data at different depths, down to 80 cm into the soil, was available. Given the importance of the number of model evaluations required to conduct the Sobol' sensitivity analysis (Nossent and Bauwens, 2012) and the stability of sensitivity indices, we also check the convergence of the Sobol' indices through a visual assessment of diagnostic plots.

#### 485 2.2.4 Parameter estimation

Based on the results of sensitivity analysis, informative and non-informative parameters are identified. Later, we fixed the non-informative parameters to their corresponding reported values in literature (see Table 3 for details) and the remaining informative parameters are inferred using a Monte Carlo approach (Kuczera and Parent, 1998). The parameters were calibrated against the GPP\_NT\_VUT\_REF time series from the corresponding flux tower measurements (global Fluxnet Tier1 network accessed on 13 February 2021) (Pastorello et al., 2020). It is important to note that besides the maximum LAI value we did not use LAI field observations in the calibration process as LAI is not readily available from the FLUXNET dataset. Instead some LAI observations (obtained from site contacts) were used in the model ~~verification-validation~~ step. The first year of the dataset is considered a spin-up period. The rest of the time-series are divided into two sub-periods. The first half is used for the calibration phase, and the remaining years to independently evaluate the model performance (i.e., over the out-of-

495 calibration set). A total of 10 000 parameter sets was sampled from their a priori defined ranges (Table 3) in each study site to estimate the parameters and simulate the GPP flux and LAI. Model performance was quantified using a group of performance metrics, including Kling-Gupta efficiency (KGE) (Gupta et al., 2009), Root Mean Square Error (RMSE), and coefficient of determination ( $R^2$ ). We selected an ensemble of informative model runs that simultaneously lie within the top 5% of all the performance metrics.

## 500 2.2.5 Site-specific ~~verification~~-validation and model generalization

The second half of the GPP time series at each study site was used for the model ~~verification~~-validation step. In addition to the at-site ~~verification~~validation, it is also equally important to consider the generality of the model structure including underlying model parameterizations. To this end, we considered an independent (spatial) ~~verification~~-validation approach – so called cross-validation – for assessing the robustness of model parameterizations beyond the conditions during which they were calibrated.

505 The relevance of the cross-validation to the modeling framework, is that transferable models can be used beyond the spatial and temporal limits of their underlying data, especially in the face of pervasive scarcity of observational data to constrain model parameterizations (Yates et al., 2018). Therefore, as the next step in our modeling framework, and after performing the site-specific calibration and ~~verification~~validation, a cross-validation of the model is conducted to come up with a compromise solution (here parameter set) applicable across the study sites, following the approach of Zink et al. (2016). In doing so, the

510 behavioral parameter sets found from on-site calibration for each study site are grouped together as one unique set of all possible behavioral parameters. Then the model is run using all possible parameter sets and the respective performance metric (i.e., KGE) for each parameter set at each investigated site is estimated. After that, the mean values of KGEs corresponding to each parameter set over all study sites are calculated. Finally, a set of parameters associated with the highest mean KGE score is recognised as a compromise solution. Here the goal of this analysis is to investigate the generality of the underlying model

515 structure, and to allow inference of a common (compromise) set of model parameters for the PCM for a broader applicability (i.e., beyond the calibration sites).

## 3 Results and Discussion

In the following, we first show and discuss findings from the global sensitivity analysis and site-specific parameter calibration. This is followed by a discussion of the site-specific model performance. Finally, we present the results of a cross-validation to

520 test the generality of underlying model parameterizations. This also allows us to propose a standard set of PCM parameters for locations where calibration is not possible.

### 3.1 Sensitivity analysis

Here, we explore the sensitivity of the output variables (i.e. GPP and LAI) to the model parameter variations using Sobol' method at each study site. Although a direct comparison of PCM parameters sensitivities from this study with similar models

525 in other studies is difficult due to difference in model structures and representation of photosynthesis processes, one can gain

insights by comparative assessments among conducted studies. For instance, the light utilization in LUE-oriented GPP models is based on photon absorption and photosynthetic efficiency of incident light (Frost-Christensen and Sand-Jensen, 1992). Hence, one can compare the significance of the LUE parameter of our model with that of the quantum yield of photosynthesis which is a measure of photosynthetic efficiency in the Farquhar equation (Farquhar et al., 1980) in several land surface models.

530 As it can be seen from Figure 3a (mean GPP) and b (mean LAI), different sensitive parameters are associated with the different output variables. However, for the same output variable, all sites more or less share a similar informative set of parameters, although the magnitudes differ. Furthermore, the evaluation of Sobol' indices convergence (see Figure 4) showed relative stability of sensitivity indices at around 8 000 model evaluations. In the following, we show and discuss the sensitivity of the model outputs to different PCM parameters.

### 535 3.1.1 Parameter sensitivity for GPP estimation

We first investigate the sensitivity of GPP output to the model parameters. Figure 3a shows the total-order Sobol' index of all parameters contributing to the GPP output. The boxes in Figure 3a indicate variation of the sensitivity of a given parameter across different sites. Only a small number of them have ultimate control on the simulated GPP out of the 34 model parameters (Figure 3a). This is in agreement with previous studies using LPJ-DGVM (Zaehle et al., 2005), BETHY (White et al., 2000),

540 and BIOME-BGC (Knorr, 2000) models showing only a few of investigated parameters significantly influence the modelled carbon fluxes outputs (including GPP).

The most sensitive parameter for the GPP estimates turned out to be the light use efficiency, ~~LUE-in~~ (LUE in Eq. 3). This agrees with numerous other studies confirming that the light use efficiency is a significant parameter affecting GPP. For instance, Zaehle et al. (2005) conducted a probability-based sensitivity analysis using the LPJ-DGVM ecosystem model,

545 utilizing the Farquhar photosynthesis scheme, and found that carbon fluxes (including GPP) are highly sensitive to parameters related to the photosynthesis process, particularly the intrinsic quantum efficiency parameter (so called  $\alpha_q$  in their model), which is related to the ~~LUE-LUE~~ in PCM. Similarly, Ma et al. (2020) using a GSA in the Flux-based Ecosystem Model and based on the Farquhar photosynthesis scheme, found canopy quantum efficiency of photon conversion among the most sensitive parameters with a strong influence on forest GPP. The multiplicative coefficient of canopy reflectance,  ~~$\epsilon C$~~ , and the

550 light extinction coefficient,  ~~$k$~~ , parameters in the fPAR formulation (Eq. 4) based on Lambert-Beer's law ~~show also also showed~~ substantial sensitivities. Notably, these parameters are ~~typically~~-fixed to constant values by default in the fPAR formulation ~~controlling PAR availability and utilization~~, in similar studies ~~Xiao et al. (e.g. 2004); Xin et al. (e.g. 2019);~~

(e.g., Xiao et al. (2004) and Xin et al. (2019)); whereas, here, we let these parameters ( $C$  and  $k$ ) vary at  $\pm 20\%$  level of their fixed values. The next group of sensitive parameters are those involved in the imposed environmental stresses on GPP: I) The

555  $v_{min}$  parameter (Eq. 10) exhibits some sensitivity and controls the impact of vapour pressure deficit stress on simulated GPP (fVPD). Balzarolo et al. (2019) also reported the strong impact of VPD ~~variable~~ in general on radiation use efficiency and on resultant GPP. II) ~~Next the next~~ environmental factor constraining the GPP is soil moisture stress. Here, we identify  $\beta$  (Eq. 11) and  $\theta_r$  (Eq. 15) as sensitive parameters. We can only consider and discuss the soil moisture stress-related parameters ~~in-at~~ the DE-HoH site due to the lack of soil moisture data at other sites. The investigated sensitivity of fSM-related parameters are shown in

the supplementary Figure S3. Similar findings of a pronounced impact of parameters controlling soil moisture availability (e.g.,  $\theta_r$  and  $\beta$ ) on simulated GPP has been reported by Li et al. (2016) for the CABLE and JULES models. From a soil science perspective, ~~the~~  $\theta_r$  is often a fixed value of soil water content corresponding to a soil matric potential of 1500 kPa (Zhang and Han, 2019) and is typically not considered as a parameter. However, our result shows that ~~the~~  $\theta_r$  might not be considered as fixed. ~~While the functional form of  $\theta_r$  can be deduced based on pedo-transfer functions (Zacharias and Wessolek, 2007), empirical coefficients of such functions representing the linkages between  $\theta_r$  and~~ Pedo-transfer functions (PTFs) link soil textural properties (e.g., sand, clay contents) ~~can to soil parameters (e.g.,  $\theta_r$ ) and various functional forms have been developed in past decades (Van Looy et al., 2017). Empirical coefficients of PTFs can also~~ be regarded as model parameters (Samaniego et al., 2010; Kumar et al., 2013; Schweppe et al., 2021). Hirmas et al. (2018) also showed that soil retention properties can change in time. For example, climate change may induce rapid changes in the soil macroporosity and the associated soil hydraulic properties. Those may alter the feedback between climate and land surface.

The ~~SLA~~ SLA parameter (Eq. 2), as one of the structural parameters, is also a major contributor to ~~the~~ simulated GPP. Its sensitivity can be explained by the direct effect of SLA on the LAI calculation (Eq. 2) through which the carbon assimilation (GPP) is eventually taking place (Eq. 4, 3). Arsenault et al. (2018) and Li et al. (2016) also reported the ~~SLA~~ SLA parameter among very sensitive model parameters, when simulating carbon fluxes (including GPP) in the Noah-MP and CABLE land surface models, respectively.

Finally, the last group of sensitive parameters in modeled GPP are those involved in the phenology submodel. The parameter  $F_s$  (Eq. 21), determining the timing of leaf fall, appeared as a major informative parameter for all sites. Although, some parameters were only sensitive ~~in at~~ some sites including those for the leaf budburst threshold- namely, ~~b and r~~ b and r (Eq. 19). The ~~b~~ b parameter appeared sensitive only at DE-HoH and the parameter ~~r~~ r is sensitive at CA-Oas and US-Oho. Generally, the implemented phenology submodel controls the plant active period and at the same time accounts for the impact of the temperature factor on leaf development and resultant GPP. This might be a reason why temperature-related parameters in the temperature stress factors (Eqs. 8 and 9) are not found to be informative in the sensitivity analysis. ~~This is because temperature mainly controls the start and end~~ In other words, temperature stress limits the  $\text{CO}_2$  assimilation and gross primary productivity outside of the growing season ~~in the phenology submodel. Phenology parameters play their roles during the growing season.~~ This period indicates favourable condition for plant growth when the temperature stress is mostly not active. Therefore, ~~corresponding temperature stress~~ parameters do not significantly influence the modelled GPP. In agreement with our results, Yuan et al. (2007) also reported little impact of environmental stresses due to temperature on GPP during the growing season. It is worth mentioning that the temperature stress is still applied during the growing season, but as the upper-most limits of temperature ( $T_{low}=-2$  and  $T_{high}=38$  °C) do not occur frequently, unless during cold, heat stresses (such as heat years in 2018 and 2019 at the DE-HoH site), the sensitivity of GPP to temperature parameters are less pronounced during the growing season.

Another interesting point emerging from Figure 3a is the insensitivity of GPP output to the LAI balanced (maximum),  $L_b$ . This effect can also be seen in the LAI simulation (e.g., at DE-HoH site) where ~~a group of daily LAI at an ensemble of simulated LAI at each time step during~~ the maturity phase, ~~(i.e., in Figure 7 lead to not much of the-), did not cause much~~ difference in the corresponding GPP ~~outputs-output~~ (i.e., in Figure 5). This is in agreement with the previous stud-



ies of [Lee et al. \(2019\)](#); [Jung et al. \(2007\)](#) [Jung et al. \(2007\)](#) and [Lee et al. \(2019\)](#), which showed that GPP output saturates and becomes insensitive at LAI values above  $4 \text{ m}^2 \text{ m}^{-2}$ .

### 3.1.2 Parameter sensitivity for LAI estimation

We further explore the parameter sensitivity for LAI output similar to the GPP described above. In general, a similar set of sensitive parameters were identified for GPP and LAI outputs across sites (Figure 3b). However, some differences were also detected: parameters such as  $L_b$ ,  $f_{cov}$ ,  $L_g$ ,  $p_2$ , and  $p_3$  show substantial sensitivity, while the sensitivity to  $v_{min}$  was almost negligible. Regarding the similarity of parameters between GPP and LAI, it is worth noting that the calculations of GPP and LAI depend on each other since assimilated carbon (i.e., GPP) is partly converted to leaf biomass from which the LAI is calculated, and used in turn for the GPP calculation in the next time step. Therefore, LAI output should roughly be sensitive to the same set of parameters as the GPP output. The result in Figure 3b shows that [LUE, C, and k](#) [LUE, C, and k](#), directly involved in the GPP formulation, have considerable influence on the LAI output. These parameters, in particular the LUE, strongly control the assimilated carbon and consequently affect the modelled LAI.

Figure 3b also shows a major contribution of [SLA](#) [SLA](#) (Eq. 2),  $f_{cov}$  (Eq. 2), and  $L_b$  (Eq. 24) to the LAI output. Similarly to the [LUE](#) [LUE](#) for GPP, the [SLA](#) [SLA](#) is central for the calculation of LAI (Eq. 2) and thus shows by far the largest sensitivity. Since the LAI output in the model depends on GPP, the studies [reporting the SLA mentioned above reporting the SLA](#) impact on GPP [might likely](#) apply for LAI output as well (Li et al., 2016; Arsenault et al., 2018). The  $f_{cov}$  parameter represents the fractional vegetation coverage per unit area and is a critical parameter in calculating forest GPP (Ma et al., 2015). Ma et al. (2015) assumed 100% forest coverage in their calculation of GPP, from which LAI was calculated. They showed how this inappropriate assumption (i.e., 100% forest coverage) can exaggerate the forest area when calculating forest GPP (and consequently the LAI) rather than considering a realistic coverage. Here in the PCM, the  $f_{cov}$  parameter is allowed to vary between 60% to 95% as an adjustable parameter (based on [the Fluxnet2015 Dataset description of percent coverage greater than 60% at DBF sites; http://sites.fluxdata.org/](#)). We observe that fractional vegetation coverage substantially influences the simulation of LAI. In agreement with Ma et al. (2015), our result supports the importance of the fractional coverage ( $f_{cov}$ ) as an important structural parameter in carbon cycle modelling studies. The  $L_b$  parameter (Eq. 24), also exhibits a marked sensitivity for the LAI output (Figure 3b) because [this parameter is a direct factor allowing the canopy to it directly affects how long carbon allocation to the leaf pool continues until the canopy LAI reach to its maximum](#) [Next important contribution of parameters to value at canopy closure \(see \(Eq. 26\). Other parameters](#) the LAI output [is sensitive to](#) are those governing the leaf phenology in the phenology submodel,  $L_g$  (Eq. 18),  $F_s$  (Eq. 22), [b](#) [b](#) (Eq. 20), [r](#) [r](#) (Eq. 20) (i.e., in Figure 3b). To the best of our knowledge, these parameters have not been studied elsewhere within a sensitivity analysis framework, and therefore we could not perform any comparative assessment. Parameters [b and r](#) [b and r](#) contribute to the simulation of leaf budburst day,  $F_s$  contributes to the identification of leaf fall day, and  $L_g$  [parameter](#) influences the LAI output estimation through its influence on the length of the growing season. The  $F_s$  parameter exhibits higher sensitivity and a larger between-site variation than other parameters (Figure 3b). This parameter represents [the necessary amount of cold accumulation a coldness threshold for leaf fall in degree day to trigger the leaf fall event. If the cumulative cold degree days from summer solstice \(FDD\) becomes equal or](#)



less than this threshold, then leaves start falling (more detail can be found in (Yue and Unger, 2015)). For instance, ~~lower-cold~~  
630 ~~degree-days-accumulation-a higher threshold~~ would lead to an early leaf ~~fall-and-leaf-shedding~~shedding, especially in the cold  
climates where cumulative cold degree days can be reached faster. Therefore, the ~~between-site~~ between site variation of this  
parameter ~~might-not-be~~ is not surprising, given the differences in temperature and accumulated cold degree days among study  
sites.

Other additional parameters that showed sensitivity for the LAI output are  $p_2$ , and  $p_3$  (Eq. 17). These parameters belong to  
635 the canopy respiration process in the modified Arrhenius equation (Eq. 17). They are typically considered as fixed parameters  
(e.g., in TETIS-VEG model (Perez, 2016), in LPJ-ML model (Schaphoff et al., 2017)), while here we varied these parameters  
within 20% of their nominal value. Notably, these parameters showed greater sensitivity for the LAI estimation than that of the  
GPP. It might partly be due to the reduced/raised assimilated carbon (GPP) by canopy respiration which ~~in turn might decrease,~~  
in turn, might decrease/increases the available carbon to be allocated to leaf biomass and affect the resultant LAI. ~~Furthermore,~~  
640 ~~the evaluation of Sobol' indices convergence (see Figure 4) showed relative stability of sensitivity indices at around 8 000 model~~  
~~evaluations.~~ In addition to that, to best of our knowledge, it is the first time that these parameters are thoroughly analysed within  
a sensitivity analysis framework, and we yet might not be able to find a reason or explanation for this pattern in this study. This  
calls for future studies to further investigate this aspect.

### 3.2 Site specific model assessment

645 We conduct site-specific parameter estimation for all available eddy-covariance (EC) flux tower study sites (Figure 5). For this,  
only ~~informative-parameters~~ the most sensitive parameters (depending on the sensitivity analysis result at each site number  
of the most sensitive parameters vary between 8 to 14 parameters) identified in the sensitivity analysis are calibrated and  
the others are fixed (Table 3). For model parameter calibrations we used the first half of the available time series and the  
remaining years for ~~verification-validation~~ (Table 1). Calibration and ~~verification-validation~~ of the model are only performed  
650 for the GPP flux because direct LAI measurements are not available at all of the flux sites. Figure 5 shows the seven-day mean  
of simulated GPP for a set of ensemble members for each study site during both the calibration and ~~verification-validation~~  
periods. Since the different sites were operational at different times and some sites (e.g., DE-Hai) cover a relatively long time  
period, we show only five years of simulation at each site: the last three years of calibration and the first two years of ~~verification~~  
validation periods (Figure 5). A complete simulation for each site during the entire available times series is provided in the  
655 Supplementary Figure S4. In addition, Table 4 summarizes the model performance in simulating GPP during calibration and  
~~verification-validation~~ periods at different sites. In general, the model achieved KGE values of above 0.65, RMSE of less than  
 $2.5 \text{ gC m}^{-2} \text{ day}^{-1}$ , and  $R^2$  values of above 0.65 over all study sites. We compare the performance of our model to other  
modeling studies, whenever there is either an identical site to our study or a similar biome type (i.e., DBF) presented. To this  
end, our results are similar to Yue and Unger (2015) who found a high correlation of more than 0.8 and RMSE lower than 3  
660  $\text{g C m}^{-2} \text{ d}^{-1}$  for the GPP simulations at DBF forest sites in a global setting using the Yale Interactive terrestrial Biosphere  
model. Another study conducted by Asaadi et al. (2018) showed a quite good model performance using the CLASS-CTEM  
land surface model (Melton and Arora, 2014) applied at US-Ha1 (1998-2013) and US-MMs (1999-2006) flux tower sites, with

$R^2$  value of 0.99 accompanying RMSE of 0.62, and  $R^2$  value of 0.98 accompanying RMSE of  $1.07 \text{ g C m}^{-2} \text{ d}^{-1}$  at US-Ha1 and US-MMs, respectively. In a recent study, Holtmann et al. (2021) assessed the daily carbon fluxes over the DE-HoH forest during 2015-2017 using the FORMIND model (Fischer et al., 2016). They showed that the simulated and measured GPP correlates with an  $R^2$  of 0.82 and RMSE of  $9 \text{ MgCha}^{-1} \text{ a}^{-1}$  equivalent to  $2.46 \text{ g C m}^{-2} \text{ d}^{-1}$  using FORMIND model.

Taken together, our model exhibits a reasonable ~~validity~~-performance and performs equally well in estimating temporal dynamics of GPP (Table 4) compared to other more complex land surface and biogeochemical models. The PCM shows skill in capturing GPP at most of the investigated sites; although it overestimates GPP at the IT-Ro1 during summer. IT-Ro1 is located in a Mediterranean climate exposed to dry summers (Vicca et al., 2016). The forest ecosystems in Mediterranean type climate are affected by water limitation which can affect the GPP flux significantly (Cueva et al., 2021). The lack of soil moisture data probably contributed to the misrepresentation of GPP at this site. This is in agreement with previous studies that found similarly poor modeling performance across sites located in the Mediterranean climate in central Italy in dry summer periods when simulating GPP (Maselli et al., 2012; Chiesi et al., 2011; Fibbi et al., 2019). ~~In~~ Vargas et al. (2013), also discussed the interannual dynamics of soil moisture effect on GPP flux in Mediterranean ecosystems using five process-oriented ecosystem models including water balance. They observed a systematically underestimation of GPP in the models that were accounting for soil water balance. Those underestimations may have been related to the complex nature of Mediterranean ecosystems, e.g., due to deep roots and an important role of the lower canopy. In contrast, here we overestimate the GPP and believe that this is due to lack of local information on soil moisture stress. More information of soil moisture stress is therefore expected to improve the model. Overall, they emphasize the importance of drought conditions and the complex nature of Mediterranean ecosystems in representing forest dynamics, including GPP flux. In addition, water limitation impact on GPP could be related to the irregular occurrence of extreme events (e.g., European-wide drought 2018). Such conditions were observed at DE-HoH and DE-Hai sites, where the model overestimated GPP during late summer of 2018 coincided with Europe-wide drought 2018 (Buras et al., 2020). In the next step, we also examine the model's overall performance in reproducing GPP in terms of multi-year average of GPP at each site. Figure 6 shows that the model can generally explain the spatial variation of GPP with an  $R^2$  as high as 0.90.

As an independent ~~verification~~-validation step, we evaluate the PCM simulations of LAI against field-measurements data at some study sites where observational data were made available via personal contacts with site investigators. Figure 7 compares simulated values of LAI with their field measurements at four sites (US-MMS, US-Ha1, DE-Hai, and DE-HoH). In general, a good spatial and temporal consistency between the simulated LAI and the field-measurement LAI can be seen from the plots (Figure 7). The  $R^2$  corresponding to the US-MMS, US-Ha1, DE-Hai, and DE-HoH sites are 0.90, 0.85, 0.78, and 0.90, respectively. Furthermore, the comparisons yield RMSE of 0.96, 1.58, 2.21,  $1.4 \text{ m}^2 \text{ m}^{-2}$  to the US-MMS, US-Ha1, DE-Hai, and DE-HoH sites, respectively. Table 5 summarizes the model performance in simulating LAI during a common period of observed and modeled data.

The simulated LAI captures reasonably well the observed LAI seasonality at almost all the sites. It demonstrates the capability of the model in capturing canopy status at different phenophases. However, there are some pronounced deviations between modelled and observed LAI at some sites (US-Ha1, DE-HoH) during the dormancy phase and autumn leaf decline period.

Given the deciduous nature of those ecosystems, it is likely that the higher winter values of field measurements compared to simulated LAI reflects the presence of understory vegetation (Asaadi et al., 2018) or instrument's reading of present stand and/or dead leaf on trees after onset of leaf shedding. We also notice a slightly lagging phase in simulated LAI during the spring as compared to the field-measurements data, for instance at the DE-Hai site. Such discrepancy may be due to the lack of accounting for dependence of green-up rate on non-structural carbohydrate from previous years as a buffer to initiate leaf onset (Asaadi et al., 2018), which is currently not represented in the PCM.

### 3.3 Spatial model ~~verification~~ validation and model generalization

~~Eventually, we~~ We conduct cross-validation of parameter transferability for all sites against tower-derived GPP data (Section 2.2.5). Figure 8 summarizes the results of this analysis, providing a comparison between the range of obtained Kling-Gupta efficiency performance metric (KGE) from on-site calibration and KGE obtained from a compromised solution. It can be seen that the model with a compromise parameter set still shows a reasonable predictive skill ( $KGE > 0.5$ ), while leaving space for skill improvement with a site-specific parameter ( $\Delta KGE \approx 0.10$ ). The poorest performances are associated with the northernmost site DK-Sor and the Mediterranean IT-Ro1 site. The associated bias in those sites is likely related to GPP response to the maximum LUE parameter obtained from compromise solution applied over all the sites. As it was shown in the sensitivity analysis (see Section 3.1.1), the variation of GPP is predominantly driven by the LUE-LUE variation thus a constant fixed maximum LUE across all sites might be a reason for the limited performance at the sites located in maximum latitude and water-limited regions. It has been shown that maximum LUE-LUE varies in different geographical locations (Jung et al., 2007), and this is in line with our on-site calibration result indicating largest maximum LUE-LUE at DK-Sor (northernmost site with a cold and moist climate) and lowest at IT-Ro1 (a relatively drier Mediterranean site) sites. Thus applying a compromise value for LUE-LUE at these two site would result in a bias in GPP estimation. Previous studies (Wang et al., 2010; Madani et al., 2014) showed a large variation in maximum LUE-LUE not only between different biomes but also ~~even~~ within an individual biome and plant functional type. Concerning the large spatial variability of maximum LUE-LUE, several factors such as spatial heterogeneity of vegetation, canopy densities, ages, soil nutrition, leaf nutrient content have been mentioned in previous studies (Wang et al., 2010; Madani et al., 2014). Some methods such as spatially explicit estimation of optimum LUE (Madani et al., 2014) or introducing pixel-level maximum LUE-LUE (Wang et al., 2010) have been employed in satellite-based LUE-LUE models to overcome this shortcoming. They argued that the assumption of a constant maximum LUE-LUE (i.e. based on standard MODIS-base GPP algorithm and a Biome Property Look-Up Table; Heinsch et al., 2003), needs to be reexamined so that spatial heterogeneity between individual plant functional types is represented. Therefore, the uncertainty introduced by the fixed maximum LUE-LUE may be reduced and ecosystem productivity modeling would be improved.

### 3.4 Limitation and opportunities

While the model performs well, in general, on simulating the GPP, some inconsistencies in the observed and modelled GPP across sites help to identify the model limitation and introduce future opportunities to improve the model performance. One of the mismatches is that the model lacks to adequately capture the observed decline in GPP during 2019 (Figure 5) at the

DE-HoH. This may be related to a possible legacy impact of the drought year 2018 into the successive year 2019 (Buras et al., 2020; Schuldt et al., 2020; Schnabel et al., 2021; Reichstein et al., 2013). Here we infer that the reduction in the tower GPP in 2019 might be due to a change in the ~~LUE~~LUE parameter. Based on calibration from previous non-drought years, the obtained ~~LUE~~LUE value might lead the model to overestimate GPP in early 2019. Indeed, calibrating the model to the  
735 drought years of 2018 and 2019 yielded a lower ~~LUE~~LUE parameter (reduction of ~~LUE~~LUE value by 12%), which might support the possible legacy impact of last year drought on ~~LUE~~LUE parameter. Another possible explanation, alternatively or collectively to the plant legacy effect, would be variation/depletion of deep soil moisture storage (Jung et al., 2009). Since the model does not represent established internal feedback for carrying over effect after extreme events (Reichstein et al., 2013) and only consider the soil moisture up to 80 cm depth, thus the current model version would not reflect on such a process and  
740 GPP is likely to be overestimated.

Another limitation in our simulation is a lack to account for a possible effect of diffuse light on GPP response in the current model structure. We observed the potential role of diffuse light on GPP during some mismatch periods between eddy flux tower and modelled GPP across some of the sites (e.g., DE-HoH year 2107, FR-Fon year 2012, and US-Ha1 year 2010) (see Figure S1). The model underestimates GPP during these periods based on a lower PAR input, however, the observations show  
745 greater GPP despite lower input PAR. This is in line with findings of Knohl and Baldocchi (2008), where they investigated the effect of diffuse light on the forest ecosystem and discussed how diffuse radiation can lead to an increase in carbon uptake. Enhancement of GPP due to diffuse light is related to more evenly distribution and more efficient light penetration within the canopy (Yuan et al., 2014). Integration of such effect in the current model by introducing a time-varying ~~LUE~~LUE (condition-varying) (Wei et al., 2017) instead of the fixed LUE would improve the simulation result. In particular, under unprecedented  
750 global warming and climate change, future changes in cloud cover and aerosol ~~concentration~~concentrations are expected to modify the solar radiation and the subsequent ecosystem productivity (Durand et al., 2021; Meyer et al., 2014). Regarding LAI simulation, one limitation is that, at some points, the model cannot increase in LAI in the initial onset of LAI as fast as that of observation in the early growing period. In previous studies, it has been shown that the inclusion of non-structural carbon storage at the beginning of green-up might help to overcome this issue (Asaadi et al., 2018) and refine the model  
755 simulation results further. Aside from the current model limitations subjected to further improvement, the model exhibits a reasonable validity and performs equally well in estimating the temporal dynamics of GPP and LAI development compared to more complex land surface and biogeochemical models. The PCM being parsimonious makes it suitable for further reaching applications in coupled models. Dynamic development of LAI is relevant to GPP estimation and beneficial for hydrologic models providing them with prognostically driven LAI time series based on vegetation responses to temperature, particularly  
760 in the context of water budget responses to climate variability.

We aim, as a next step, to implement the presented model into the existing open-source mesoscale Hydrologic Model (mHM; Samaniego et al., 2010; Kumar et al., 2013, available at <https://www.ufz.de/mhm>) with a proven predictive power in simulating root-zone soil moisture dynamics (Boeing et al., 2021). The spatially simulated soil moisture derived from mHM would provide an alternative to (limited) soil moisture observations required for GPP simulation. In particular, in the face of  
765 ongoing and future climate changes and increasing occurrence of droughts (Harper et al., 2021), reliable simulations of soil

moisture are invaluable information to capture plant drought responses for the carbon cycle and climate feedbacks (Harper et al., 2021). Finally, in doing so, we expect an improved capability of the hydrological model to represent the coupled water and carbon (i.e., GPP/LAI in this study) components.

#### 4 Conclusion

770 In view of ongoing natural and anthropogenic changes, assessing the extent to which terrestrial plants can sequester atmospheric carbon and affect the water balance through LAI ~~implication-are-is~~ essential for effective climate-adaptation and resilience plans. ~~In this study, we developed~~ Here, we present a parsimonious canopy model (PCM) with a medium level of complexity to simulate canopy GPP and LAI. In the PCM model the carbon uptake drives leaf biomass accumulation based on a mass balance approach. The model employs the light use efficiency principle in which the core concept is the conversion of  
775 absorbed photosynthetically active radiation (PAR) into biomass. An integrated phenology submodel, from which allocation of carbon to and decay from the leaf pool is guided, is incorporated to predict the timing of leaf development and characterising different phenological stages. The PCM model performed reasonably well in reproducing the daily development of GPP and LAI in deciduous broad-leaved forest ~~biome~~ biomes across Europe and North America. The model runs with a few required inputs: ~~air~~ air temperature, vapour pressure deficit, PAR, and soil moisture (optional, recommended in dry regions and drought  
780 events). Although the proposed model runs with a number of parameters for representing the relevant processes (29 parameters without the soil moisture-related parameters), a global sensitivity analysis showed that only 10 parameters (on average across sites) were sensitive and had to be inferred via calibration. The result reaffirms that light use efficiency and specific leaf area index parameters are by far the most informative parameters in GPP and LAI simulations, respectively. The on-site calibrated maximum ~~LUE-LUE~~ parameter showed relatively large variation within the sites with greater maximum ~~LUE-at~~ LUE in  
785 Denmark (Dk-Sor site) and lower value ~~at-in Italy~~ (IT-Ro1 site). It implies that applying a fixed biome-specific maximum ~~LUE~~ LUE does not hold applicable over different locations. Moreover, modelled GPP during growing season was shown to be almost insensitive to LAI changes. This indicates that GPP is saturated at a particular value of LAI and any further increase in LAI does not necessarily increase the resultant GPP. We also tested the robustness and generality of the underlying model structure, identifying a compromise set of model parameters applicable to all sites (region-wide). The results show that the  
790 model application is possible without site-specific calibration and yet yielding reasonable model quality. The model's skill in capturing the LAI dynamics – that was not used in the parameter inference process – further confirms the robustness of the presented model structure. Given the scarce soil moisture information, we expect that simulated soil moisture derived from a hydrological model would improve the representation of GPP simulations, particularly at semiarid regions or ~~in~~ during drought events. We envision that the medium complexity of the presented model allows a seamless integration into large scale hydrolog-  
795 ical models to better represent ecohydrological aspects of ecosystems. We plan to implement the PCM model into the existing hydrologic models (e.g., open-source mesoscale Hydrologic Model; mHM), thereby enabling an improved representation of coupled water and carbon fluxes, in the face of a changing environment. To allow for a seamless estimation of carbon and water fluxes, we plan to include implementation of a robust regional parameter inference approach (e.g., establishing regionalized

~~LUE~~-LUE parameter through a multiscale parameterization approach (Samaniego et al., 2010)) and performing extensive  
800 cross-validation experiments to ensure credible model simulations across a wide range of spatial domains.

*Code availability.* The PCM is archived at <https://doi.org/10.5281/zenodo.6373776> (Bahrami et al., 2022) (last access: 21 march 2022). It is also publicly available at <https://git.ufz.de/bahrami/pcm> (last access: 21 march 2022).

805 *Data availability.* The flux tower dataset for DK-Sor, CA-Oas, DE-Hai, FR-Fon, IT-Ro1, US-Ha1, US-Oho, and US-MMS can be accessed from the FLUXNET 2015 Tier 1 at <https://fluxnet.org/data/fluxnet2015-dataset/> (accessed on 20 july 2021). Data from DE-HoH are available by contact [corinna.bebmann@ufz.de](mailto:corinna.bebmann@ufz.de) and [felix.pohl@ufz.de](mailto:felix.pohl@ufz.de). LAI field measurements for US-Ha1 can be downloaded from <https://harvardforest1.fas.harvard.edu/exist/apps/datasets/showData.html?id=hf069> (accessed on 20 January 2022)

*Author contributions.* BB coded and scripted the model. BB performed the sensitivity analysis. BB also prepared the manuscript. RK, AH, and ST were involved in interpretation of the results and discussions. All authors contributed to results discussion, reviewing, and editing the manuscript.

810 *Competing interests.* The contact author has declared that neither they nor their co-authors have any competing interests.

*Acknowledgements.* We acknowledge the FLUXNET data network for providing the data at participant flux sites: DK-Sor, CA-Oas, DE-Hai, FR-Fon, US-Ha1, US-Oho, US-MMS, IT-Ro1 used in our study. We would like to thank F. ~~Paul~~Pohl for providing data ~~at~~from the DE-HoH flux site. We thank A. Klosterhalfen for helpful information on data ~~at~~for DE-Hai. We would also like to thank C. Rebmann (DE-HoH), M. Mund (DE-Hai), T. Whitby (US-Ha1), M.P. Voyles (US-MMS) for sharing the LAI data in this study.

## 815 References

- Ariza-Carricondo, C., Mauro, F., Op de Beeck, M., Roland, M., Gielen, B., Vitale, D., Ceulemans, R., and Papale, D.: A comparison of different methods for assessing leaf area index in four canopy types, *Central European Forestry Journal*, 65, <https://doi.org/10.2478/forj-2019-0011>, 2019.
- Arora, V.: Modeling vegetation as dynamic component in soil-vegetation-atmosphere transfer schemes and hydrological models, *Reviews of Geophysics - REV GEOPHYS*, 40, <https://doi.org/10.1029/2001RG000103>, 2002.
- 820 Arsenault, K., Nearing, G., Wang, S., Yatheendradas, S., and Peters-Lidard, C.: Parameter Sensitivity of the Noah-MP Land Surface Model with Dynamic Vegetation, *Journal of Hydrometeorology*, 19, <https://doi.org/10.1175/JHM-D-17-0205.1>, 2018.
- Asaadi, A., Arora, V. K., Melton, J. R., and Bartlett, P.: An improved parameterization of leaf area index (LAI) seasonality in the Canadian Land Surface Scheme (CLASS) and Canadian Terrestrial Ecosystem Model (CTEM) modelling framework, *Biogeosciences*, 15, 6885–6907, <https://doi.org/10.5194/bg-15-6885-2018>, 2018.
- 825 Balzarolo, M., Valdameri, N., Fu, Y. H., Schepers, L., Janssens, I. A., and Campioli, M.: Different determinants of radiation use efficiency in cold and temperate forests, *Global Ecology and Biogeography*, 28, 1649–1667, <https://doi.org/https://doi.org/10.1111/geb.12985>, 2019.
- Beer, C., Reichstein, M., Tomelleri, E., Ciais, P., Jung, M., Carvalhais, N., Rodenbeck, C., Arain, M., Baldocchi, D., Bonan, G., Bondeau, A., Cescatti, A., Lasslop, G., Lindroth, A., Lomas, M., Luyssaert, S., Margolis, H., Oleson, K., Rouspard, O., and Papale, D.: Terrestrial Gross Carbon Dioxide Uptake: Global Distribution and Covariation with Climate, *Science*, 329, 834–838, <https://doi.org/10.1126/science.1184984>, 2010.
- Boeing, F., Rakovech, O., Kumar, R., Samaniego, L., Schrön, M., Hildebrandt, A., Rebmann, C., Thober, S., Müller, S., Zacharias, S., Bogena, H., Schneider, K., Kiese, R., and Marx, A.: High-resolution drought simulations and comparison to soil moisture observations in Germany, *Hydrology and Earth System Sciences Discussions*, 2021, 1–35, <https://doi.org/10.5194/hess-2021-402>, 2021.
- 835 Bohn, F. J., Frank, K., and Huth, A.: Of climate and its resulting tree growth: Simulating the productivity of temperate forests, *Ecological Modelling*, 278, 9–17, <https://doi.org/https://doi.org/10.1016/j.ecolmodel.2014.01.021>, 2014.
- Bonhomme, R. and Chartier, P.: The interpretation and automatic measurement of hemispherical photographs to obtain sunlit foliage area and gap frequency, *Israel J. Agric. Res.*, 22, 53–61, 1972.
- Boons-Prins, E.: Grassland simulation with the LPJmL model : version 3.4.018, no. 172 in *WOt-werkdocument*, Wettelijke Onderzoekstaken Natuur and Milieu, 2010.
- 840 Buras, A., Rammig, A., and Zang, C. S.: Quantifying impacts of the 2018 drought on European ecosystems in comparison to 2003, *Biogeosciences*, 17, 1655–1672, <https://doi.org/10.5194/bg-17-1655-2020>, 2020.
- Che, M.-L., Chen, B.-Z., Wang, Y., and Guo, X.-Y.: Review of dynamic global vegetation models (DGVMs), *Ying yong sheng tai xue bao = The journal of applied ecology / Zhongguo sheng tai xue xue hui*, *Zhongguo ke xue yuan Shenyang ying yong sheng tai yan jiu suo zhu ban*, 25, 263–71, 2014.
- 845 Chen, Y., Gu, H., Wang, M., Gu, Q., Ding, Z., Mingguo, M., Liu, R., and Tang, X.: Contrasting Performance of the Remotely-Derived GPP Products over Different Climate Zones across China, *Remote Sensing*, 11, 1855, <https://doi.org/10.3390/rs11161855>, 2019.
- Cheng, Y.-B., Zhang, Q., Lyapustin, A., Wang, Y., and Middleton, E.: Impacts of light use efficiency and fPAR parameterization on gross primary production modeling, *Agricultural and Forest Meteorology*, s 189–190, 187–197, <https://doi.org/10.1016/j.agrformet.2014.01.006>, 2014.
- 850



- Chiesi, M., Fibbi, L., Genesio, L., Gioli, B., Magno, R., Maselli, F., Moriondo, M., and Vaccari, F.: Integration of ground and satellite data to model Mediterranean forest processes, *International Journal of Applied Earth Observation and Geoinformation*, 13, 504–515, <https://doi.org/https://doi.org/10.1016/j.jag.2010.10.006>, 2011.
- Cholet, C., Houle, D., Sylvain, J.-D., Doyon, F., and Maheu, A.: Climate Change Increases the Severity and Duration of Soil Water Stress in the Temperate Forest of Eastern North America, *Frontiers in Forests and Global Change*, 5, 879–882, <https://doi.org/10.3389/ffgc.2022.879382>, 2022.
- Collatz, G., Ribas-Carbo, M., and Berry, J.: Coupled Photosynthesis-Stomatal Conductance Model for Leaves of C<sub>4</sub> Plants, *Functional Plant Biology*, 19, <https://doi.org/10.1071/PP9920519>, 1992.
- Coops, N. C., Waring, R. H., and Law, B. E.: Assessing the past and future distribution and productivity of ponderosa pine in the Pacific Northwest using a process model, 3-PG, *Ecological Modelling*, 183, 107–124, <https://doi.org/https://doi.org/10.1016/j.ecolmodel.2004.08.002>, 2005.
- Cox, P., Betts, R., Bunton, C., Essery, R., Rowntree, P., and Smith, J.: The impact of new land surface physics on the GCM simulation of climate and climate sensitivity, *Climate Dynamics*, 15, 183–203, <https://doi.org/10.1007/s003820050276>, 1999.
- Cueva, A., Bullock, S. H., Méndez-Alonzo, R., López-Reyes, E., and Vargas, R.: Foliage Senescence as a Key Parameter for Modeling Gross Primary Productivity in a Mediterranean Shrubland, *Journal of Geophysical Research: Biogeosciences*, 126, e2020JG005839, <https://doi.org/https://doi.org/10.1029/2020JG005839>, e2020JG005839 2020JG005839, 2021.
- Cuntz, M., Mai, J., Samaniego, L., Clark, M., Wulfmeyer, V., Branch, O., Attinger, S., and Thober, S.: The impact of standard and hard-coded parameters on the hydrologic fluxes in the Noah-MP land surface model, *Journal of Geophysical Research: Atmospheres*, 121, 10,676–10,700, <https://doi.org/https://doi.org/10.1002/2016JD025097>, 2016.
- Durand, M., Murchie, E. H., Lindfors, A. V., Urban, O., Aphalo, P. J., and Robson, T. M.: Diffuse solar radiation and canopy photosynthesis in a changing environment, *Agricultural and Forest Meteorology*, 311, 108–114, <https://doi.org/https://doi.org/10.1016/j.agrformet.2021.108684>, 2021.
- Dyderski, M. K., Chmura, D., Dylewski, Ł., Horodecki, P., Jagodziński, A. M., Pietras, M., Robakowski, P., and Woźniak, B.: Biological Flora of the British Isles: *Quercus rubra*, *Journal of Ecology*, 108, 1199–1225, <https://doi.org/https://doi.org/10.1111/1365-2745.13375>, 2020.
- Estoque, R., Dasgupta, R., Winkler, K., Avitabile, V., Johnson, B., Myint, S., Gao, Y., Ooba, M., Murayama, Y., and Lasco, R.: Spatiotemporal pattern of global forest change over the past 60 years and the forest transition theory, *Environmental Research Letters*, 17, 084–022, <https://doi.org/10.1088/1748-9326/ac7df5>, 2022.
- Fang, H., Baret, F., Plummer, S., and Schaepman-Strub, G.: An Overview of Global Leaf Area Index (LAI): Methods, Products, Validation, and Applications, *Reviews of Geophysics*, 57, 739–799, <https://doi.org/https://doi.org/10.1029/2018RG000608>, 2019.
- Farquhar, G. D., von Caemmerer, S., and Berry, J. A.: A biochemical model of photosynthetic CO<sub>2</sub> assimilation in leaves of C<sub>3</sub> species, *Planta*, 149, 78–90, <https://doi.org/10.1007/BF00386231>, 1980.
- Fibbi, L., Moriondo, M., Chiesi, M., Bindi, M., and Maselli, F.: Impacts of climate change on the gross primary production of Italian forests, *Annals of Forest Science*, 76, 59, <https://doi.org/10.1007/s13595-019-0843-x>, 2019.
- Fischer, R., Armstrong, A., Shugart, H. H., and Huth, A.: Simulating the impacts of reduced rainfall on carbon stocks and net ecosystem exchange in a tropical forest, *Environmental Modelling and Software*, 52, 200–206, <https://doi.org/https://doi.org/10.1016/j.envsoft.2013.10.026>, 2014.

- Fischer, R., Bohn, F., Dantas de Paula, M., Dislich, C., Groeneveld, J., Gutiérrez, A. G., Kazmierczak, M., Knapp, N., Lehmann, S., Paulick, S., Pütz, S., Rödig, E., Taubert, F., Köhler, P., and Huth, A.: Lessons learned from applying a forest gap model to understand ecosystem and carbon dynamics of complex tropical forests, *Ecological Modelling*, 326, 124–133, <https://doi.org/https://doi.org/10.1016/j.ecolmodel.2015.11.018>, next generation ecological modelling, concepts, and theory: structural realism, emergence, and predictions, 2016.
- Fleischer, K., Rebel, K. T., van der Molen, M. K., Erisman, J. W., Wassen, M. J., van Loon, E. E., Montagnani, L., Gough, C. M., Herbst, M., Janssens, I. A., Gianelle, D., and Dolman, A. J.: The contribution of nitrogen deposition to the photosynthetic capacity of forests, *Global Biogeochemical Cycles*, 27, 187–199, <https://doi.org/https://doi.org/10.1002/gbc.20026>, 2013.
- Foley, J. and Ramankutty, N.: A primer on the terrestrial carbon cycle: What we don't know but should, 2003.
- Forzieri, G., Girardello, M., Ceccherini, G., Spinoni, J., Feyen, L., Hartmann, H., Beck, P. S. A., Camps-Valls, G., Chirici, G., Mauri, A., and Cescatti, A.: Emergent vulnerability to climate-driven disturbances in European forests, *Nature Communications*, 12, 1081, <https://doi.org/10.1038/s41467-021-21399-7>, 2021.
- Francés, F., Velez, J., and Velez, J.: Split-parameter structure for the automatic calibration of distributed hydrological models, *Journal of Hydrology*, 332, 226–240, <https://doi.org/10.1016/j.jhydrol.2006.06.032>, 2007.
- Friedlingstein, P., Joel, G., Field, C. B., and Fung, I. Y.: Toward an allocation scheme for global terrestrial carbon models, *Glob. Change Biol.*, 5, 755–770, <https://doi.org/10.1046/j.1365-2486.1999.00269.x>, 1999.
- Frost-Christensen, H. and Sand-Jensen, K.: The quantum efficiency of photosynthesis in macroalgae and submerged angiosperms, *Oecologia*, 91, 377–384, <https://doi.org/10.1007/BF00317627>, 1992.
- Gamon, J. A.: Reviews and Syntheses: optical sampling of the flux tower footprint, *Biogeosciences*, 12, 4509–4523, <https://doi.org/10.5194/bg-12-4509-2015>, 2015.
- Gim, H.-J., Park, S. K., Kang, M., Thakuri, B. M., Kim, J., and Ho, C.-H.: An improved parameterization of the allocation of assimilated carbon to plant parts in vegetation dynamics for Noah-MP, *Journal of Advances in Modeling Earth Systems*, 9, 1776–1794, <https://doi.org/https://doi.org/10.1002/2016MS000890>, 2017.
- Göhler, M., Mai, J., and Cuntz, M.: Use of eigendecomposition in a parameter sensitivity analysis of the Community Land Model, *Journal of Geophysical Research: Biogeosciences*, 118, 904–921, <https://doi.org/https://doi.org/10.1002/jgrg.20072>, 2013.
- Gower, S. and Norman, J.: Rapid Estimation of Leaf Area Index in Conifer and Broad-Leaf Plantations, *Ecology*, 72, 1896–1900, <https://doi.org/10.2307/1940988>, 1991.
- Granier, A., Bréda, N., Biron, P., and Villette, S.: A lumped water balance model to evaluate duration and intensity of drought constraints in forest stands, *Ecological Modelling*, 116, 269–283, [https://doi.org/https://doi.org/10.1016/S0304-3800\(98\)00205-1](https://doi.org/https://doi.org/10.1016/S0304-3800(98)00205-1), 1999.
- Granier, A., Ceschia, E., Damesin, C., Dufrêne, E., Epron, D., Gross, P., Lebaube, S., Le Dantec, V., Le Goff, N., Lemoine, D., Lucot, E., Ottorini, J. M., Pontailler, J. Y., and Saugier, B.: The carbon balance of a young Beech forest, *Functional Ecology*, 14, 312–325, <https://doi.org/https://doi.org/10.1046/j.1365-2435.2000.00434.x>, 2000.
- Grimm, N., Chapin III, F. S., Bierwagen, B., Gonzalez, P., Groffman, P., Luo, Y., Melton, F., Nadelhoffer, K., Pairis, A., Raymond, P., Schimel, J., and Williamson, C.: The impacts of climate change on ecosystem structure and function, *Frontiers in Ecology and the Environment*, 11, 474–482, <https://doi.org/10.1890/120282>, 2013.
- Guan, X., Chen, J., Shen, H., and Xie, X.: A modified two-leaf light use efficiency model for improving the simulation of GPP using a radiation scalar, 2021.

- 925 Gupta, H., Kling, H., Yilmaz, K., and Martinez, G.: Decomposition of the Mean Squared Error and NSE Performance Criteria: Implications for Improving Hydrological Modelling, *Journal of Hydrology*, 377, 80–91, <https://doi.org/10.1016/j.jhydrol.2009.08.003>, 2009.
- Harper, A., Williams, K., McGuire, P., Carolina, M., Rojas, D., Verhoef, A., Huntingford, C., Rowland, L., Marthews, T., Eller, C., Mathison, C., Nobrega, R., Gedney, N., Vidale, P., Pandey, D., Garrigues, S., Wright, A., and Wohlfahrt, G.: Improvement of modeling plant responses to low soil moisture in JULESv4.9 and evaluation against flux tower measurements, *Geoscientific Model Development*, 14, 3269–3294, <https://doi.org/10.5194/gmd-14-3269-2021>, 2021.
- 930 Hartge, K. H.: Feddes, R. A., Kowalik, P. I. und Zaradny, H.: simulation of field water use and crop yield. Pudoc (Centre for agricultural publishing and documentation) Wageningen, Niederlande, 195 Seiten, 13 Abbildungen, Paperback. Preis: hfl 30,-, *Zeitschrift für Pflanzenernährung und Bodenkunde*, 143, 254–255, <https://doi.org/https://doi.org/10.1002/jpln.19801430219>, 1980.
- Haverd, V., Smith, B., Raupach, M., Briggs, P., Nieradzik, L., Beringer, J., Hutley, L., Trudinger, C., and Cleverly, J.: Coupling carbon allocation with leaf and root phenology predicts tree–grass partitioning along a savanna rainfall gradient, *Biogeosciences*, 13, 761–779, <https://doi.org/10.5194/bg-13-761-2016>, 2016.
- 935 Heinsch, F., Reeves, M., Votava, P., Kang, S., Cristina, M., Zhao, M., Glassy, J., Jolly, W., Loehman, R., Bowker, C., Kimball, J., and Nemani, R.: User’s guide GPP and NPP (MOD17A2/A3) products NASA MODIS land algorithm, Version 2.0, 2003.
- Hidy, D., Barcza, Z., Marjanović, H., Ostrogović Sever, M. Z., Dobor, L., Gelybó, G., Fodor, N., Pintér, K., Churkina, G., Running, S., Thornton, P., Bellocchi, G., Haszpra, L., Horváth, F., Suyker, A., and Nagy, Z.: Terrestrial ecosystem process model Biome-BGCMuSo v4.0: summary of improvements and new modeling possibilities, *Geoscientific Model Development*, 9, 4405–4437, <https://doi.org/10.5194/gmd-9-4405-2016>, 2016.
- 940 Hidy, D., Barcza, Z., Hollós, R., Dobor, L., Ács, T., Zacháry, D., Filep, T., Pásztor, L., Incze, D., Dencsó, M., Tóth, E., Merganičová, K., Thornton, P., Running, S., and Fodor, N.: Soil-related developments of the Biome-BGCMuSo v6.2 terrestrial ecosystem model, *Geoscientific Model Development*, 15, 2157–2181, <https://doi.org/10.5194/gmd-15-2157-2022>, 2022.
- 945 Hirmas, D., Giménez, D., Nemes, A., Kerry, R., Brunzell, N., and Wilson, C.: Climate-induced changes in continental-scale soil macroporosity may intensify water cycle, *Nature*, 561, <https://doi.org/10.1038/s41586-018-0463-x>, 2018.
- Holtmann, A., Huth, A., Pohl, F., Rebmann, C., and Fischer, R.: Carbon Sequestration in Mixed Deciduous Forests: The Influence of Tree Size and Species Composition Derived from Model Experiments, *Forests*, 12, <https://doi.org/10.3390/f12060726>, 2021.
- 950 Hou, Z., Huang, M., Leung, L. R., Lin, G., and Ricciuto, D. M.: Sensitivity of surface flux simulations to hydrologic parameters based on an uncertainty quantification framework applied to the Community Land Model, *Journal of Geophysical Research: Atmospheres*, 117, <https://doi.org/https://doi.org/10.1029/2012JD017521>, 2012.
- Huang, X., Zheng, Y., Zhang, H., Lin, S., Liang, S., Li, X., Ma, M., and Yuan, W.: High spatial resolution vegetation gross primary production product: Algorithm and validation, *Science of Remote Sensing*, 5, 100 049, <https://doi.org/https://doi.org/10.1016/j.srs.2022.100049>, 2022.
- 955 Imadi, S., Gul, A., Dikilitas, M., Karakas, S., Sharma, I., and Ahmad, P.: Water stress: Types, causes, and impact on plant growth and development, pp. 343–355, <https://doi.org/10.1002/9781119054450.ch21>, 2016.
- Iooss, B. and Lemaître, P.: A Review on Global Sensitivity Analysis Methods, *Operations Research/ Computer Science Interfaces Series*, 59, [https://doi.org/10.1007/978-1-4899-7547-8\\_5](https://doi.org/10.1007/978-1-4899-7547-8_5), 2014.
- 960 IPCC: Climate Change 2021: The Physical Science Basis. Contribution of Working Group I to the Sixth Assessment Report of the Intergovernmental Panel on Climate Change, Masson-Delmotte, V., P. Zhai, A. Pirani, S.L. Connors, C. Péan, S. Berger, N. Caud, Y. Chen, L.

- Goldfarb, M.I. Gomis, M. Huang, K. Leitzell, E. Lonnoy, J.B.R. Matthews, T.K. Maycock, T. Waterfield, O. Yelekçi, R. Yu, and B. Zhou, Cambridge University Press. In Press., 2021.
- Istanbulluoglu, E., Wang, T., and Wedin, D. A.: Evaluation of ecohydrologic model parsimony at local and regional scales in a semiarid grassland ecosystem, *Ecohydrology*, 5, 121–142, <https://doi.org/https://doi.org/10.1002/eco.211>, 2012.
- Jackson, R. B., Canadell, J., Ehleringer, J. R., Mooney, H. A., Sala, O. E., and Schulze, E. D.: A global analysis of root distributions for terrestrial biomes, *Oecologia*, 108, 389–411, <https://doi.org/10.1007/BF00333714>, 1996.
- Jolly, W. M., Nemani, R., and Running, S. W.: A generalized, bioclimatic index to predict foliar phenology in response to climate, *Global Change Biology*, 11, 619–632, <https://doi.org/https://doi.org/10.1111/j.1365-2486.2005.00930.x>, 2005.
- Jung, M., Vetter, M., Herold, M., Churkina, G., Reichstein, M., Zaehle, S., Ciais, P., Viovy, N., Bondeau, A., Chen, Y., Trusilova, K., Feser, F., and Heimann, M.: Uncertainties of modeling gross primary productivity over Europe: A systematic study on the effects of using different drivers and terrestrial biosphere models, *Global Biogeochemical Cycles*, 21, <https://doi.org/10.1029/2006GB002915>, 2007.
- Jung, M., Reichstein, M., and Bondeau, A.: Towards global empirical upscaling of FLUXNET eddy covariance observations: Validation of a model tree ensemble approach using a biosphere model, *Biogeosciences*, 6, <https://doi.org/10.5194/bgd-6-5271-2009>, 2009.
- Kattge, J., Diaz, S., Lavorel, S., Prentice, I., Leadley, P., Bönsch, G., Garnier, E., Westoby, M., Reich, P., Wright, I., Cornelissen, J., Violle, C., Harrison, S., Bodegom, P., Reichstein, M., Enquist, B., Soudzilovskaia, N., Ackerly, D., Anand, M., and Wirth, C.: TRY - a global database of plant traits, *Global Change Biology*, 17, 2905–2935, <https://doi.org/10.1111/j.1365-2486.2011.02451.x>, 2011.
- Kennedy, D., Swenson, S., Oleson, K. W., Lawrence, D. M., Fisher, R., Lola da Costa, A. C., and Gentine, P.: Implementing Plant Hydraulics in the Community Land Model, Version 5, *Journal of Advances in Modeling Earth Systems*, 11, 485–513, <https://doi.org/https://doi.org/10.1029/2018MS001500>, 2019.
- Knohl, A. and Baldocchi, D.: Effects of diffuse radiation on canopy gas exchange processes in a forest ecosystem, *Journal of Geophysical Research*, *Biogeosciences*, 113, G02 023, doi:10.1029/2007JG000 663, <https://doi.org/10.1029/2007JG000663>, 2008.
- Knorr, W.: Annual and interannual CO<sub>2</sub> exchanges of the terrestrial biosphere: process-based simulations and uncertainties, *Global Ecology and Biogeography*, 9, 225–252, <https://doi.org/https://doi.org/10.1046/j.1365-2699.2000.00159.x>, 2000.
- Konings, A. G., Williams, A. P., and Gentine, P.: Sensitivity of grassland productivity to aridity controlled by stomatal and xylem regulation, *Nature Geoscience*, 10, 284–288, <https://doi.org/10.1038/ngeo2903>, 2017.
- Kuczera, G. and Parent, E.: Monte Carlo assessment of parameter uncertainty in conceptual catchment models: the Metropolis algorithm, *Journal of Hydrology*, 211, 69–85, [https://doi.org/https://doi.org/10.1016/S0022-1694\(98\)00198-X](https://doi.org/https://doi.org/10.1016/S0022-1694(98)00198-X), 1998.
- Kumar, R., Samaniego, L., and Attinger, S.: Implications of distributed hydrologic model parameterization on water fluxes at multiple scales and locations, *Water Resources Research*, 49, <https://doi.org/10.1029/2012WR012195>, 2013.
- Lal, R. and Lorenz, K.: Carbon Sequestration in Temperate Forests, pp. 187–202, [https://doi.org/10.1007/978-94-007-4159-1\\_9](https://doi.org/10.1007/978-94-007-4159-1_9), 2012.
- Law, B., Anthoni, P., and Aber, J.: Measurements of gross and net ecosystem productivity and water vapour exchange of a *Pinus ponderosa* ecosystem, and an evaluation of two generalized models, *Global Change Biology - GLOB CHANGE BIOL*, 6, 155–168, <https://doi.org/10.1046/j.1365-2486.2000.00291.x>, 2000.
- Lee, H., Park, J., Cho, S., Lee, M., and Kim, H.: Impact of leaf area index from various sources on estimating gross primary production in temperate forests using the JULES land surface model, *Agricultural and Forest Meteorology*, p. 107614, 2019.
- Li, J., Wang, Y., Duan, Q., Lu, X., Pak, B., Wiltshire, A., Robertson, E., and Ziehn, T.: Quantification and attribution of errors in the simulated annual gross primary production and latent heat fluxes by two global land surface models, *Journal of Advances in Modeling Earth Systems*, 8, <https://doi.org/10.1002/2015MS000583>, 2016.

- 1000 Li, Q., Lu, X., Wang, Y., Huang, X., Cox, P. M., and Luo, Y.: Leaf area index identified as a major source of variability in modeled CO<sub>2</sub> fertilization, *Biogeosciences*, 15, 6909–6925, <https://doi.org/10.5194/bg-15-6909-2018>, 2018.
- Lloyd, J. and Taylor, J. A.: On the temperature dependence of soil respiration, *Functional Ecology*, 8, 315–323, 1994.
- Luyssaert, S., Inglisma, I., Jungs, M., Richardson, A., Reichsteins, M., Papale, D., Piao, S., Schulzes, E., Wingate, L., Matteucci, G., Aragaoss, L., Aubinet, M., Beers, C., Bernhofer, C., Black, K., Bonal, D., Bonnefonds, J., Chambers, J., Ciais, P., and Janssens, I.: CO<sub>2</sub> balance of boreal, temperate, and tropical forests, *Global Change Biology* 13 (2007) 12, 2007.
- 1005 Ma, H., Ma, C., Li, X., Yuan, W., Liu, Z., and Zhu, G.: Sensitivity and Uncertainty Analyses of Flux-based Ecosystem Model towards Improvement of Forest GPP Simulation, *Sustainability*, 12, <https://doi.org/10.3390/su12072584>, 2020.
- Ma, J., Yan, X., Dong, W., and Chou, J.: Gross primary production of global forest ecosystems has been overestimated, *Scientific reports*, 5, 10820, <https://doi.org/10.1038/srep10820>, 2015.
- 1010 Madani, N., Kimball, J. S., Affleck, D. L. R., Kattge, J., Graham, J., van Bodegom, P. M., Reich, P. B., and Running, S. W.: Improving ecosystem productivity modeling through spatially explicit estimation of optimal light use efficiency, *Journal of Geophysical Research: Biogeosciences*, 119, 1755–1769, <https://doi.org/https://doi.org/10.1002/2014JG002709>, 2014.
- Malhi, Y., Doughty, C., and Galbraith, D.: The allocation of ecosystem net primary productivity in tropical forests, *Philosophical Transactions of the Royal Society B: Biological Sciences*, 366, 3225–3245, <https://doi.org/10.1098/rstb.2011.0062>, 2011.
- 1015 Malhi, Y., Franklin, J., Seddon, N., Solan, M., Turner, M., Field, C., and Knowlton, N.: Climate change and ecosystems: Threats, opportunities and solutions, *Philosophical Transactions of the Royal Society B: Biological Sciences*, 375, 20190104, <https://doi.org/10.1098/rstb.2019.0104>, 2020.
- Maselli, F., Pasqui, M., Chirici, G., Chiesi, M., L. F., Salvati, R., and Corona, P.: Modeling primary production using a 1 km daily meteorological data set, *Climate Research*, 54, 271–285, <https://doi.org/10.3354/cr01121>, 2012.
- 1020 Melton, J. R. and Arora, V. K.: Sub-grid scale representation of vegetation in global land surface schemes: implications for estimation of the terrestrial carbon sink, *Biogeosciences*, 11, 1021–1036, <https://doi.org/10.5194/bg-11-1021-2014>, 2014.
- Melton, J. R. and Arora, V. K.: Competition between plant functional types in the Canadian Terrestrial Ecosystem Model (CTEM) v. 2.0, *Geoscientific Model Development*, 9, 323–361, <https://doi.org/10.5194/gmd-9-323-2016>, 2016.
- Meyer, L., Brinkman, S., van Kesteren, L., Leprince-Ringuet, N., and van Boxmeer, F. E.: Climate Change 2014: Synthesis Report. Contribution of Working Groups I, II and III to the Fifth Assessment Report of the Intergovernmental Panel on Climate Change, Cambridge University Press, Geneva, Switzerland, 2014.
- 1025 Monsi, M. and Saeki, T.: Ober den Lichtfaktor in den Pflanzengesllschat\*en und seine Bedeutung ffor die Stoffproductkti, *Bot.*, 14, 22–52, 1953.
- Monteith, J. L.: Solar Radiation and Productivity in Tropical Ecosystems, *Journal of Applied Ecology*, 9, 20, 1972.
- 1030 Monteith, J. L.: Climate and the Efficiency of Crop Production in Britain, *Philosophical Transactions of the Royal Society of London Series B*, 281, 277–294, <https://doi.org/10.1098/rstb.1977.0140>, 1977.
- Nathalie, B.: Ground-based measurements of leaf area index: A review of methods, instruments and current controversies, *Journal of experimental botany*, 54, 2403–17, <https://doi.org/10.1093/jxb/erg263>, 2003.
- Nathalie, B., Huc, R., Granier, A., and Dreyer, E.: Temperate forest trees and stands under severe drought: A review of ecophysiological responses, adaptation processes and long-term consequences, <http://dx.doi.org/10.1051/forest:2006042>, 63, <https://doi.org/10.1051/forest:2006042>, 2006.

- Nigatu, M.: Review on Effect of Climate Change on Forest Ecosystem, *International Journal of Environmental Sciences and Natural Resources*, 17, <https://doi.org/10.19080/IJESNR.2019.17.555968>, 2019.
- Nossent, J. and Bauwens, W.: Optimising the convergence of a Sobol' sensitivity analysis for an environmental model: application of an appropriate estimate for the square of the expectation value and the total variance, 2012.
- Ostle, N. J., Smith, P., Fisher, R., Ian Woodward, F., Fisher, J. B., Smith, J. U., Galbraith, D., Levy, P., Meir, P., McNamara, N. P., and Bardgett, R. D.: Integrating plant–soil interactions into global carbon cycle models, *Journal of Ecology*, 97, 851–863, <https://doi.org/10.1111/j.1365-2745.2009.01547.x>, 2009.
- Pan, N., Wang, S., Wei, F., Shen, M., and Fu, B.: Inconsistent changes in NPP and LAI determined from the parabolic LAI versus NPP relationship, *Ecological Indicators*, 131, 108 134, <https://doi.org/10.1016/j.ecolind.2021.108134>, 2021.
- Pan, Y., Birdsey, R., Fang, J., Houghton, R., Kauppi, P., Kurz, W., Phillips, O., Shvidenko, A., Lewis, S., Canadell, J., Ciais, P., Jackson, R., Pacala, S., McGuire, A., Piao, S., Rautiainen, A., Sitch, S., and Hayes, D.: A Large and Persistent Carbon Sink in the World's Forests, *Science (New York, N.Y.)*, 333, 988–93, <https://doi.org/10.1126/science.1201609>, 2011.
- Pasquato, M., Medici, C., Friend, A., and Frances, F.: Comparing two approaches for parsimonious vegetation modelling in semiarid regions using satellite data, *ECOHYDROLOGY*, 8, 1024–1036, 2015.
- Pastorello, G., Trotta, C., Canfora, E., Chu, H., Christianson, D., Cheah, Y.-W., Poindexter, C., Chen, J., Elbashandy, A., Humphrey, M., Isaac, P., Polidori, D., Ribeca, A., Ingen, C., Zhang, L., Amiro, B., Ammann, C., Arain, M., Ardö, J., and Papale, D.: The FLUXNET2015 dataset and the ONEFlux processing pipeline for eddy covariance data, *Scientific Data*, 7, <https://doi.org/10.1038/s41597-020-0534-3>, 2020.
- Perez, G. R.: On the use of satellite data to calibrate a parsimonious ecohydrological model in ungauged basins, Ph.D. thesis, Departamento de Ingenieria Hidraulica y Medio Ambiente, Universitat Politecnica de Valencia, 2016.
- Potter, C. S., Randerson, J. T., Field, C. B., Matson, P. A., Vitousek, P. M., Mooney, H. A., and Klooster, S. A.: Terrestrial ecosystem production: A process model based on global satellite and surface data, *Global Biogeochemical Cycles*, 7, 811–841, <https://doi.org/10.1029/93GB02725>, 1993.
- Prince, S. and Goward, S.: Global Primary Production: A Remote Sensing Approach, *Journal of Biogeography*, 22, 815, 1995.
- Rahman, A., Zhang, X., Houser, P., Sauer, T., and Maggioni, V.: Global Assimilation of Remotely Sensed Leaf Area Index: The Impact of Updating More State Variables Within a Land Surface Model, *Frontiers in Water*, 3, 789 352, <https://doi.org/10.3389/frwa.2021.789352>, 2022.
- Rakovec, O., Hill, M. C., Clark, M. P., Weerts, A. H., Teuling, A. J., and Uijlenhoet, R.: Distributed Evaluation of Local Sensitivity Analysis (DELSA), with application to hydrologic models, *Water Resources Research*, 50, 409–426, <https://doi.org/10.1002/2013WR014063>, 2014.
- Reichstein, M., Bahn, M., Ciais, P., Frank, D., Mahecha, M., Seneviratne, S., Zscheischler, J., Beer, C., Buchmann, N., Frank, D., Papale, D., Rammig, A., Smith, P., Thonicke, K., Velde, M., Vicca, S., Walz, A., and Wattenbach, M.: Climate extremes and the carbon cycle, *Nature*, 500, 287–95, <https://doi.org/10.1038/nature12350>, 2013.
- Reinmann, A. B. and Hutya, L. R.: Edge effects enhance carbon uptake and its vulnerability to climate change in temperate broadleaf forests, *Proceedings of the National Academy of Sciences*, 114, 107–112, <https://doi.org/10.1073/pnas.1612369114>, 2017.
- Rödig, E., Huth, A., Bohn, F., Rebmann, C., and Cuntz, M.: Estimating the carbon fluxes of forests with an individual-based forest model, *Forest Ecosystems*, 4, 4, <https://doi.org/10.1186/s40663-017-0091-1>, 2017.

- Ruimy, A., Saugier, B., and Dedieu, G.: Methodology for the estimation of terrestrial net primary production from remotely sensed data, *Journal of Geophysical*, 99, 5263–5283, 1994.
- Ruimy, A., Kergoat, L., Bondeau, A., and Intercomparison, T. P. O. T. P. N. M.: Comparing global models of terrestrial net primary productivity (NPP): analysis of differences in light absorption and light-use efficiency, *Global Change Biology*, 5, 56–64, <https://doi.org/https://doi.org/10.1046/j.1365-2486.1999.00007.x>, 1999.
- Ruiz-Perez, G., Koch, J., Manfreda, S., Caylor, K., and Frances, F.: Calibration of a parsimonious distributed ecohydrological daily model in a data-scarce basin by exclusively using the spatio-temporal variation of NDVI, *Hydrology and Earth System Sciences*, 21, 6235–6251, <https://doi.org/10.5194/hess-21-6235-2017>, 2017.
- Running, S., Nemani, R., Heinsch, F., Zhao, M., Reeves, M., and Hashimoto, H.: A Continuous Satellite-Derived Measure of Global Terrestrial Primary Production, *BioScience*, 54, 547–560, [https://doi.org/10.1641/0006-3568\(2004\)054\[0547:ACSMOG\]2.0.CO;2](https://doi.org/10.1641/0006-3568(2004)054[0547:ACSMOG]2.0.CO;2), 2004.
- Running, S. W., Thornton, P. E., Nemani, R., and Glassy, J. M.: Global Terrestrial Gross and Net Primary Productivity from the Earth Observing System, pp. 44–57, Springer New York, New York, NY, [https://doi.org/10.1007/978-1-4612-1224-9\\_4](https://doi.org/10.1007/978-1-4612-1224-9_4), 2000.
- Saltelli, A.: Making best use of model evaluations to compute sensitivity indices, *Computer Physics Communications*, 145, 280–297, [https://doi.org/https://doi.org/10.1016/S0010-4655\(02\)00280-1](https://doi.org/https://doi.org/10.1016/S0010-4655(02)00280-1), 2002.
- Saltelli, A., Tarantola, S., and Chan, K. P.-S.: A Quantitative Model-Independent Method for Global Sensitivity Analysis of Model Output, *Technometrics*, 41, 39–56, <https://doi.org/10.1080/00401706.1999.10485594>, 1999.
- Samaniago, L., Kumar, R., and Attinger, S.: Multiscale parameter regionalization of a grid-based hydrologic model at the mesoscale, *Water Resources Research*, 46, <https://doi.org/https://doi.org/10.1029/2008WR007327>, 2010.
- Schaefer, K., Schwalm, C. R., Williams, C., Arain, M. A., Barr, A., Chen, J. M., Davis, K. J., Dimitrov, D., Hilton, T. W., Hollinger, D. Y., Humphreys, E., Poulter, B., Raczka, B. M., Richardson, A. D., Sahoo, A., Thornton, P., Vargas, R., Verbeeck, H., Anderson, R., Baker, I., Black, T. A., Bolstad, P., Chen, J., Curtis, P. S., Desai, A. R., Dietze, M., Dragoni, D., Gough, C., Grant, R. F., Gu, L., Jain, A., Kucharik, C., Law, B., Liu, S., Lokipitiya, E., Margolis, H. A., Matamala, R., McCaughey, J. H., Monson, R., Munger, J. W., Oechel, W., Peng, C., Price, D. T., Ricciuto, D., Riley, W. J., Roulet, N., Tian, H., Tonitto, C., Torn, M., Weng, E., and Zhou, X.: A model-data comparison of gross primary productivity: Results from the North American Carbon Program site synthesis, *Journal of Geophysical Research: Biogeosciences*, 117, <https://doi.org/https://doi.org/10.1029/2012JG001960>, 2012.
- Schaphoff, S., von Bloh, W., Rammig, A., Thonicke, K., Biemans, H., Forkel, M., Gerten, D., Heinke, J., Jägermeyr, J., Knauer, J., Langerwisch, F., Lucht, W., Mueller, C., Rolinski, S., and Waha, K.: LPJmL4 a dynamic global vegetation model with managed land Part 1: Model description, *Geoscientific Model Development*, 11, 1343–1375, 2017.
- Schnabel, F., Purucker, S., Schmitt, L., Engelmann, R. A., Kahl, A., Richter, R., Seele-Dilbat, C., Skiadaresis, G., and Wirth, C.: Cumulative growth and stress responses to the 2018-2019 drought in a European floodplain forest, *bioRxiv*, <https://doi.org/10.1101/2021.03.05.434090>, 2021.
- Schuldt, B., Buras, A., Arend, M., Vitasse, Y., Beierkuhnlein, C., Damm, A., Gharun, M., Grams, T. E., Hauck, M., Hajek, P., Hartmann, H., Hiltbrunner, E., Hoch, G., Holloway-Phillips, M., Körner, C., Larysch, E., Lübke, T., Nelson, D. B., Rammig, A., Rigling, A., Rose, L., Ruehr, N. K., Schumann, K., Weiser, F., Werner, C., Wohlgemuth, T., Zang, C. S., and Kahmen, A.: A first assessment of the impact of the extreme 2018 summer drought on Central European forests, *Basic and Applied Ecology*, 45, 86–103, <https://doi.org/https://doi.org/10.1016/j.baae.2020.04.003>, 2020.

- 1110 Schweppe, R., Thober, S., Kelbling, M., Kumar, R., Attinger, S., and Samaniego, L.: MPR 1.0: A stand-alone Multiscale Parameter Regionalization Tool for Improved Parameter Estimation of Land Surface Models, *Geoscientific Model Development Discussions*, 2021, 1–40, <https://doi.org/10.5194/gmd-2021-103>, 2021.
- Senf, C., Pflugmacher, D., Zhiqiang, Y., Sebal, J., Knorn, J., Neumann, M., Hostert, P., and Seidl, R.: Canopy mortality has doubled in Europe’s temperate forests over the last three decades, *Nature Communications*, 9, <https://doi.org/10.1038/s41467-018-07539-6>, 2018.
- 1115 Seo, H. and Kim, Y.: Role of remotely sensed leaf area index assimilation in eco-hydrologic processes in different ecosystems over East Asia with Community Land Model version 4.5 – Biogeochemistry, *Journal of Hydrology*, 594, 125 957, <https://doi.org/https://doi.org/10.1016/j.jhydrol.2021.125957>, 2021.
- Sitch, S., Smith, B., Prentice, I. C., Arneth, A., Bondeau, A., Cramer, W., Kaplan, J. O., Levis, S., Lucht, W., Sykes, M. T., Thonicke, K., and Venevsky, S.: Evaluation of ecosystem dynamics, plant geography and terrestrial carbon cycling in the LPJ dynamic global vegetation model, *Global Change Biology*, 9, 161–185, <https://doi.org/https://doi.org/10.1046/j.1365-2486.2003.00569.x>, 2003.
- 1120 Spielmann, F. M., Wohlfahrt, G., Hammerle, A., Kitz, F., Migliavacca, M., Alberti, G., Ibrom, A., El-Madany, T. S., Gerdel, K., Moreno, G., Kolle, O., Karl, T., Peressotti, A., and Delle Vedove, G.: Gross Primary Productivity of Four European Ecosystems Constrained by Joint CO<sub>2</sub> and COS Flux Measurements, *Geophysical Research Letters*, 46, 5284–5293, <https://doi.org/https://doi.org/10.1029/2019GL082006>, 2019.
- 1125 Springer, K., Wang, R., and Gamon, J.: Parallel Seasonal Patterns of Photosynthesis, Fluorescence, and Reflectance Indices in Boreal Trees, *Remote Sensing*, 9, 691, <https://doi.org/10.3390/rs9070691>, 2017.
- Street, L. E., SHAVER, G. R., WILLIAMS, M., and VAN WIJK, M. T.: What is the relationship between changes in canopy leaf area and changes in photosynthetic CO<sub>2</sub> flux in arctic ecosystems?, *Journal of Ecology*, 95, 139–150, <https://doi.org/https://doi.org/10.1111/j.1365-2745.2006.01187.x>, 2007.
- 1130 Tang, Y., Reed, P., Wagener, T., and van Werkhoven, K.: Comparing sensitivity analysis methods to advance lumped watershed model identification and evaluation, *Hydrology and Earth System Sciences*, 11, 793–817, <https://doi.org/10.5194/hess-11-793-2007>, 2007.
- Turner, D., RITTS, W., STYLES, J., YANG, Z., COHEN, W., Law, B., and THORNTON, P.: A diagnostic carbon flux model to monitor the effects of disturbance and interannual variation in climate on regional NEP, *Tellus B*, 58, 476 – 490, <https://doi.org/10.1111/j.1600-0889.2006.00221.x>, 2006.
- 1135 Van Looy, K., Bouma, J., Herbst, M., Koestel, J., Minasny, B., Mishra, U., Montzka, C., Nemes, A., Pachepsky, Y. A., Padarian, J., Schaap, M. G., Tóth, B., Verhoef, A., Vanderborght, J., van der Ploeg, M. J., Weihermüller, L., Zacharias, S., Zhang, Y., and Vereecken, H.: Pedotransfer Functions in Earth System Science: Challenges and Perspectives, *Reviews of Geophysics*, 55, 1199–1256, <https://doi.org/https://doi.org/10.1002/2017RG000581>, 2017.
- Vargas, R., Sonnentag, O., Abramowitz, G., Carrara, A., Chen, J., Ciais, P., Correia, A., Keenan, T., Kobayashi, H., Ourcival, J., Papale, D., Pearson, D., Pereira, J., Piao, S., Rambal, S., and Baldocchi, D.: Drought Influences the Accuracy of Simulated Ecosystem Fluxes: A Model-Data Meta-analysis for Mediterranean Oak Woodlands, *Ecosystems*, 16, 749–764, <https://doi.org/10.1007/s10021-013-9648-1>, 2013.
- 1140 Vicca, S., Balzarolo, M., Filella, I., Granier, A., Herbst, M., Knohl, A., Bernard, L., Mund, M., Nagy, Z., Pintér, K., Rambal, S., Verbesselt, J., Verger, A., Zeileis, A., Zhang, C., and Penuelas, J.: Remotely-sensed detection of effects of extreme droughts on gross primary production, *Scientific Reports*, 6, <https://doi.org/10.1038/srep28269>, 2016.
- 1145



- Wang, H., Jia, G., Fu, C., Feng, J., Zhao, T., and Ma, Z.: Deriving maximal LUE from coordinated flux measurements and satellite data for regional gross primary production modeling, *Remote Sensing of Environment*, 114, 2248–2258, <https://doi.org/10.1016/j.rse.2010.05.001>, 2010.
- Wang, L., Zhu, H., Lin, A., Zou, L., Qin, W., and Du, Q.: Evaluation of the Latest MODIS GPP Products across Multiple Biomes Using Global Eddy Covariance Flux Data, *Remote Sensing*, 9, <https://doi.org/10.3390/rs9050418>, 2017.
- 1150 Wang, Y., Cao, G., Wang, Y., Webb, A. A., Yu, P., and Wang, X.: Response of the daily transpiration of a larch plantation to variation in potential evaporation, leaf area index and soil moisture, *Scientific Reports*, 9, 4697, <https://doi.org/10.1038/s41598-019-41186-1>, 2019.
- Wegehenkel, M.: Modeling of vegetation dynamics in hydrological models for the assessment of the effects of climate change on evapotranspiration and groundwater recharge, *Advances in Geosciences*, 21, 109–115, <https://doi.org/10.5194/adgeo-21-109-2009>, 2009.
- 1155 Wei, S., Yi, C., Fang, W., and Hendrey, G.: A global study of GPP focusing on light-use efficiency in a random forest regression model, *Ecosphere*, 8, e01724, <https://doi.org/10.1002/ecs2.1724>, 2017.
- White, M., Thornton, P., Running, S., and Nemani, R.: Parameterization and Sensitivity Analysis of the BIOME-BGC Terrestrial Ecosystem Model: Net Primary Production Controls, *Earth Interactions - EARTH INTERACT*, 4, [https://doi.org/10.1175/1087-3562\(2000\)004<0003:PASAOT>2.0.CO;2](https://doi.org/10.1175/1087-3562(2000)004<0003:PASAOT>2.0.CO;2), 2000.
- 1160 Wu, C.: Use of a vegetation index model to estimate gross primary production in open grassland, *Journal of Applied Remote Sensing*, 6, <https://doi.org/10.1117/1.JRS.6.063532>, 2012.
- Xia, J., Yuan, W., Wang, Y.-P., and Zhang, Q.: Adaptive Carbon Allocation by Plants Enhances the Terrestrial Carbon Sink, *Scientific Reports*, 7, 3341, <https://doi.org/10.1038/s41598-017-03574-3>, 2017.
- Xiao, X., Zhang, Q., Braswell, B., Urbanski, S., Boles, S., Wofsy, S., Moore, B., and Ojima, D.: Modeling gross primary production of temperate deciduous broadleaf forest using satellite images and climate data, *Remote Sensing of Environment*, 91, 256–270, <https://doi.org/10.1016/j.rse.2004.03.010>, 2004.
- 1165 Xin, Q., Dai, Y., and Liu, X.: A simple time-stepping scheme to simulate leaf area index, phenology, and gross primary production across deciduous broadleaf forests in the eastern United States, *Biogeosciences*, 16, 467–484, <https://doi.org/10.5194/bg-16-467-2019>, 2019.
- Yang, H., Yang, X., Heskell, M., Sun, S., and Tang, J.: Seasonal variations of leaf and canopy properties tracked by ground-based NDVI imagery in a temperate forest, *Scientific Reports*, 7, <https://doi.org/10.1038/s41598-017-01260-y>, 2017.
- 1170 Yates, K. L., Bouchet, P. J., Caley, M. J., Mengersen, K., Randin, C. F., Parnell, S., Fielding, A. H., Bamford, A. J., Ban, S., Barbosa, A. M., Dormann, C. F., Elith, J., Embling, C. B., Ervin, G. N., Fisher, R., Gould, S., Graf, R. F., Gregr, E. J., Halpin, P. N., Heikkinen, R. K., Heinänen, S., Jones, A. R., Krishnakumar, P. K., Lauria, V., Lozano-Montes, H., Mannocci, L., Mellin, C., Mesgaran, M. B., Moreno-Amat, E., Mormede, S., Novacek, E., Oppel, S., Ortúño Crespo, G., Peterson, A. T., Rapacciuolo, G., Roberts, J. J., Ross, R. E., Scales, K. L., Schoeman, D., Snelgrove, P., Sundblad, G., Thuiller, W., Torres, L. G., Verbruggen, H., Wang, L., Wenger, S., Whittingham, M. J., Zharikov, Y., Zurell, D., and Sequeira, A. M.: Outstanding Challenges in the Transferability of Ecological Models, *Trends in Ecology and Evolution*, 33, 790–802, <https://doi.org/10.1016/j.tree.2018.08.001>, 2018.
- Yuan, W., Liu, S., Zhou, G., Zhou, G., Tieszen, L., Baldocchi, D., Bernhofer, C., Gholz, H., Goldstein, A., Goulden, M., Hollinger, D., Hu, Y., Law, B., Stoy, P., Vesala, T., and Wofsy, S.: Deriving a light use efficiency model from eddy covariance flux data for predicting daily gross primary production across biomes, *Agricultural and Forest Meteorology*, 143, 189–207, <https://doi.org/10.1016/j.agrformet.2006.12.001>, 2007.
- 1180

- Yuan, W., Liu, S., Yu, G., Bonnefond, J.-M., Chen, J., Davis, K., Desai, A. R., Goldstein, A. H., Gianelle, D., Rossi, F., Suyker, A. E., and Verma, S. B.: Global estimates of evapotranspiration and gross primary production based on MODIS and global meteorology data, *Remote Sensing of Environment*, 114, 1416–1431, <https://doi.org/https://doi.org/10.1016/j.rse.2010.01.022>, 2010.
- 1185 Yuan, W., Cai, W., Xia, J., Chen, J., Liu, S., Dong, W., Merbold, L., Law, B., Arain, A., Beringer, J., Bernhofer, C., Black, A., Blanken, P. D., Cescatti, A., Chen, Y., Francois, L., Gianelle, D., Janssens, I. A., Jung, M., Kato, T., Kiely, G., Liu, D., Marcolla, B., Montagnani, L., Raschi, A., Rouspard, O., Varlagin, A., and Wohlfahrt, G.: Global comparison of light use efficiency models for simulating terrestrial vegetation gross primary production based on the LaThuile database, *Agricultural and Forest Meteorology*, 192–193, 108–120, <https://doi.org/https://doi.org/10.1016/j.agrformet.2014.03.007>, 2014.
- 1190 Yuan, W., Zheng, Y., Piao, S., Ciais, P., Lombardozi, D., Wang, Y., Ryu, Y., Chen, G., Dong, W., Hu, Z., Jain, A. K., Jiang, C., Kato, E., Li, S., Lienert, S., Liu, S., Nabel, J. E., Qin, Z., Quine, T., Sitch, S., Smith, W. K., Wang, F., Wu, C., Xiao, Z., and Yang, S.: Increased atmospheric vapor pressure deficit reduces global vegetation growth, *Science Advances*, 5, <https://doi.org/10.1126/sciadv.aax1396>, 2019.
- Yue, X. and Unger, N.: The Yale Interactive terrestrial Biosphere model version 1.0: description, evaluation and implementation into NASA GISS ModelE2, *Geoscientific Model Development*, 8, 2399–2417, <https://doi.org/10.5194/gmd-8-2399-2015>, 2015.
- 1195 Zacharias, S. and Wessolek, G.: Excluding Organic Matter Content from Pedotransfer Predictors of Soil Water Retention, *Soil Science Society of America Journal*, 71, 43–50, <https://doi.org/https://doi.org/10.2136/sssaj2006.0098>, 2007.
- Zaehle, S., Sitch, S., Smith, B., and Hatterman, F.: Effects of parameter uncertainties on the modeling of terrestrial biosphere dynamics, *Global Biogeochemical Cycles*, 19, <https://doi.org/https://doi.org/10.1029/2004GB002395>, 2005.
- Zhang, L. and Han, J.: Improving water retention capacity of an aeolian sandy soil with feldspathic sandstone, *Scientific Reports*, 9, 1–8, <https://doi.org/10.1038/s41598-019-51257-y>, 2019.
- 1200 Zhang, L., Zhou, D., Fan, J.-W., and Hu, Z.: Comparison of four light use efficiency models for estimating terrestrial gross primary production, *Ecological Modelling*, 300, 30–39, <https://doi.org/10.1016/j.ecolmodel.2015.01.001>, 2015.
- Zhou, H., Yue, X., Lei, Y., Tian, C., Ma, Y., and Cao, Y.: Large Contributions of Diffuse Radiation to Global Gross Primary Productivity During 1981–2015, *Global Biogeochemical Cycles*, 35, <https://doi.org/10.1029/2021GB006957>, 2021.
- 1205 Zhu, Z., Bi, J., Pan, Y., Ganguly, S., Anav, A., Xu, L., Samanta, A., Piao, S., Nemani, R. R., and Myneni, R. B.: Global Data Sets of Vegetation Leaf Area Index (LAI)3g and Fraction of Photosynthetically Active Radiation (FPAR)3g Derived from Global Inventory Modeling and Mapping Studies (GIMMS) Normalized Difference Vegetation Index (NDVI3g) for the Period 1981 to 2011, *Remote Sensing*, 5, 927–948, <https://doi.org/10.3390/rs5020927>, 2013.
- Zink, M., Kumar, R., Cuntz, M., and Samaniego, L.: A High-Resolution Dataset of Water Fluxes and States for Germany Accounting for Parametric Uncertainty, *Hydrology and Earth System Sciences Discussions*, pp. 1–29, <https://doi.org/10.5194/hess-2016-443>, 2016.
- 1210

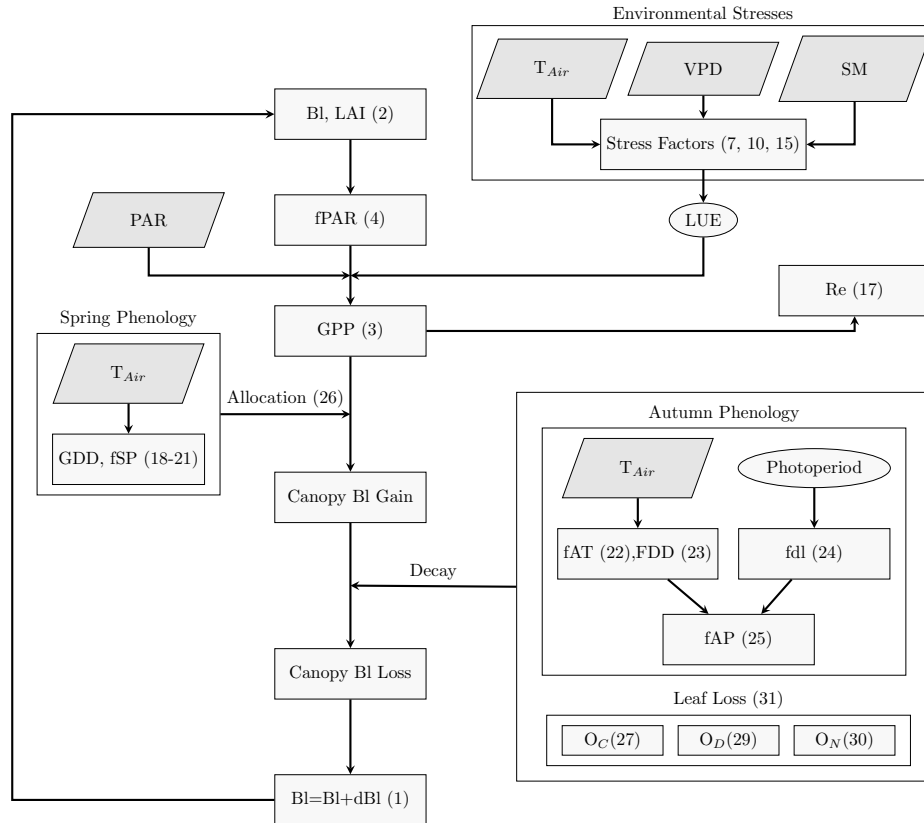


**Figure 1.** Schematic representation of the PCM model. The parallelograms indicate the model inputs;  $T_{Air}$ : air temperature, VPD: vapor pressure deficit, SM: soil moisture, and PAR: ~~photosynthetically~~ photosynthetically active radiation. Rectangles are the processes in the model (~~f~~ Variables in ellipse show LUE is model parameter and photoperiod. Photoperiod is day-length-calculated based on latitudinal distribution). Numbers refer to the corresponding equations in the text.

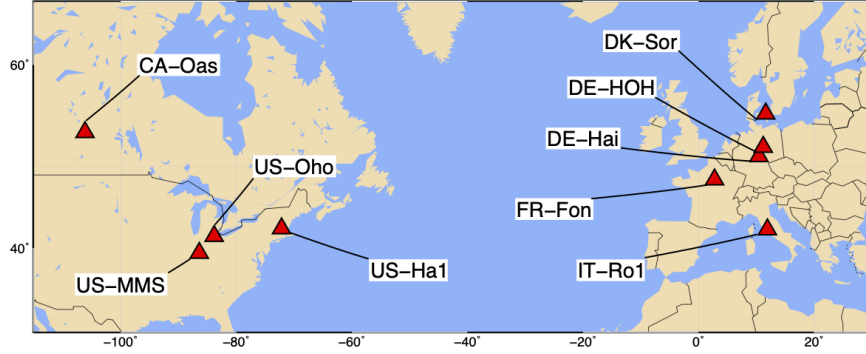


**Figure 2.** Location of the FLUXNET2015 sites investigated in this study.

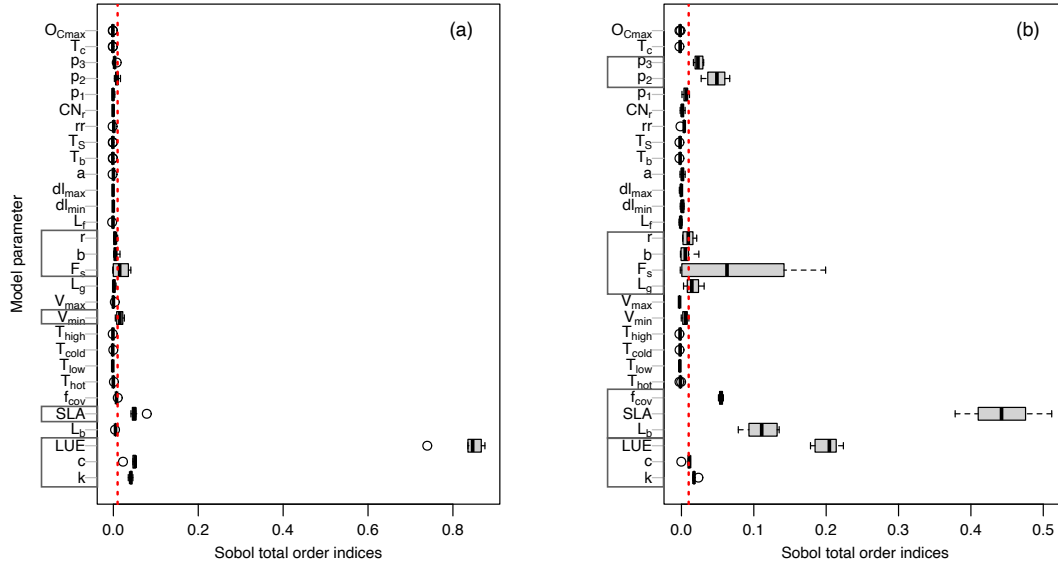


**Figure 3.** Distribution of total-order Sobol' indices for GPP (a) and LAI (b) outputs across all sites. Each **colored-grey** box on the Y-axis represents parameters involved in a specific process as following: **brown**-GPP-related parameters (Eq. 3, 4); **dark green**-LAI-related parameters (Eq. 2, 26); **Cyan**-Environmental stresses-related parameters (Eq. 10); **blue**-phenology-related parameters (Eq. 18, 20, 22); **grey**-canopy respiration-related parameters (Eq. 17). The vertical dotted red line corresponds to the threshold of 1%

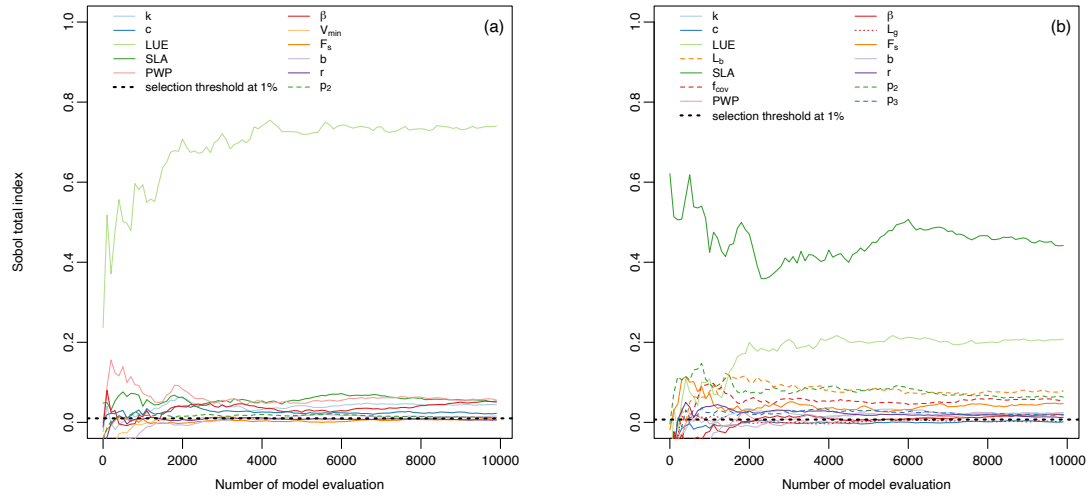


**Figure 4.** Illustration of evolution of total-order Sobol' indices (total-order indices convergence) for sensitive parameters with increasing number of samples for GPP (a) and LAI (b) outputs, at DE-HoH site taken as an example including soil moisture stress-related parameters.

**Table 1.** Descriptions of flux tower sites from FLUXNET2015 global database collection. Note that since phenology submodel for simulating budburst in each year needs the temperature data from 10-11 last days of previous year, therefore the very first year of investigated time period at each site is not included in the simulations.

Site ID	Site Name	Latitude	Longitude	Elevation(m)	Mean Annual Temperature ( $^{\circ}\text{C}$ )	Mean Annual Precipitation (mm)	Downloaded Period	Simulation period	Source
DK-Sor	Soroe	55.48	11.64	40	8.2	660	1996-2014	2006-2013	DOI: 10.18140/FLX/1440155
CA-Oas	Saskatchewan - Western Boreal	53.62	-106.19	530	0.34	428.53	1996-2010	1996-2010	DOI: 10.18140/FLX/1440043
DE-HoH	Hohes Holz	52.08	11.21	193	9.1	563	2014-2019	2014-2019	Own dataset
DE-Hai	Hainich	51.07	10.45	430	8.3	720	2000-2018	2000-2018	DOI: 10.18140/FLX/1440148
FR-Fon	Fontainebleau-Barbeau	48.47	2.78	103	10.2	720	2005-2014	2005-2014	DOI: 10.18140/FLX/1440161
IT-Ro1	Roccarespanpani 1	42.40	11.93	235	15.15	876.2	2000-2008	2001-2006	DOI: 10.18140/FLX/1440174
US-Ha1	Harvard Forest EMS Tower	42.53	-72.17	340	6.62	1071	1991-2012	2003-2012	DOI: 10.18140/FLX/1440071
US-Oho	Oak Openings	41.55	-83.84	230	10.1	849	2004-2013	2004-2013	DOI: 10.18140/FLX/1440088
US-MMS	Morgan Monroe State Forest	39.32	-86.41	275	10.58	1032	1999-2014	1999-2014	DOI: 10.18140/FLX/1440083

**Table 2.** List of input and state variables (at daily time step) in PCM.

Input variables	Unit	Description
T	$^{\circ}\text{C}$	mean air temperature
PPFD	$\mu\text{mol m}^{-2} \text{s}^{-1}$	photosynthetically active radiation
VPD	$\text{hPa}$	vapour pressure deficit
SM	%	soil moisture
Soil textural properties	%	sand, clay, and bulk density
Lat	degree	Latitude of site
State variables	Unit	Description
Bl	$\text{gC m}^{-2}$	biomass of leaf
D	$\text{gC m}^{-2}$	leaf biomass decay
LAI	$\text{m}^2 \text{m}^{-2}$	leaf area index
fPAR	%	fraction of photosynthetically active radiation

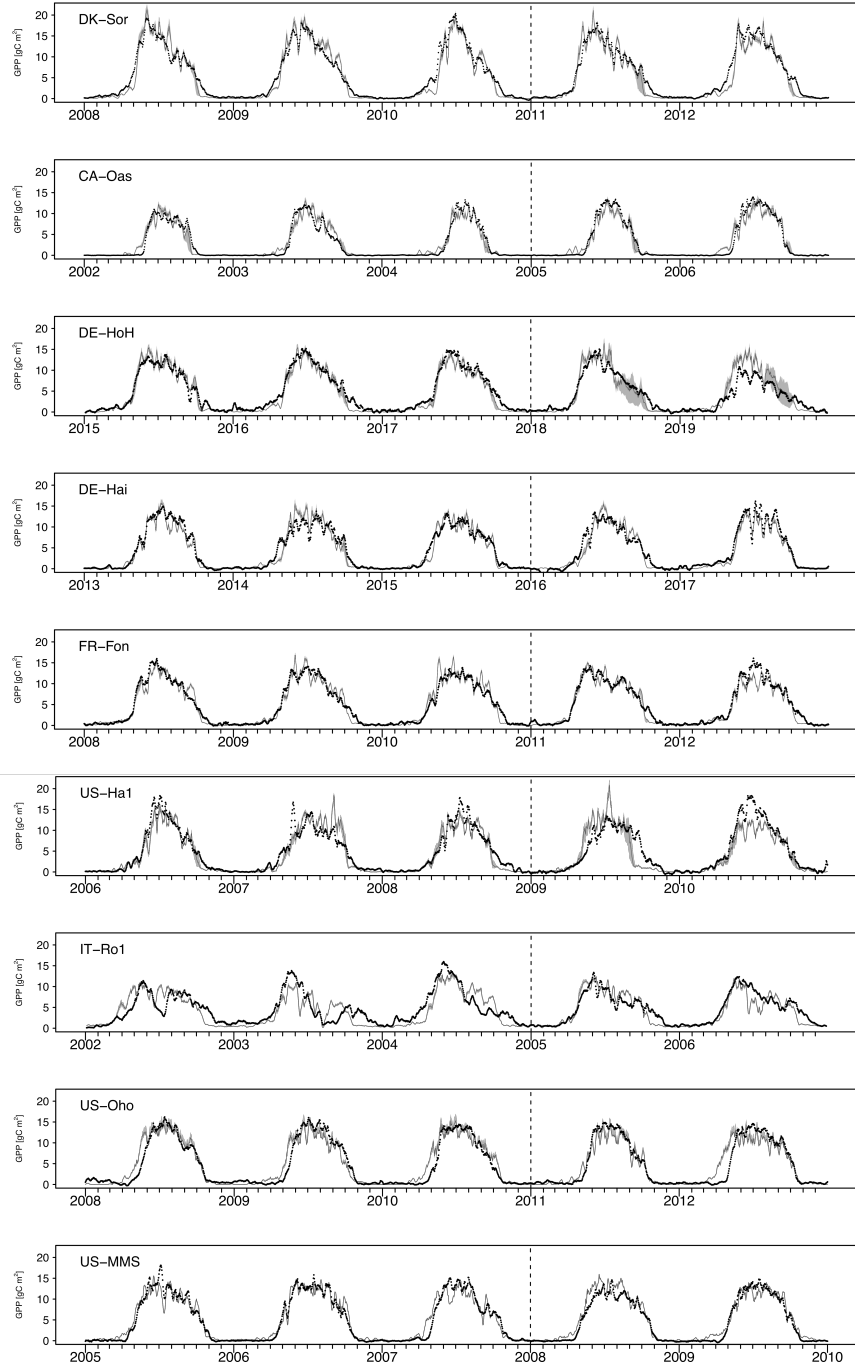


**Figure 5.** Time series of observed and simulated GPP at each study site during the three last years of calibration and the two first years of verification-validation periods. The vertical dash line marked the calibration-verification-calibration-validation periods. The black dots indicate the tower estimated GPP. The light grey shed-sheded area corresponds to the resultant ensemble sets-of-modeled-GPP-outputs-output members at each time step. The dark grey line refers to the median of model-ensemblesensemble members.

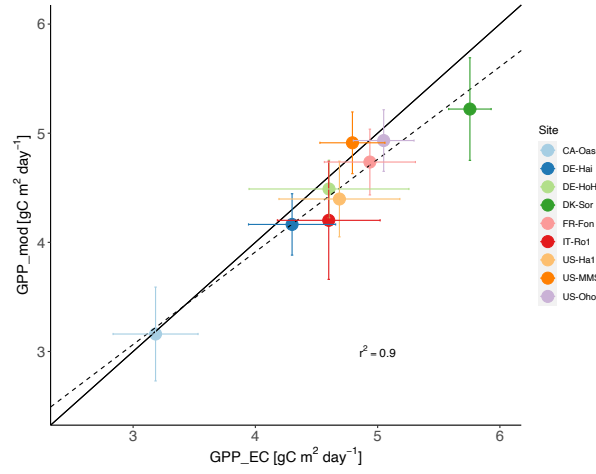


**Figure 6.** Estimated GPP based on flux tower measurements vs. modelled GPP  $\pm$  standard deviation (error bars) across the 9 studied sites. The solid line indicates the 1:1 line, and the dashed line indicates the regression line. Each dot represents one of the sites and refers to site-averaged GPP over the entire available time series.

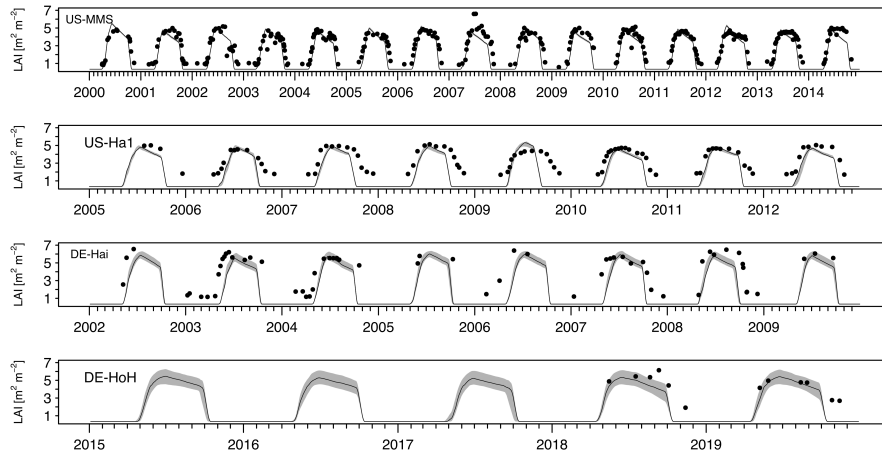


**Figure 7.** Time series of observed and simulated LAI at study flux tower sites during the common years of field measurements and simulations. The black dots indicate the field measurement LAI. The light grey shed corresponds to the ensemble sets-members of modeled the LAI outputs-output at each time step. The dark grey line refers to the median of model-ensemblesensemble members.

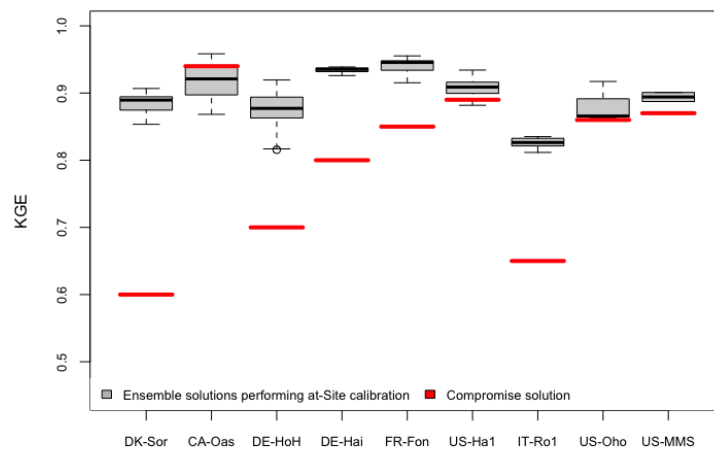


**Figure 8.** Comparison between KGE obtained from ensemble simulated GPP performing at-site calibration and the KGE obtained from compromised solution.



**Table 3.** Model parameters in PCM

Calibration model parameters, based on sensitivity analysis	Unit	Description	Lower Boundary	Upper Boundary	References
$K$	-	extinction coefficient	0.45	0.60	Ruimy et al. (1999); Yuan et al. (2007)
$C$	-	Beer–Lambert law parameter	0.85	1	Monsi and Saeki (1953)
$LUE$	$gC\ MJ^{-1}$	light use efficiency	1.04	2.25	Cheng et al. (2014); Yuan et al. (2010)
$L_b$	$m^2\ m^{-2}$	maximum balanced LAI	4	6.5	Fleischer et al. (2013)
$SLA$	$m^2\ g^{-1}$	specific leaf area	0.01	0.03	Kattge et al. (2011); Gim et al. (2017); Dyderski et al. (2020)
$f_{cov}$	%	vegetation fractional coverage per unit area	0.60	0.95	Fluxnet site description
$PWP$	%	permanent wilting point	7	13	Intermediate output of PCM model
$\beta$	-	root distribution coefficient	0.966	1	Jackson et al. (1996)
$v_{min}$	$hPa$	mean VPD at which $LUE = LUE_{potential}$	6.5	10	Heinsch et al. (2003); Cheng et al. (2014)
$L_g$	$DegreeDay$	phenological growing length	300	450	Yue and Unger (2015)
$F_s$	$DegreeDay$	phenological threshold for leaf fall	-500	-112	Yue and Unger (2015), calibrated
$b$	$DegreeDay$	phenological parameter for budburst threshold $G_b$	440	660	Yue and Unger (2015)
$r$	-	phenological parameter for budburst threshold $G_b$	-0.012	-0.008	Yue and Unger (2015)
$p_2$	-	2nd parameter in Arrhenius equation	44.96	67.44	Sitch et al. (2003)
$p_3$	-	3rd parameter in Arrhenius equation	36.96	55.44	Sitch et al. (2003)
Fixed model parameters based on sensitivity analysis					
$FC$	%	field capacity	23	23	Intermediate output of PCM model
$scw$	-	critical threshold value of soil moisture	0.4	0.4	Granier et al. (1999)
$T_{hot}$	$^{\circ}C$	mean air temperature of warmest month	19	19	Rödig et al. (2017); Sitch et al. (2003)
$T_{low}$	$^{\circ}C$	low temperature limit for $CO_2$ assimilation	-2	-2	Rödig et al. (2017); Sitch et al. (2003)
$T_{cold}$	$^{\circ}C$	mean air temperature of coldest month	10	10	Rödig et al. (2017); Sitch et al. (2003)
$T_{high}$	$^{\circ}C$	high temperature limit for $CO_2$ assimilation	38	38	Rödig et al. (2017); Sitch et al. (2003)
$v_{max}$	$hPa$	mean VPD at which $LUE = 0$	25	25	Heinsch et al. (2003); Cheng et al. (2014)
$L_f$	$DegreeDay$	phenological falling length	410	410	Yue and Unger (2015)
$dl_{min}$	<i>minutes</i>	phenological day length threshold for leaf fall	585	585	Yue and Unger (2015)
$dl_{max}$	<i>minutes</i>	phenological day length threshold for leaf fall	695	695	Yue and Unger (2015)
$a$	$DegreeDay$	phenological parameter for budburst threshold $G_b$	-110	-110	Yue and Unger (2015)
$r$	-	phenological parameter for budburst threshold $G_b$	-0.01	-0.01	Yue and Unger (2015)
$T_b$	$^{\circ}C$	base temperature for budburst occurrence	5	5	Yue and Unger (2015)
$T_s$	$^{\circ}C$	base temperature for senescence occurrence	20	20	Yue and Unger (2015)
$CNr$	$gC\ gN^{-1}$	leaf C:N ratio	25	25	White et al. (2000)
$p_1$	-	1st Arrhenius parameter	308.56	308.56	Sitch et al. (2003)
$T_c$	$^{\circ}C$	temperature threshold for determining cold stress	5	5	Melton and Arora (2016)
$rr$	$gC\ gN^{-1}$	leaf respiration coefficient	0.066	0.066	Kattge et al. (2011); Sitch et al. (2003); Rödig et al. (2017)
$O_{Dmax}$	$day^{-1}$	maximum drought stress loss rate	0.15	0.15	Melton and Arora (2016)
$O_{Cmax}$	$day^{-1}$	maximum cold stress loss rate	0.005	0.005	Melton and Arora (2016)

**Table 4.** Summary statistics for the comparison between model estimated GPP and tower estimated GPP at different sites. Statistics include KGE, root mean square error (RMSE), and  $R^2$ . GPP units are [ $g\ C\ m^{-2}\ d^{-1}$ ]. The statistics refer to ensemble medians of model estimated GPP. The linear regression is over the both calibration and validation periods.

Site	Calibration				validation				Linear regression
	Period	KGE	RMSE	$R^2$	Period	KGE	RMSE	$R^2$	$\hat{y}$
DK-Sor	2007-2010	0.89	2.09	0.89	2011-2013	0.89	2.15	0.89	$y = 0.99x - 0.51$
CA-Oas	1997-2004	0.92	1.5	0.89	2005-2010	0.90	1.4	0.91	$y = 0.9x + 0.29$
DE-HoH	2015-2017	0.88	1.8	0.88	2018-2019	0.75	2.5	0.80	$y = 1.04x - 0.34$
DE-Hai	2001-2015	0.93	1.9	0.85	2016-2018	0.91	2.01	0.84	$y = 0.96x + 0.05$
FR-Fon	2006-2010	0.95	1.7	0.91	2011-2014	0.91	1.94	0.85	$y = 0.96x + 0.04$
US-Ha1	2004-2008	0.92	2.03	0.86	2009-2012	0.88	2.56	0.80	$y = 0.91x + 0.11$
IT-Ro1	2002-2004	0.79	2.45	0.65	2005-2006	0.86	1.87	0.78	$y = 0.87x + 0.2$
US-Oho	2005-2010	0.87	2.22	0.85	2011-2013	0.85	2.39	0.82	$y = 0.84x + 0.55$
US-MMS	2000-2007	0.9	2.1	0.85	2008-2014	0.89	1.9	0.87	$y = 0.93x + 0.75$

**Table 5.** Summary statistics for the comparison between model estimated LAI and Field measurement LAI at different sites. Statistics include  $R^2$  and RMSE. LAI units are [ $m^{-2}$ ]. The statistics refer to ensemble medians of model estimated LAI.

Site	Period	RMSE	$r^2$	Linear regression
US-MMS	<u>2000-2014</u>	<u>0.96</u>	<u>0.90</u>	<u><math>y = 1.08x - 0.8</math></u>
US-Ha1	<u>2005-2012</u>	<u>1.58</u>	<u>0.85</u>	<u><math>y = 0.92x - 1.52</math></u>
DE-Hai	<u>2002-2009</u>	<u>2.21</u>	<u>0.78</u>	<u><math>y = 0.89x - 1.32</math></u>
DE-HoH	<u>2018-2019</u>	<u>1.4</u>	<u>0.90</u>	<u><math>y = 1.32x - 2.62</math></u>